Electronic Supplementary Material (ESI) for Polymer Chemistry.
This journal is © The Royal Society of Chemistry 2021

Controlled and Efficient Polymerization of Methyl Methacrylate Catalyzed by Pyridinylidenaminophosphines Based Lewis Pairs

Fang Ge[a], Sun Li[b], Zhe Wang[b], Wenzhong Zhang [c], Xiaowu Wang[b,*]

Tables of Contents

1 Synthesis of Pyridinylidenaminophosphines (PyAPs)

Synthesis of pyridyl salt 1

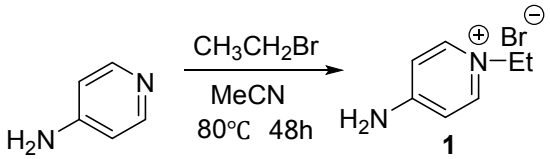

2-Aminopyridine (5.00 g, 53.1 mmol, 1 eq.) and bromoethane (5.9 mL, 79.7 mmol, 1.5 eq.) were dissolved in MeCN (50 mL) and heated at 80 °C for 48 h. The salt was precipitated out of the solution with Et_2O (100 mL), filtered off and washed with Et_2O. The colourless powder was dried in vacuo at 80 °C for16 h. Yield: 9.3g (86.2%)

^{1}H NMR (400 MHz, DMSO-d_6, 298 K): δ (ppm) = 8.48 (s, 1H), 8.12 (d, $^3J_{HH}$ = 6.7 Hz, 1H), 7.87 (dd, $^3J_{HH}$ = 8.9, 7.1 Hz, 1H), 7.09 (d, $^3J_{HH}$ = 8.9 Hz, 1H), 6.92 (t, $^3J_{HH}$ = 6.9 Hz, 0H), 4.20 (q, $^3J_{HH}$ = 7.2 Hz, 1H), 1.30 (t, $^3J_{HH}$ = 7.2 Hz, 2H).

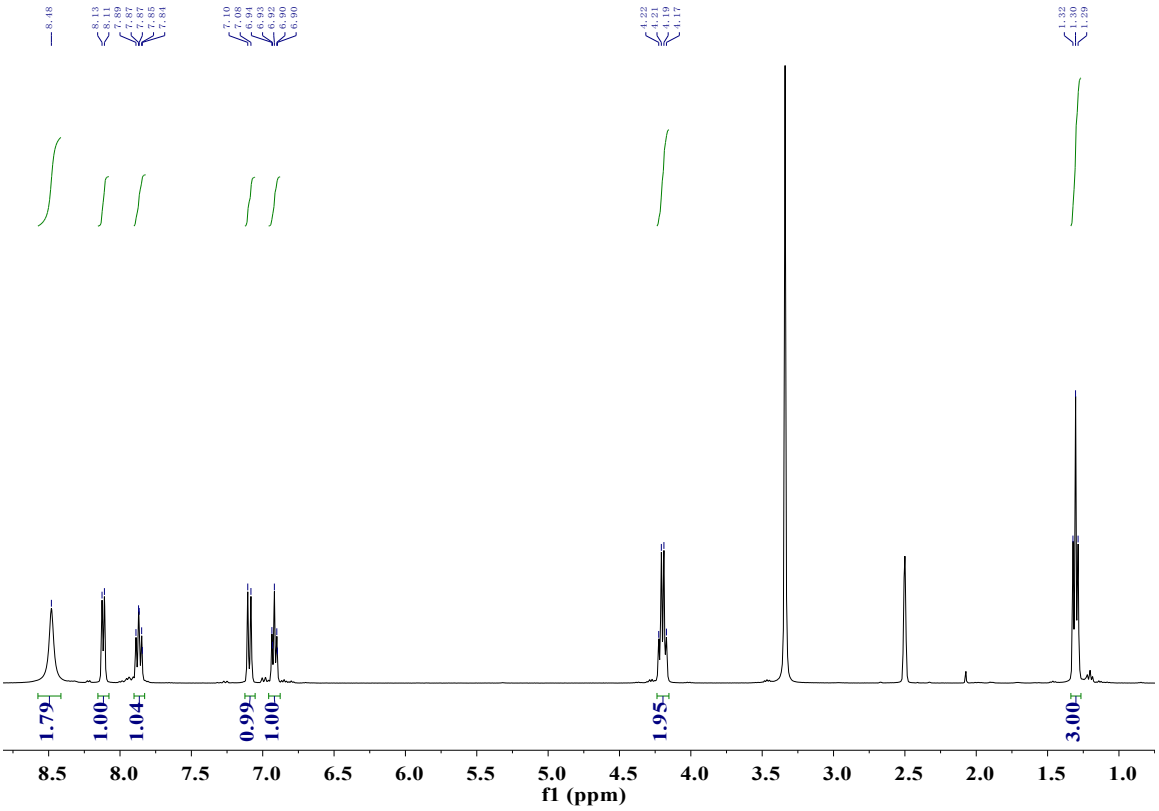

Figure S1. ^{1}H NMR (400 MHz, DMSO-d_6, 298 K)

Synthesis of PyAP-^{t}Bu

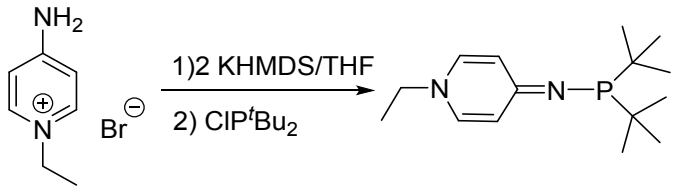

Pyridinium salt (1.015 g, 5 mmol, 1 equiv.), KHMDS (10 mL, 1 M in THF, 10 mmol, 2 equiv.) and ClP^{t}Bu$_2$ (0.95 mL, 5 mmol, 1 equiv.) were suspended in THF (10 mL). After overnight stirring, all volatile compounds were removed in *vacuo* and the residue was extracted with n-hexane (3×30 mL) to give the corresponding phosphine as bright yellow solid in 83% yield (1.10 g, 4.13 mmol). Suitable single crystals were obtained from PyAP-^{t}Bu hexane solution at -30°C for 2 days.

^{1}H NMR (400 MHz, C_6D_6, 298 K) δ (ppm) = 6.80-6.76 (m, 1H), 5.79 (d, $^3J_{HH}$ = 7.5 Hz, 1H), 2.31 (q, $^3J_{HH}$ = 7.2 Hz, 1H), 1.42 (d, $^3J_{HH}$ = 10.8 Hz, 9H), 0.39 (t, $^3J_{HH}$ = 7.3 Hz, 2H). ^{31}P{^{1}H} NMR (162 MHz, C_6D_6, 298 K) δ (ppm) = 68.9 (s).

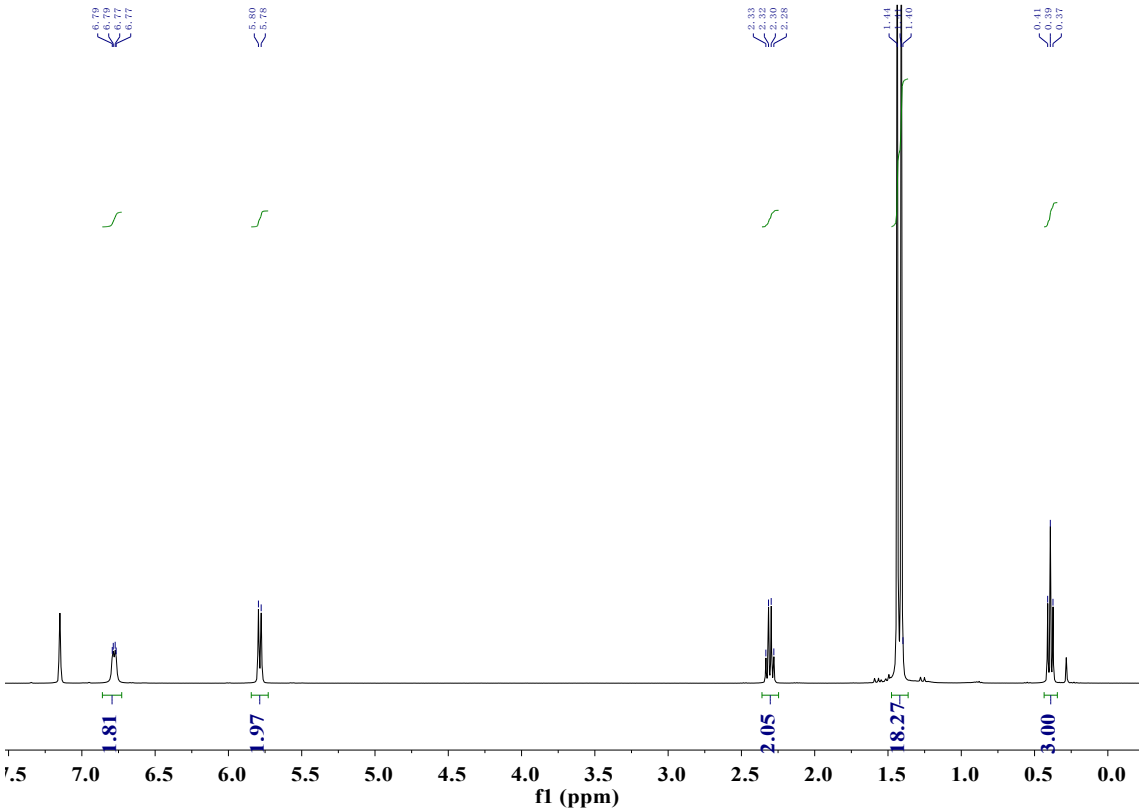

Figure S2. ^{1}H NMR spectrum of PyAP-^{t}Bu (400 MHz, C_6D_6, 298 K)

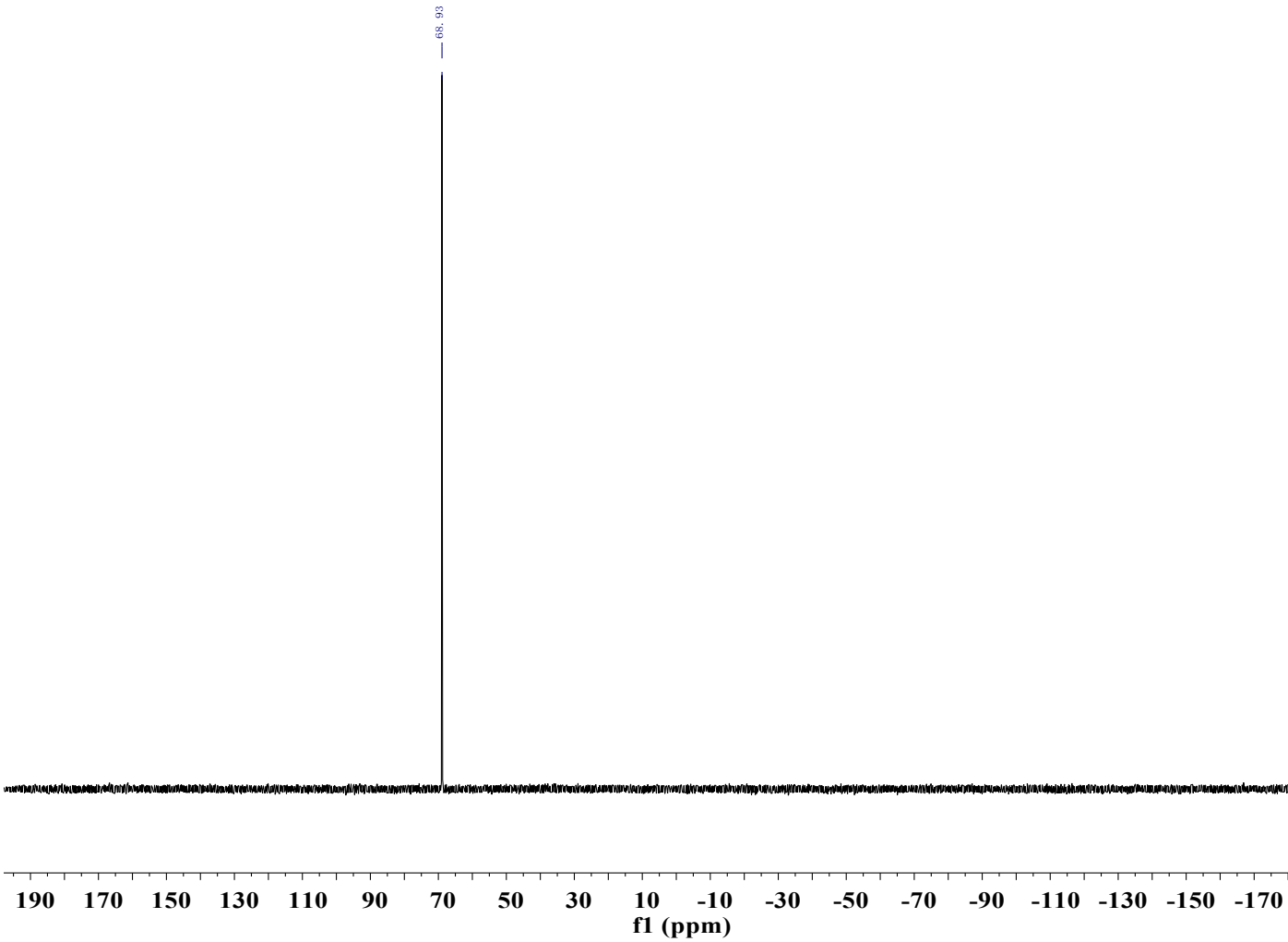

Figure S3. $^{31}P\{^{1}H\}$ NMR spectrum of PyAP-^{t}Bu (162 MHz, C_6D_6, 298 K)

Synthesis of PyAP-Cy

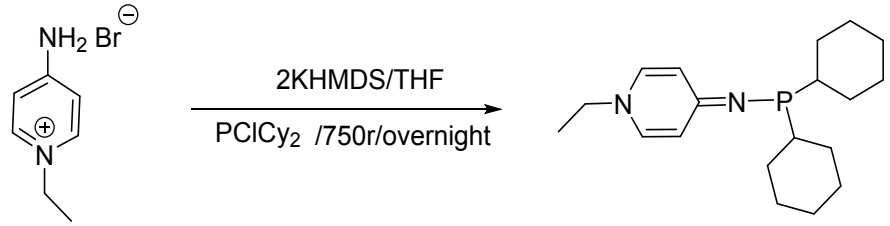

PyAP-Cy was prepared and isolated as yellow solid using the same procedure as described for the preparation of P^{i}P^{t}Bu$_2$. Pyridinium salt (1.015 g, 5 mmol, 1 equiv.), KHMDS (10 mL, 1 M in THF, 10 mmol, 2 equiv.) and ClPCy$_2$ (1.1 mL, 5 mmol, 1 equiv.) were

suspended in THF (10 mL). After overnight stirring, all volatile compounds were removed in *vacuo* and the residue was extracted with n-hexane (3×20 mL) to give the corresponding phosphine as bright yellow solid in 64% yield (1.02 g, 3.2 mmol).

^{1}H NMR (400 MHz, C_6D_6, 298 K) δ (ppm) = 6.95 (s, 0H) , 6.56 (s, 1H) , 5.59 (d, $^{3}J_{HH}$ = 7.4 Hz, 1H), 2.11 (q, $^{3}J_{HH}$ = 7.3 Hz, 1H), 2.03 (d, $^{3}J_{PH}$ = 13.0 Hz, 1H), 1.95-1.87 (m, 1H), 1.81 (td, $^{3}J_{PH}$ = 11.9, 3.5 Hz, 1H), 1.68-1.57 (m, 2H), 1.50-1.35 (m, 2H), 1.14 (dpd, *J* = 24.5, 12.2, 6.0 Hz, 3H), 0.20 (t, $^{3}J_{HH}$ = 7.3 Hz, 1H). ^{31}P{^{1}H} NMR (162 MHz, C_6D_6, 298 K) δ (ppm) = 49.5 (s).

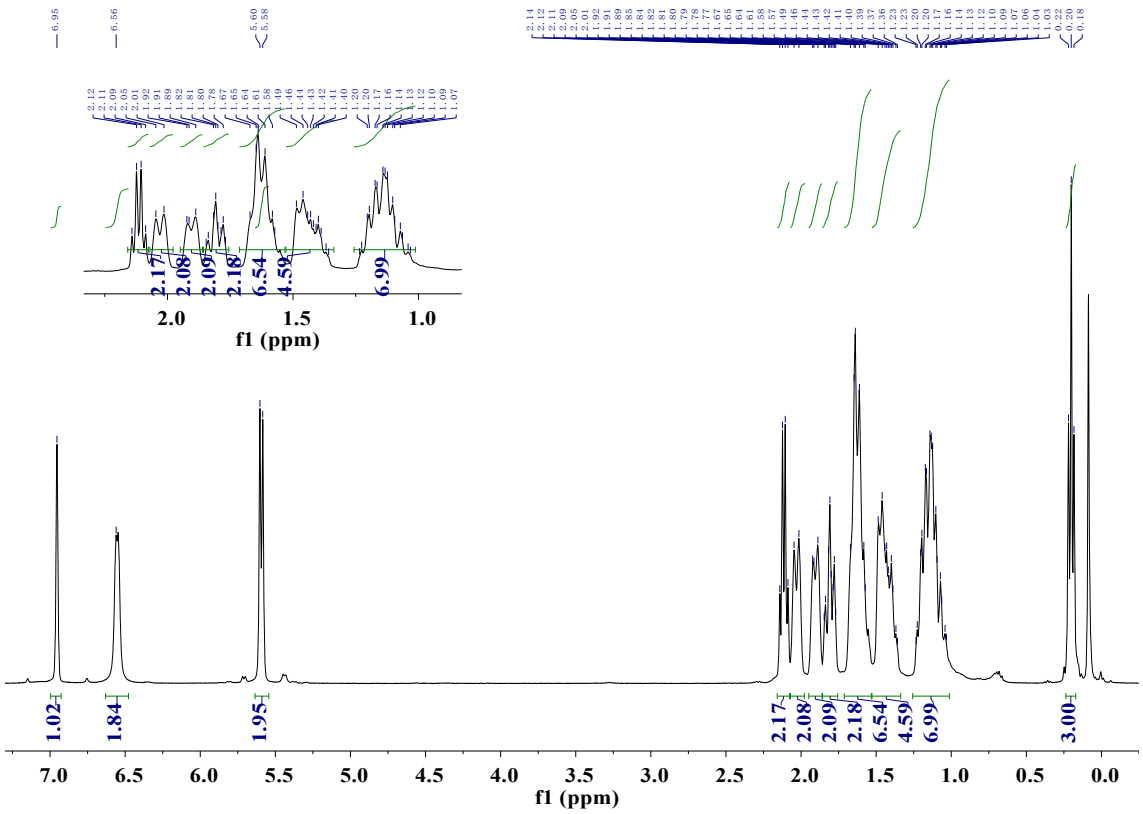

Figure S4. ^{1}H NMR spectrum of PyAP-Cy (400 MHz, C_6D_6, 298 K)

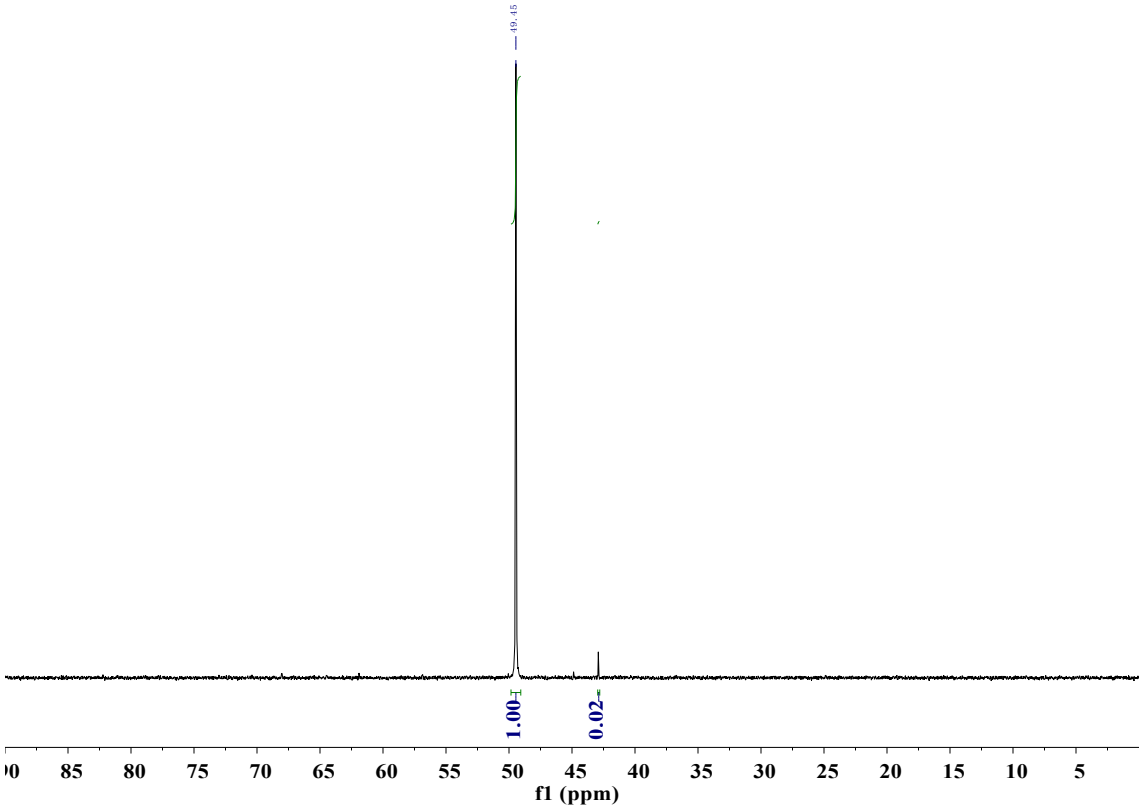

Figure S5. $^{31}P\{^{1}H\}$ NMR spectrum of PyAP-Cy (162 MHz, C_6D_6, 298 K)

Synthesis of PyAP-^{i}Pr

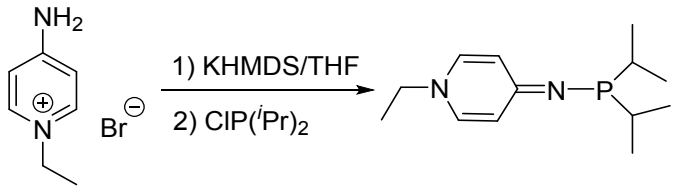

PyAP-^{i}Pr was prepared and isolated as yellow solid using the same procedure as described for the preparation of P^{i}P^{t}Bu$_2$. Pyridinium salt (1.625 g, 8 mmol, 1 equiv.), KHMDS (16 mL, 1 M in THF, 16 mmol, 2 equiv.) and ClP^{i}Pr$_2$ (1.27 mL, 8 mmol, 1 equiv.) were suspended in THF (16 mL). After overnight stirring, all volatile compounds were removed in *vacuo* and the residue was extracted with n-hexane (3× 30 mL) to give the corresponding phosphine as bright yellow solid in 81% yield (1.550 g, 6.5 mmol).

^{1}H NMR (400 MHz, C_6D_6, 298 K) δ (ppm) = 6.72 (d, $^{3}J_{HH}$ = 6.0 Hz, 2H, 2-H), 5.82 (d, $^{3}J_{HH}$ = 7.3 Hz, 2H, 3-H), 2.35 (q, $^{3}J_{HH}$ = 7.2 Hz, 2H, CH_2), 2.08 (hept, $^{3}J_{HH}$ = 7.0 Hz, 2H, $CH(CH_3)_2$), 1.30-1.40 (m, 12H, $CH(CH_3)_2$), 0.42 (t, $^{3}J_{HH}$ = 7.2 Hz, 3H, CH_3). $^{31}P\{^{1}H\}$

NMR (162 MHz, C_6D_6, 298 K) δ (ppm) = 56.3 (s).

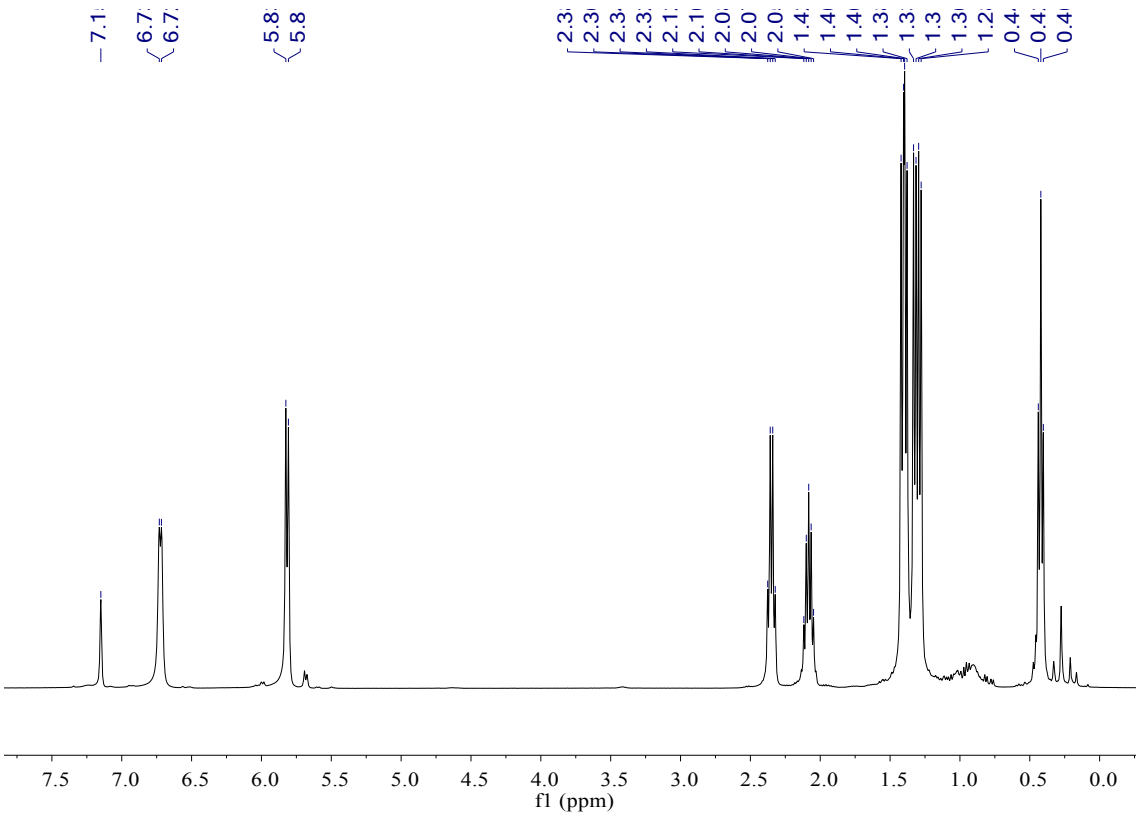

Figure S6. ^{1}H NMR spectrum of PyAP-*i*Pr (400 MHz, C_6D_6, 298 K)

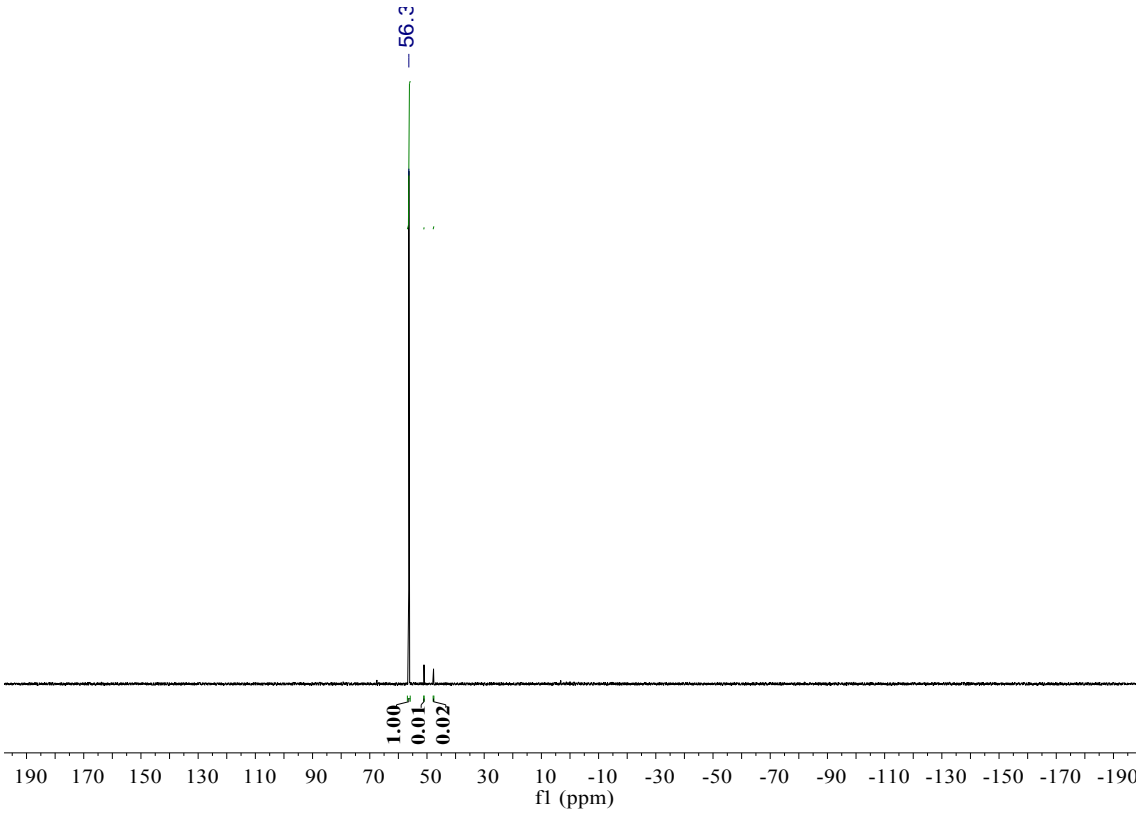

Figure S7. $^{31}P\{^{1}H\}$ NMR spectrum of PyAP-*i*Pr (162 MHz, C_6D_6, 298 K)

Synthesis of PyAP-Ph

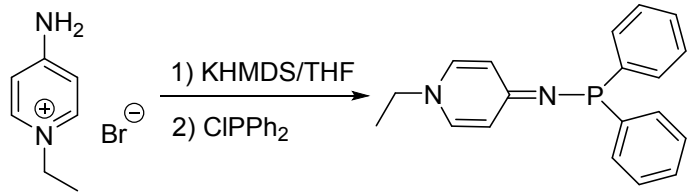

PyAP-Ph was prepared and isolated as yellow solid using the same procedure as described for the preparation of P*i*P*t*Bu$_2$. Pyridinium salt (1.015 g, 5 mmol, 1 equiv.), KHMDS (10 mL, 1 M in THF, 10 mmol, 2 equiv.) and ClPPh$_2$ (1.44 mL, 5 mmol, 1 equiv.) were suspended in THF (10 mL). After overnight stirring, all volatile compounds were removed in *vacuo* and the residue was extracted with toluene (3× 30 mL) and concentrated to 15 mL. The suspension was left in a -30℃ refidge to give the corresponding phosphine as bright yellow solid in 39.2% yield (0.60 g, 1.96 mmol).

^{1}H NMR (400 MHz, C_6D_6, 298 K) δ (ppm) = 8.07 (t, $^{3}J_{HH}$ = 7.2 Hz, 4H, *o*-Ph), 7.19 (t,

$^{3}J_{HH}$ = 7.4 Hz, 4H, *m*-Ph), 7.06 (t, $^{3}J_{HH}$ = 7.3 Hz, 2H, *p*-Ph), 6.48 (d, $^{3}J_{HH}$ = 7.2 Hz, 2H, 2-H), 5.75 (d, $^{3}J_{HH}$ = 7.1 Hz, 2H, 3-H), 2.27 (q, $^{3}J_{HH}$ = 7.3 Hz, 2H, CH_2), 0.34 (t, $^{3}J_{HH}$ = 7.2 Hz, 3H, CH_3).

$^{13}C\{^{1}H\}$ NMR (100 MHz, C_6D_6, 298 K) δ (ppm) = 163.70 (d, $^{2}J_{PC}$ = 16.0 Hz, C=N), 145.37 (d, $^{2}J_{PC}$ = 14.0 Hz, *o*-Ph_C), 135.32 (d, $^{1}J_{PC}$ = 3.0 Hz, *i*-Ph_C), 131.98 (d, $^{3}J_{PC}$ = 19.9 Hz, *m*-Ph_C), 129.3 (s, *p*-Ph_C), 116.7 (m, 3-C), 100.4 (s, 2-C), 49.8 (s, CH_2), 15.3(s, CH_3).

$^{31}P\{^{1}H\}$ NMR (162 MHz, C_6D_6, 298 K) δ (ppm) = 31.5 (s).

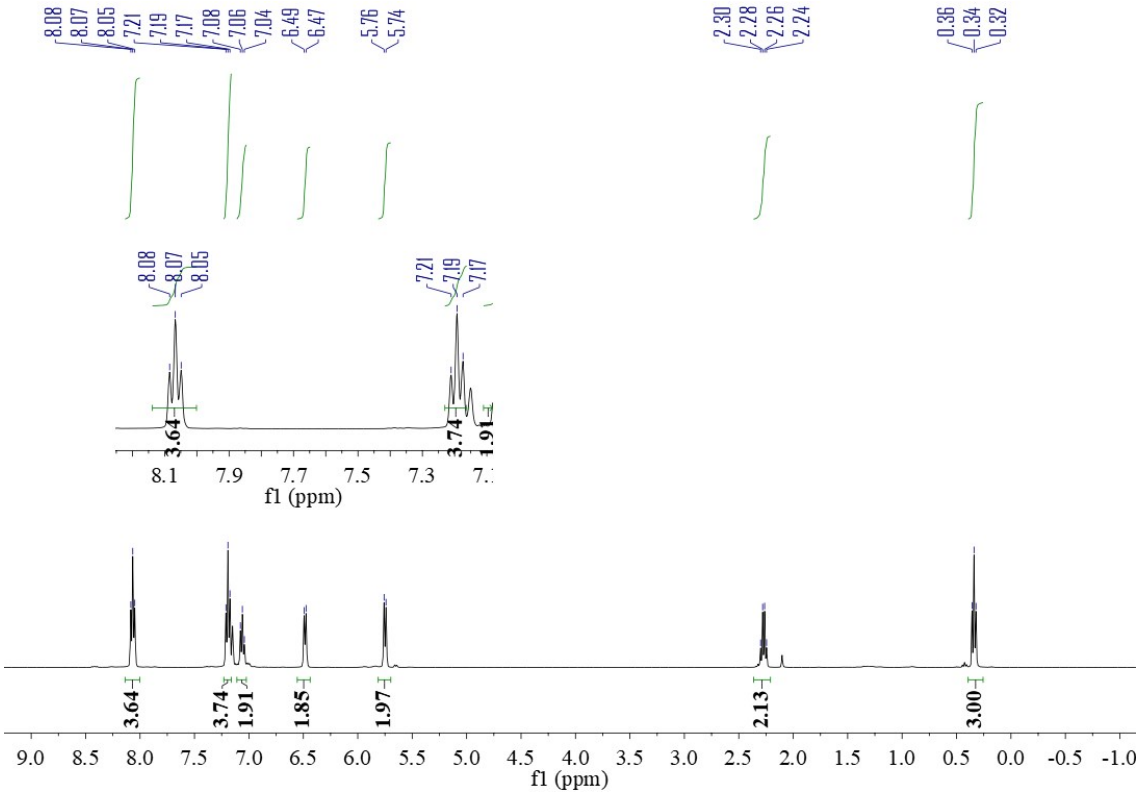

Figure S8. ^{1}H NMR spectrum of PyAP-Ph (400 MHz, C_6D_6, 298 K)

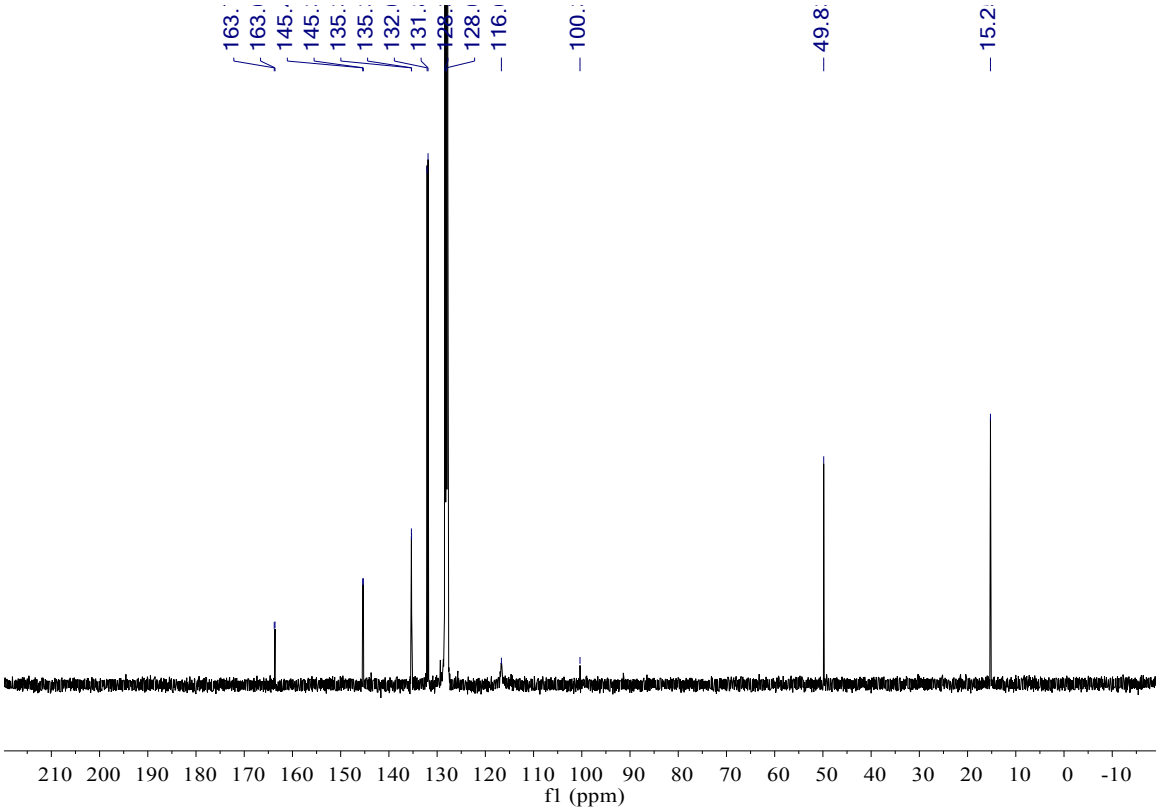

Figure S9. $^{13}C\{^{1}H\}$ NMR spectrum of PyAP-Ph (100 MHz, C_6D_6, 298 K)

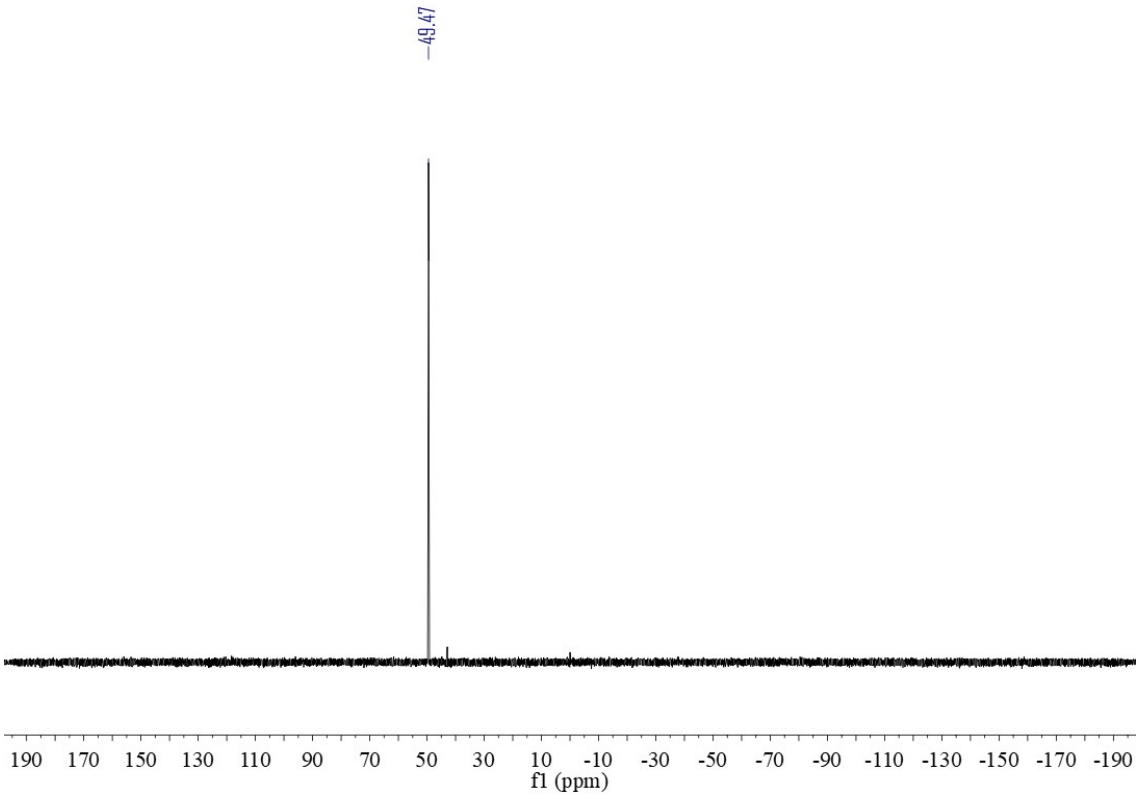

Figure S10. $^{31}P\{^{1}H\}$ NMR spectrum of PyAP-Ph (162 MHz, C_6D_6, 298 K)

2 Stoichiometric NMR Reactions

2.1 Stoichiometric NMR Reaction of PyAP-^{t}Bu with $Al(C_6F_5)_3$ in a 1:1 molar ratio

A NMR tube was charged with PyAP-^{t}Bu (6.7 mg, 0.025mmol) and 0.3 mL of C_6D_6. A solution of $Al(C_6F_5)_3$ (14.4 mg, 0.025 mmol), 0.3 mL C_6D_6 was added to this tube via pipette at ambient temperature, and the mixture was allowed to react for 5 min before analyzed by NMR spectroscopy.

Associated species : dissociated species molar ratio = 10:1, which was assigned by $^{31}P\{^{1}H\}$ NMR spectroscopy.

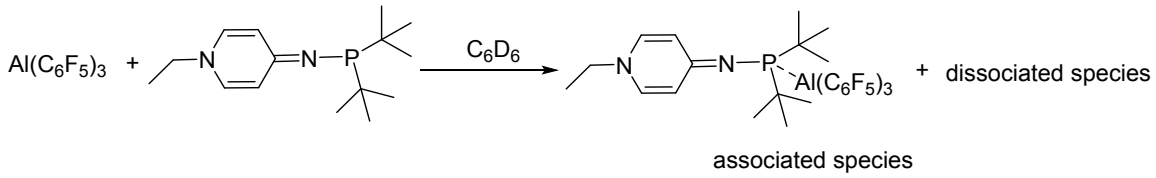

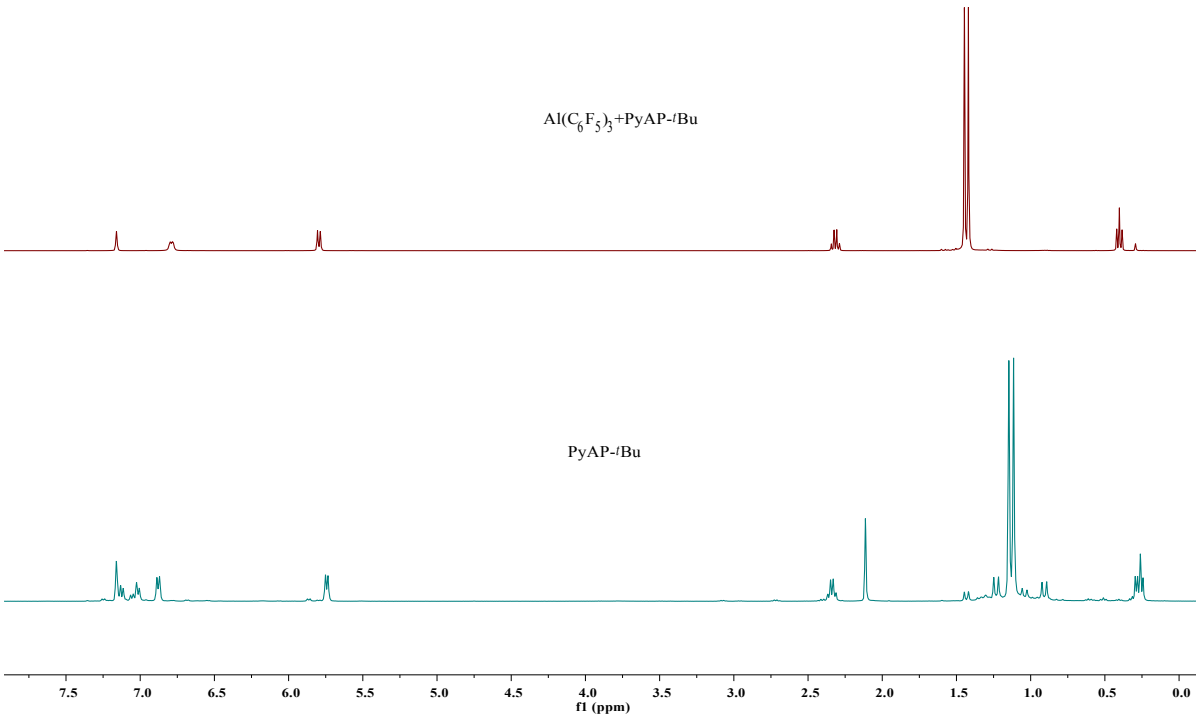

Figure S11. ^{1}H NMR spectrum for reaction of PyAP-^{t}Bu with $Al(C_6F_5)_3$ (400 MHz, C_6D_6, 298 K)

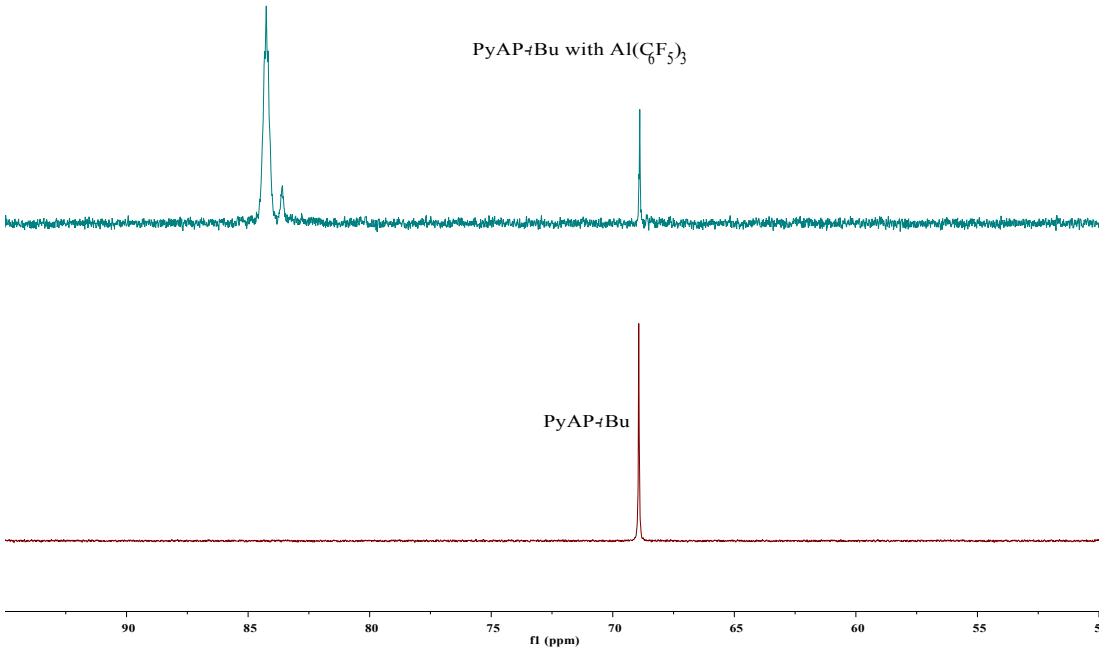

Figure S12. $^{31}P\{^{1}H\}$ NMR spectrum for reaction of PyAP-*t*Bu with $Al(C_6F_5)_3$ (162 MHz, C_6D_6, 298 K)

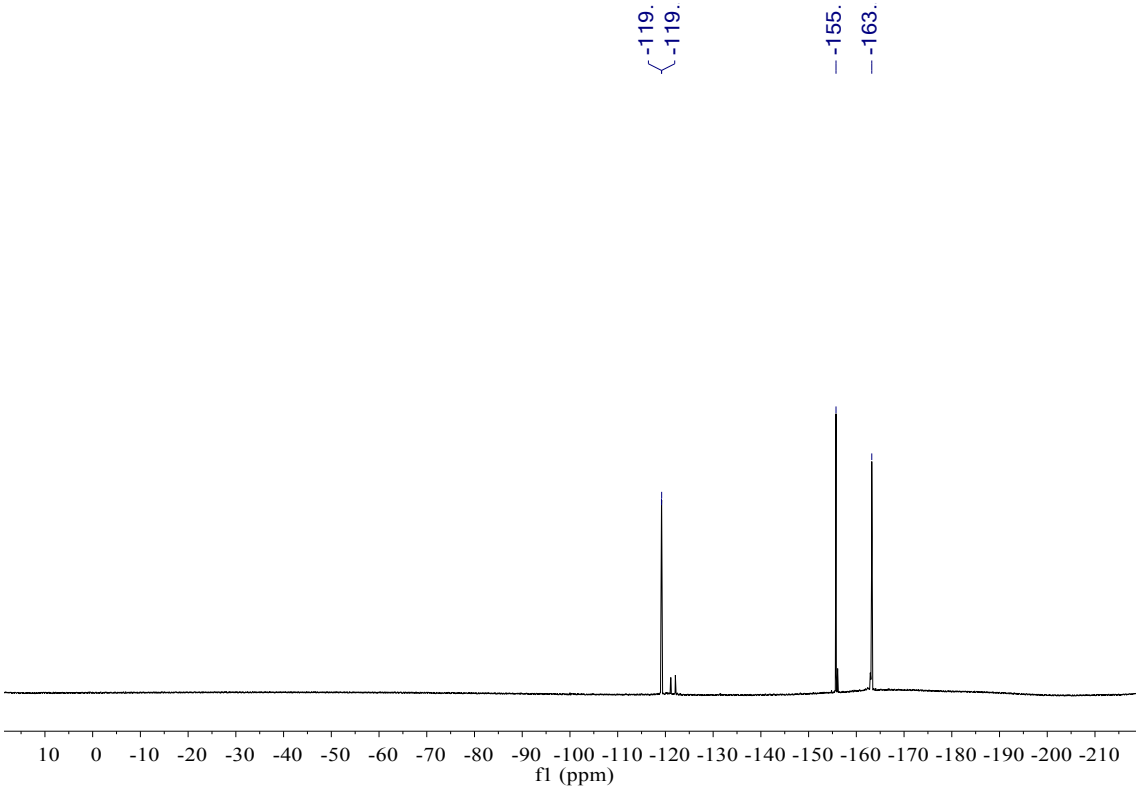

Figure S13. $^{19}F\{^{1}H\}$ NMR spectrum for reaction of PyAP-^{t}Bu with $Al(C_6F_5)_3$ (376 MHz, C_6D_6, 298 K)

2.2 Stoichiometric NMR Reaction of PyAP-Cy with ^{i}BuAl(BHT)$_2$ in a 1:1 molar ratio

A NMR tube was charged with PyAP-Cy (7.6 mg, 0.024 mmol) and 0.3 mL of C_6D_6. A solution of ^{i}BuAl(BHT)$_2$ (12.5 mg, 0.024 mmol) , 0.3 mL C_6D_6 was added to this tube via pipette at ambient temperature, and the mixture was allowed to react for 5 min before analyzed by NMR spectroscopy.

Formation of FLP was indicated by $^{31}P\{^{1}H\}$ NMR spectroscopy.

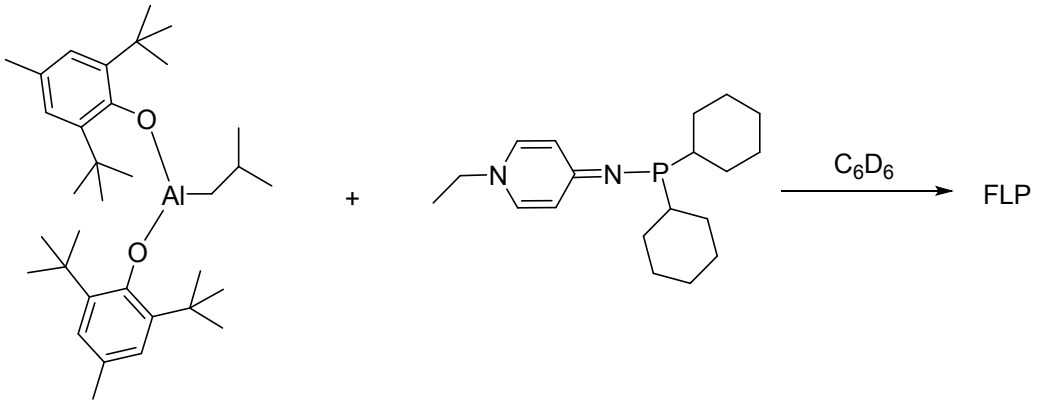

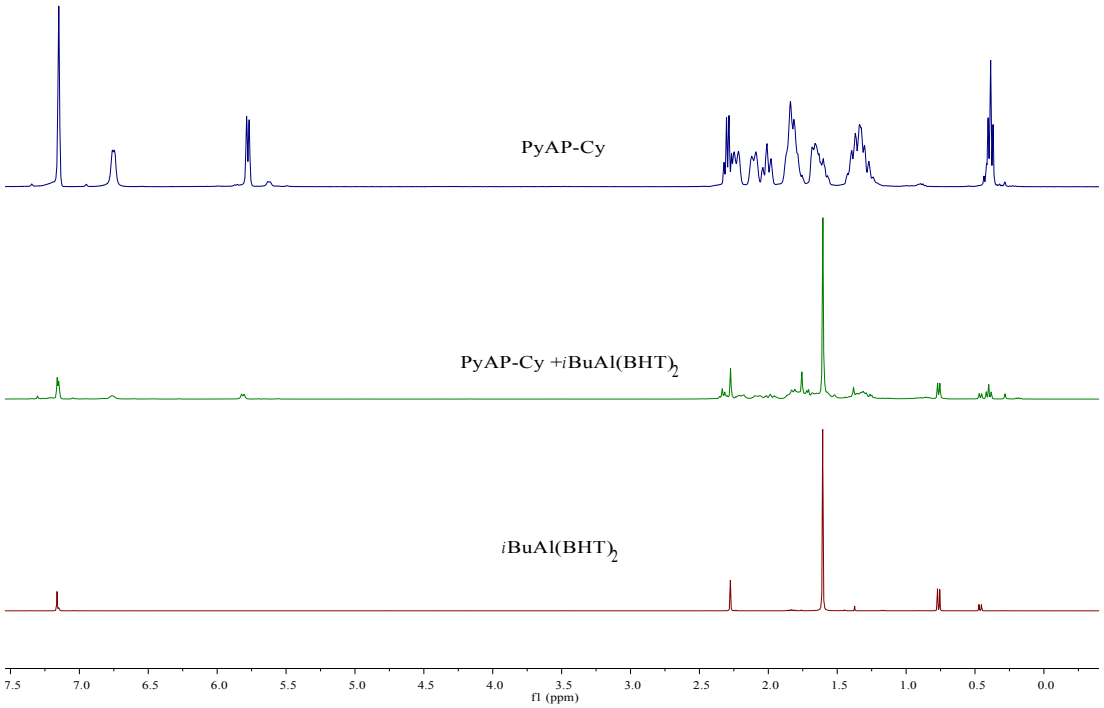

Figure S14. ^{1}H NMR spectrum for reaction of PyAP-Cy with $^{i}BuAl(BHT)_2$ (400 MHz, C_6D_6, 298 K)

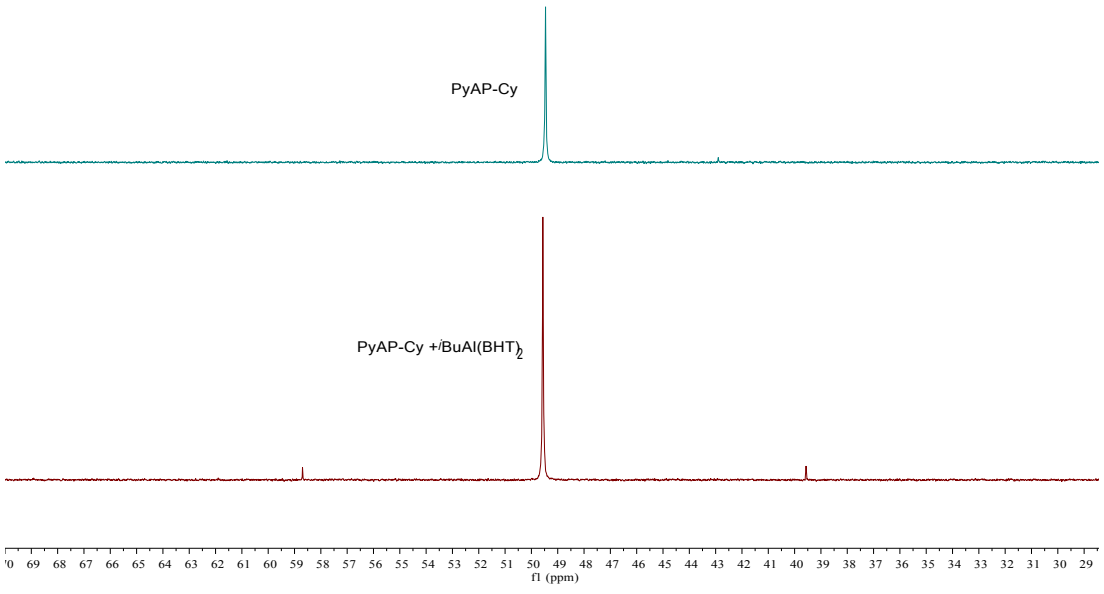

Figure S15. $^{31}P\{^{1}H\}$ NMR spectrum for reaction of PyAP-Cy with $^{i}BuAl(BHT)_2$ (162

MHz, C_6D_6, 298 K)

2.3 Stoichiometric NMR Reaction of PyAP-^{t}Bu with ^{i}BuAl(BHT)$_2$ in a 1:1 molar ratio

A NMR tube was charged with PyAP-^{t}Bu (6.4 mg, 0.024 mmol) and 0.3 mL of C_6D_6. A solution of ^{i}BuAl(BHT)$_2$ (12.5 mg, 0.024 mmol) , 0.3 mL C_6D_6 was added to this tube via pipette at ambient temperature, and the mixture was allowed to react for 5 min before analyzed by NMR spectroscopy. **PyAP-^{t}Bu**.

Formation of FLP was indicated by $^{31}P\{^1H\}$ NMR spectroscopy.

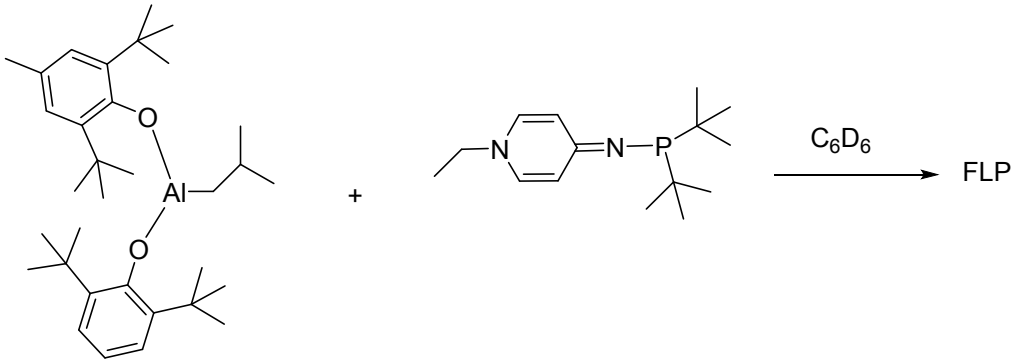

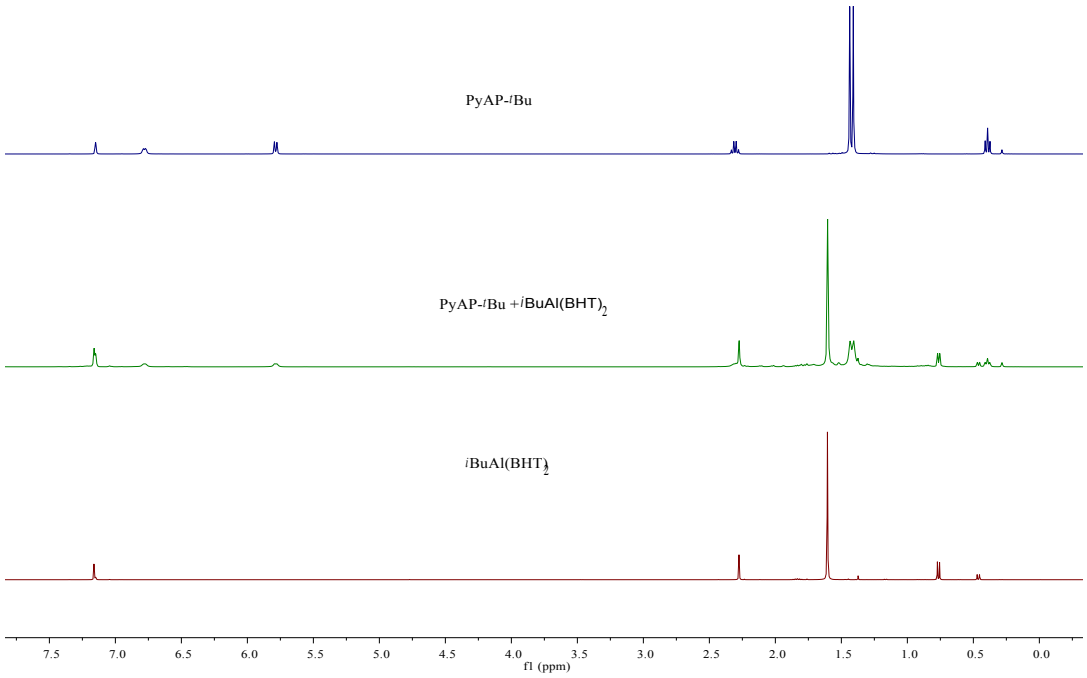

Figure S16. ^{1}H NMR spectrum for reaction of PyAP-^{t}Bu with ^{i}BuAl(BHT)$_2$ (400 MHz, C_6D_6, 298 K)

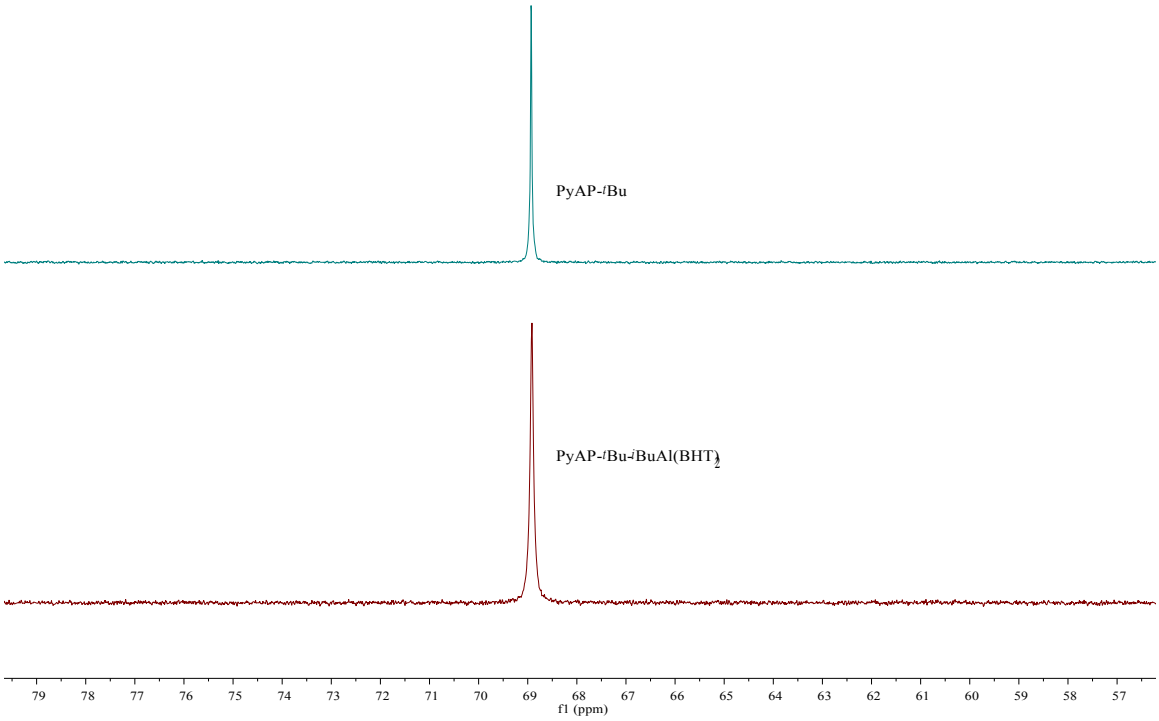

Figure S17. $^{31}P\{^{1}H\}$ NMR spectrum for reaction of PyAP-^{t}Bu with ^{i}BuAl(BHT)$_2$ (162 MHz, C_6D_6, 298 K)

2.4 Stoichiometric NMR Reaction of PyAP-^{i}P*r* with ^{i}BuAl(BHT)$_2$ in a 1:1 molar ratio

A NMR tube was charged with PyAP-^{i}P*r* (7.1 mg, 0.03 mmol) and 0.3 mL of C_6D_6. A solution of ^{i}BuAl(BHT)$_2$ (15.7 mg, 0.03 mmol) , 0.3 mL C_6D_6 was added to this tube via pipette at ambient temperature, and the mixture was allowed to react for 5 min before analyzed by NMR spectroscopy.

Formation of FLP was indicated by $^{31}P\{^{1}H\}$ NMR spectroscopy.

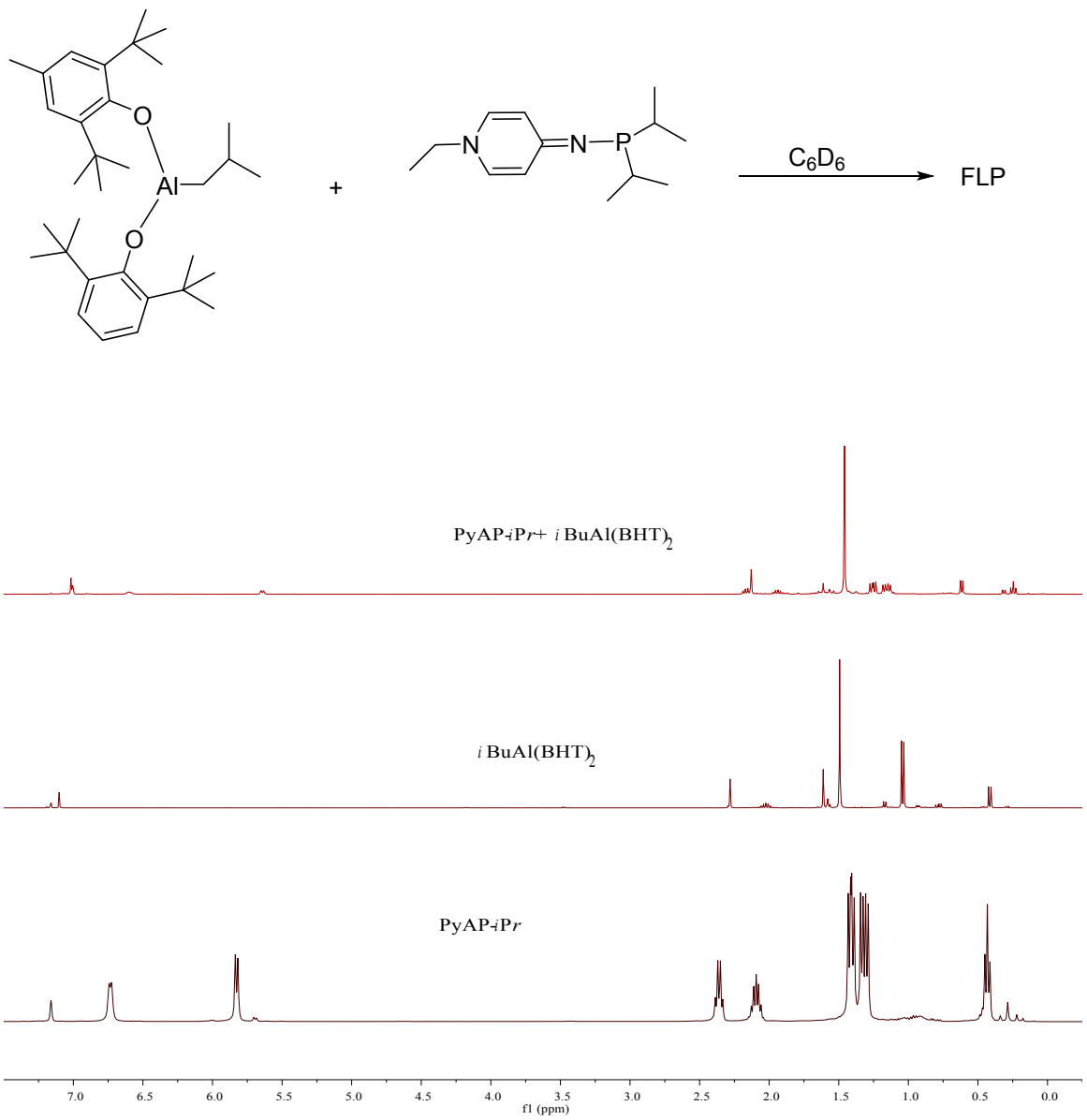

Figure S18. ^{1}H NMR spectrum for reaction of PyAP-^{i}P*r* with ^{i}BuAl(BHT)$_2$ (400 MHz, C_6D_6, 298 K)

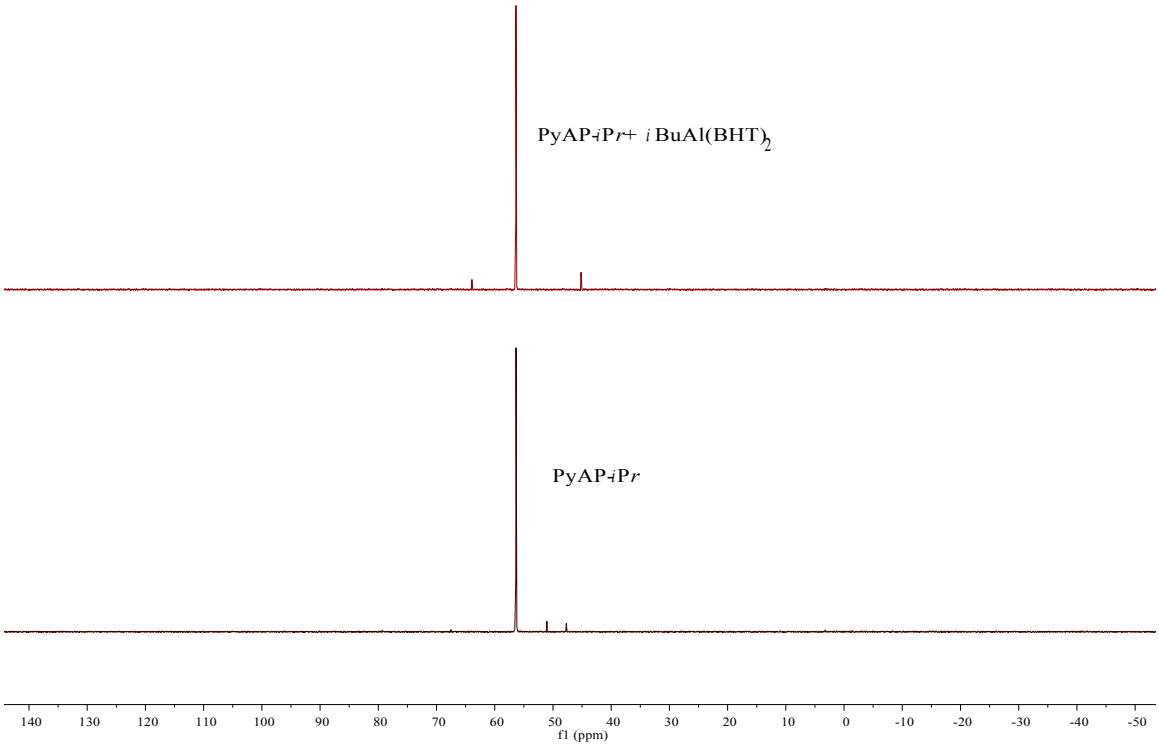

Figure S19. $^{31}P\{^{1}H\}$ NMR spectrum for reaction of PyAP-^{i}P*r* with ^{i}BuAl(BHT)$_2$ (162 MHz, C_6D_6, 298 K)

2.5 Stoichiometric NMR Reaction of PyAP-Ph with ^{i}BuAl(BHT)$_2$ in a 1:1 molar ratio

A NMR tube was charged with PyAP-Ph (9.2 mg, 0.03 mmol) and 0.3 mL of C_6D_6. A solution of ^{i}BuAl(BHT)$_2$ (15.7 mg, 0.03 mmol), 0.3 mL C_6D_6 was added to this tube via pipette at ambient temperature, and the mixture was allowed to react for 5 min before analyzed by NMR spectroscopy.

Free dissociated species and unidentified species mixture formed, which were indicated by $^{31}P\{^{1}H\}$ NMR spectroscopy.

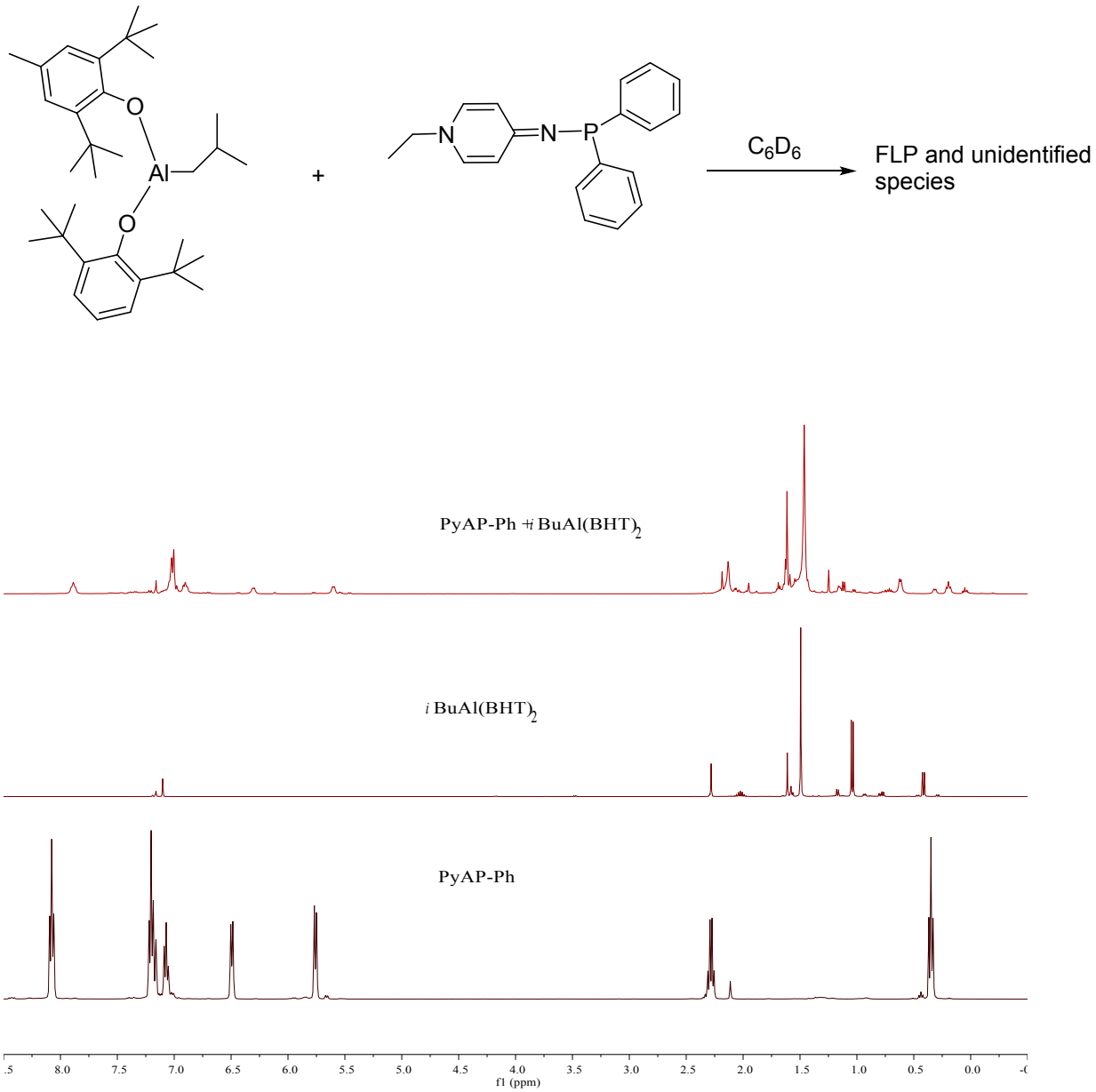

Figure S20. ^{1}H NMR spectrum for reaction of PyAP-Ph with ^{i}BuAl(BHT)$_2$ (400 MHz, C_6D_6, 298 K)

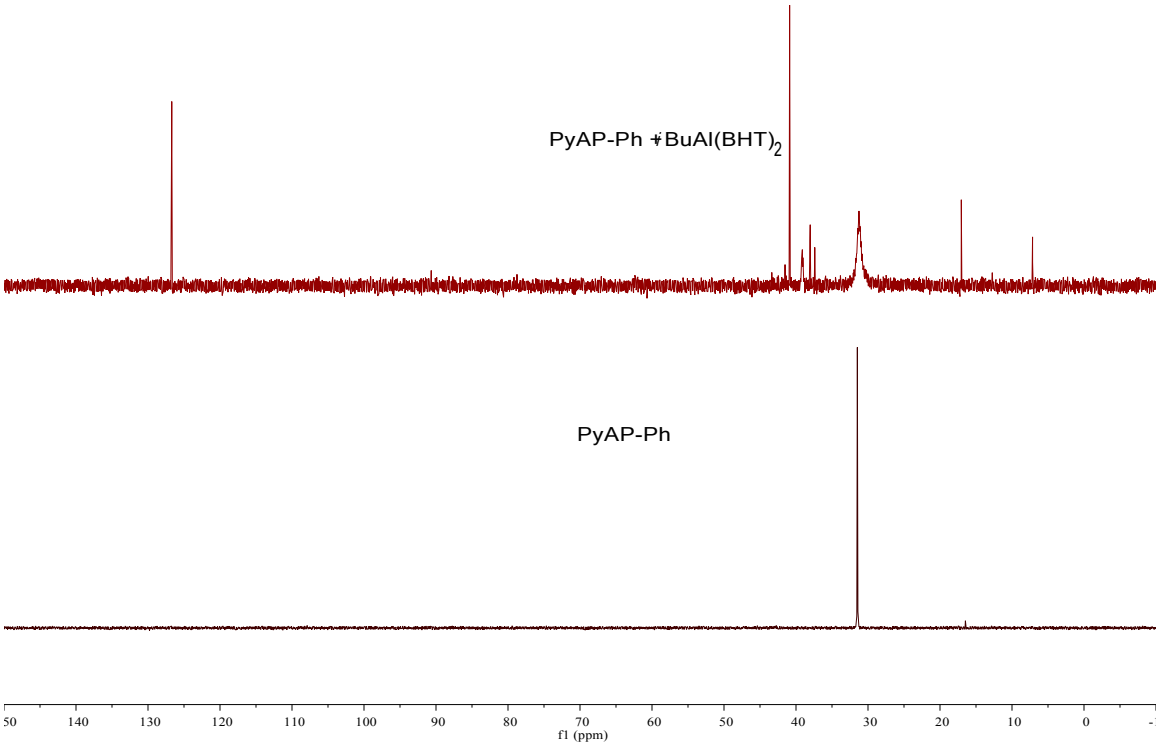

Figure S21. $^{31}P\{^{1}H\}$ NMR spectrum for reaction of PyAP-Ph with $^{i}BuAl(BHT)_2$ (162 MHz, C_6D_6, 298 K)

2.6 Stoichiometric NMR Reaction of PyAP-Cy with $MeAl(BHT)_2$ in a 1:1 molar ratio

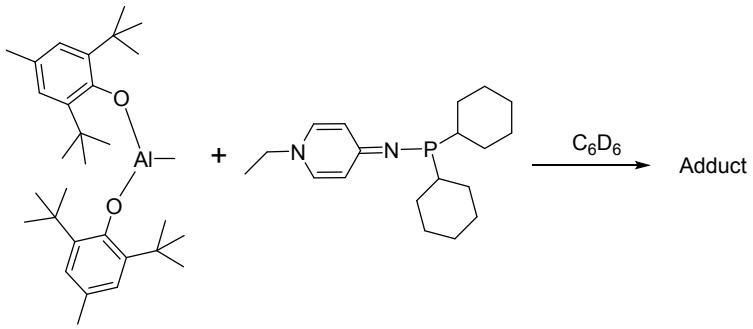

A NMR tube was charged with PyAP-Cy (9.6 mg, 0.03 mmol) and 0.3 mL of C_6D_6. A solution of $MeAl(BHT)_2$ (14 mg, 0.03 mmol) , 0.3 mL C_6D_6 was added to this tube via pipette at ambient temperature, and the mixture was allowed to react for 5 min before analyzed by NMR spectroscopy.

Associated species and dissociated species were formed, which were indicated by $^{31}P\{^{1}H\}$ NMR spectroscopy. The molar ratio of associated species to FLP is 2.5/1.

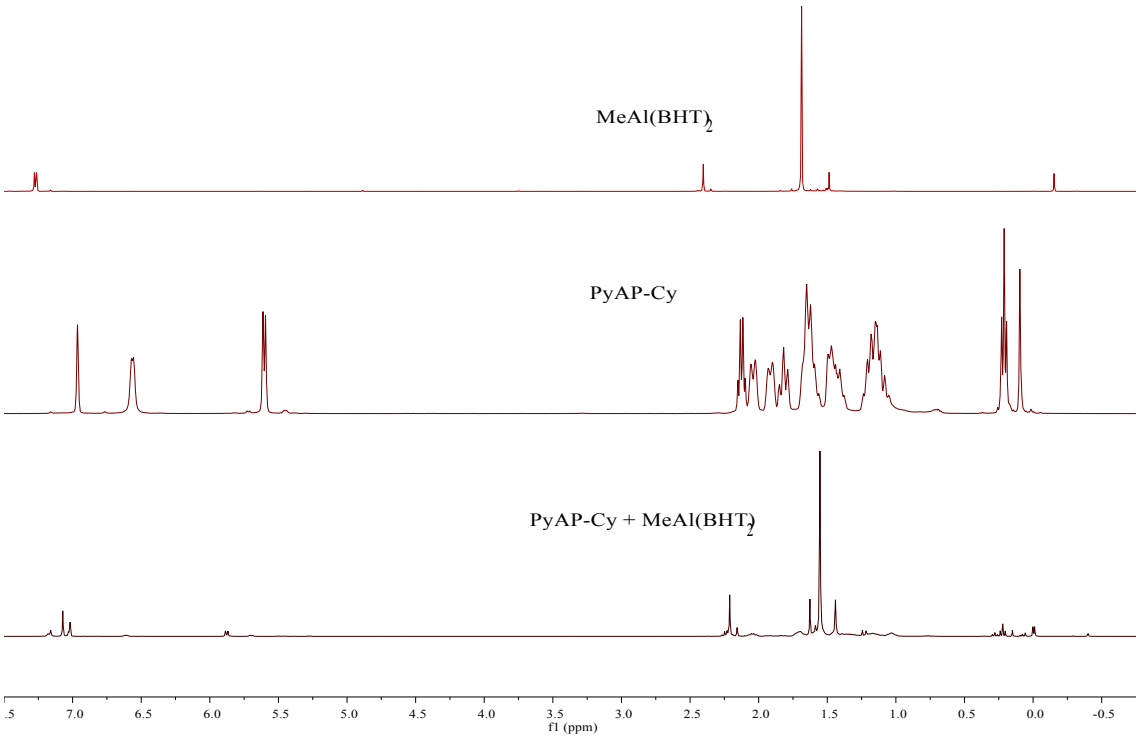

Figure S22. ^{1}H NMR spectrum for reaction of PyAP-Cy with MeAl(BHT)$_2$ (400 MHz, C_6D_6, 298 K)

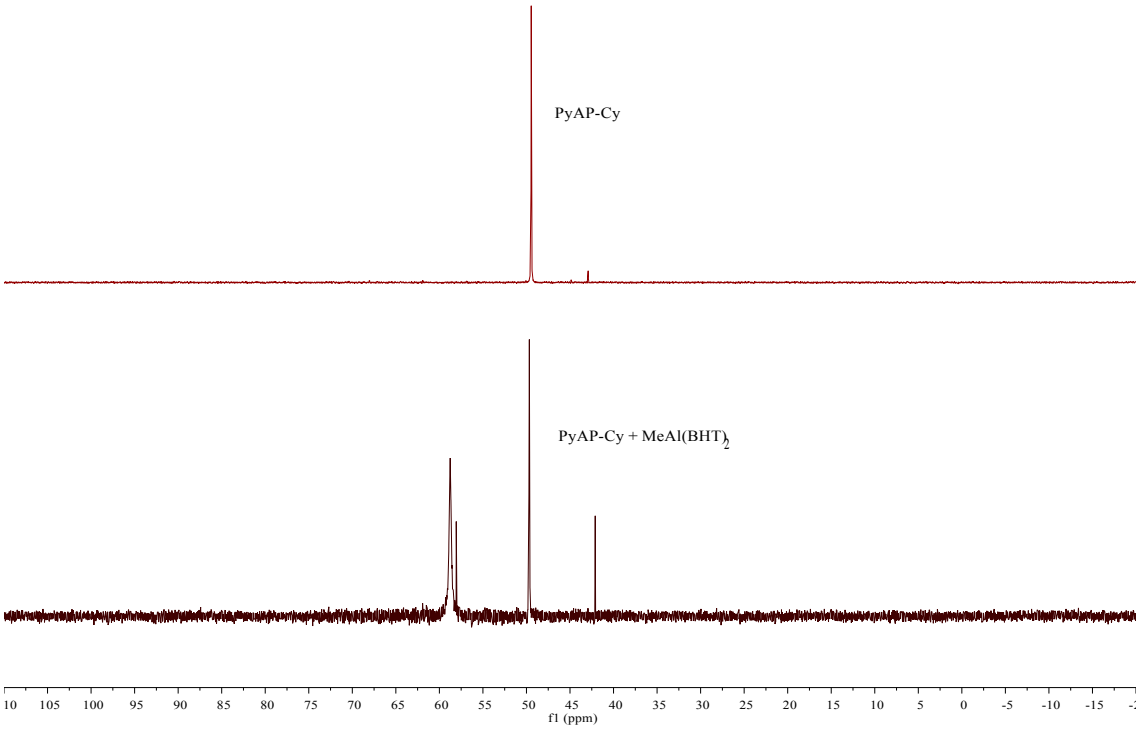

Figure S23. $^{31}P\{^{1}H\}$ NMR spectrum for reaction of PyAP-Cy with $MeAl(BHT)_2$ (162 MHz, C_6D_6, 298 K)

2.7 Stoichiometric NMR Reaction of PyAP-^{t}Bu with $MeAl(BHT)_2$ in a 1:1 molar ratio

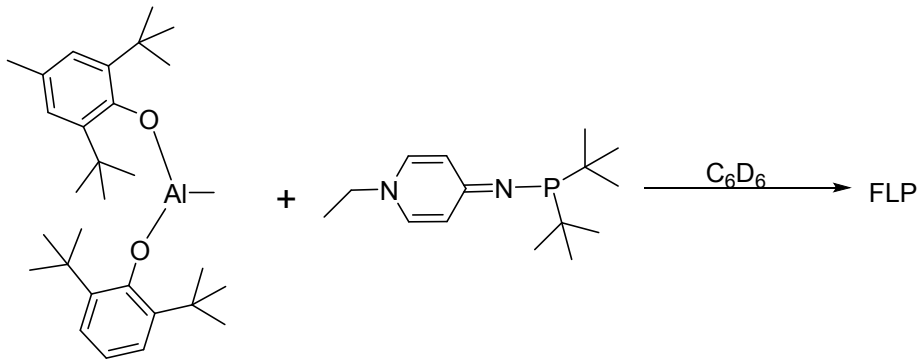

A NMR tube was charged with PyAP-^{t}Bu (8 mg, 0.03 mmol) and 0.3 mL of C_6D_6. A solution of $MeAl(BHT)_2$ (14 mg, 0.03 mmol), 0.3 mL C_6D_6 was added to this tube via pipette at ambient temperature, and the mixture was allowed to react for 5 min before analyzed by NMR spectroscopy.

Formation of FLP was indicated by $^{31}P\{^{1}H\}$ NMR spectroscopy.

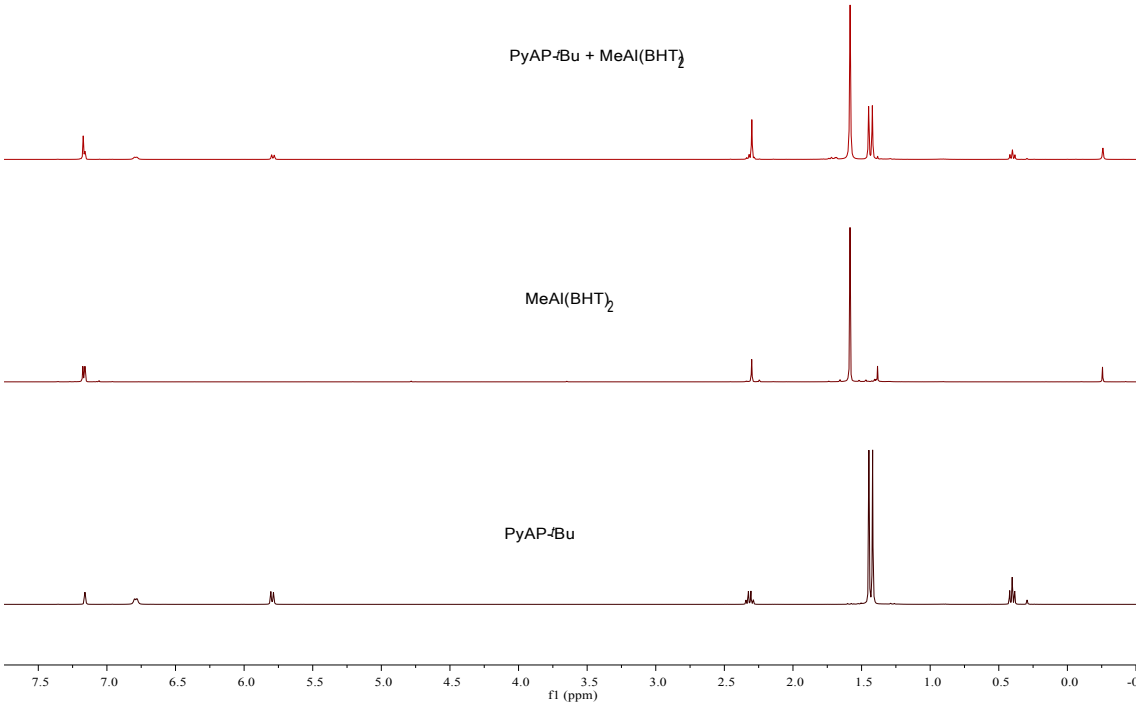

Figure S24. ^{1}H NMR spectrum for reaction of PyAP-^{t}Bu with MeAl(BHT)$_2$ (400 MHz, C_6D_6, 298 K)

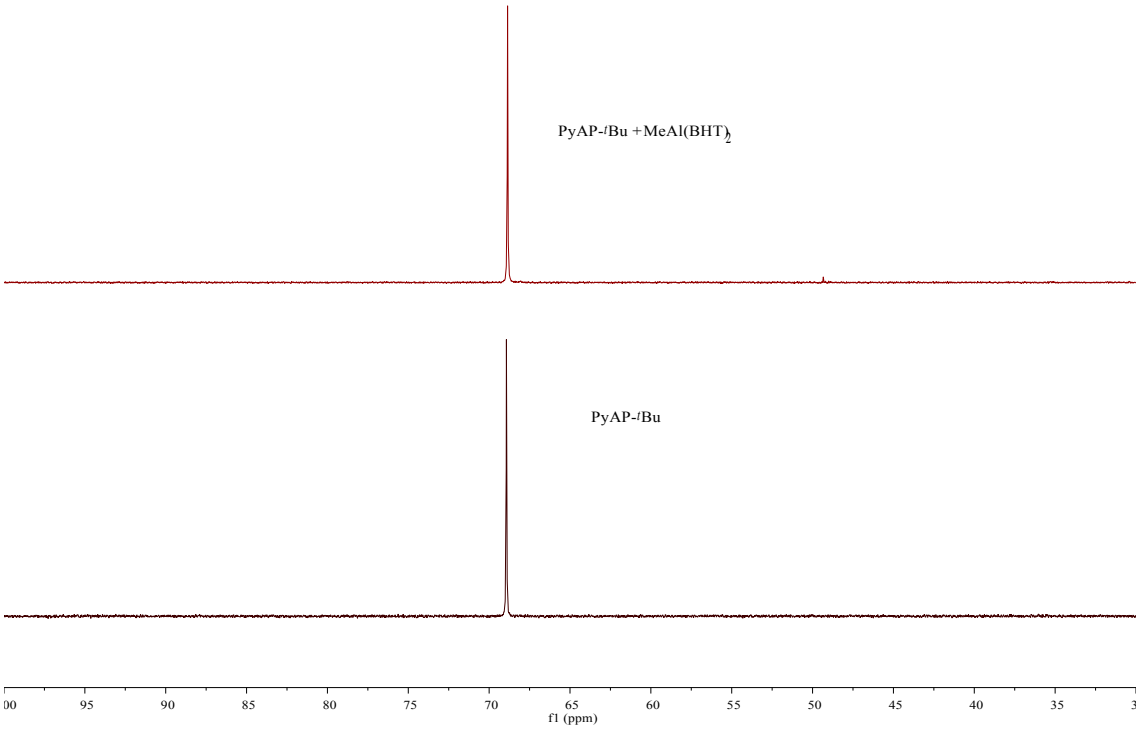

Figure S25. $^{31}P\{^{1}H\}$ NMR spectrum for reaction of PyAP-^{t}Bu with $MeAl(BHT)_2$ (162 MHz, C_6D_6, 298 K)

2.8 Stoichiometric NMR Reaction of PyAP-^{i}Pr with $MeAl(BHT)_2$ in a 1:1 molar ratio

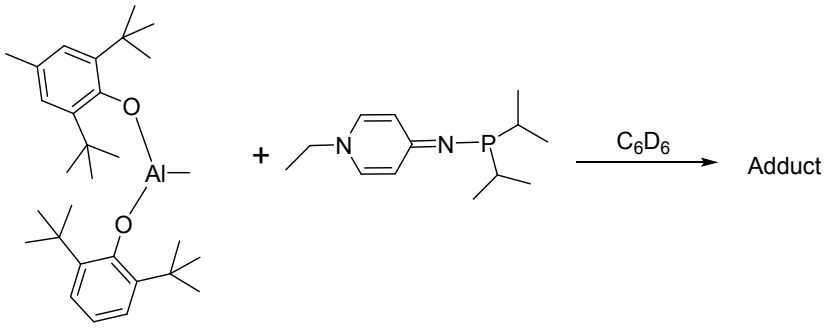

A NMR tube was charged with PyAP-^{i}Pr (7.1 mg, 0.03 mmol) and 0.3 mL of C_6D_6. A solution of $MeAl(BHT)_2$ (14 mg, 0.03 mmol) , 0.3 mL C_6D_6 was added to this tube via pipette at ambient temperature, and the mixture was allowed to react for 5 min before analyzed by NMR spectroscopy.

Associated species and dissociated species were formed, which were indicated by $^{31}P\{^{1}H\}$ NMR spectroscopy. The molar ratio of adduct to free FLP is 1/0.4.

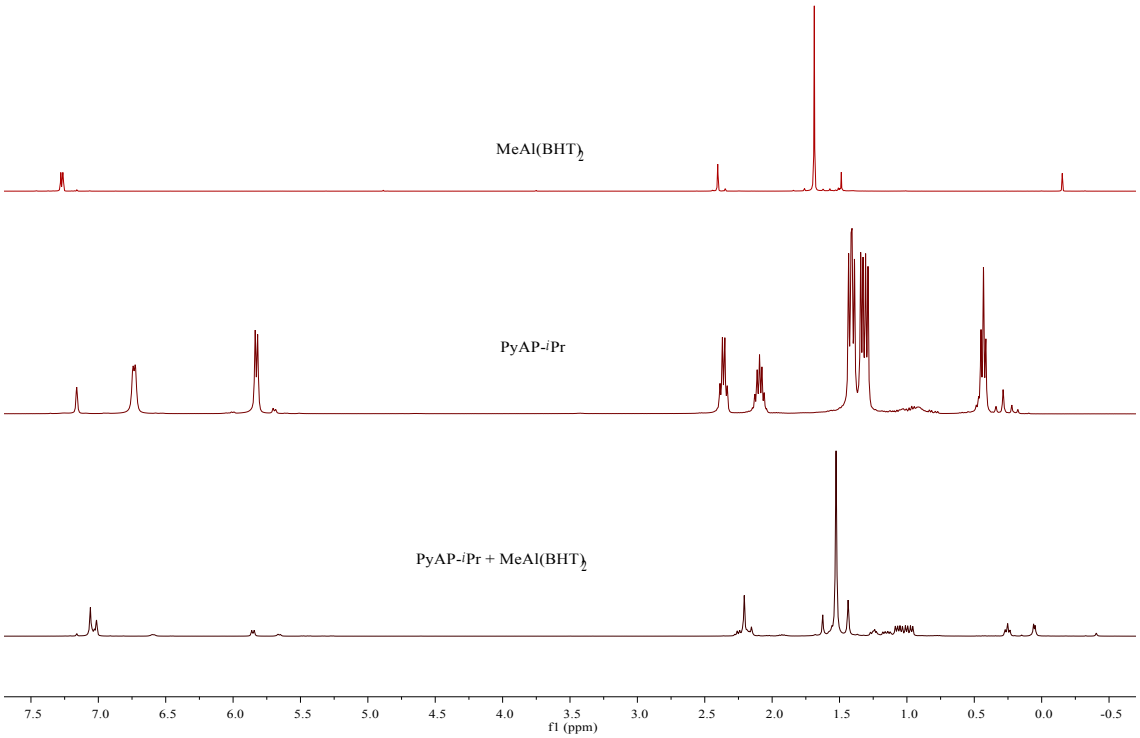

Figure S26. ^{1}H NMR spectrum for reaction of PyAP-*i*Pr with MeAl(BHT)$_2$ (400 MHz, C_6D_6, 298 K)

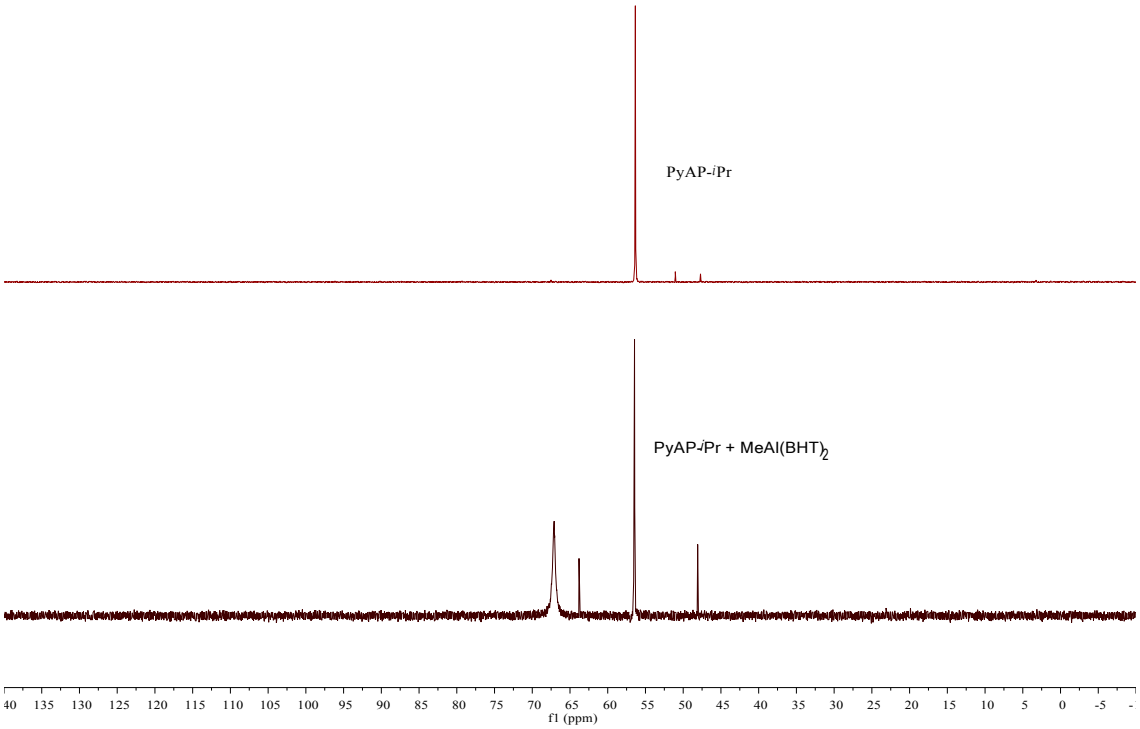

Figure S27. $^{31}P\{^{1}H\}$ NMR spectrum for reaction of PyAP-*i*Pr with $MeAl(BHT)_2$ (162 MHz, C_6D_6, 298 K)

2.9 Stoichiometric NMR Reaction of PyAP-Ph with $MeAl(BHT)_2$ in a 1:1 molar ratio

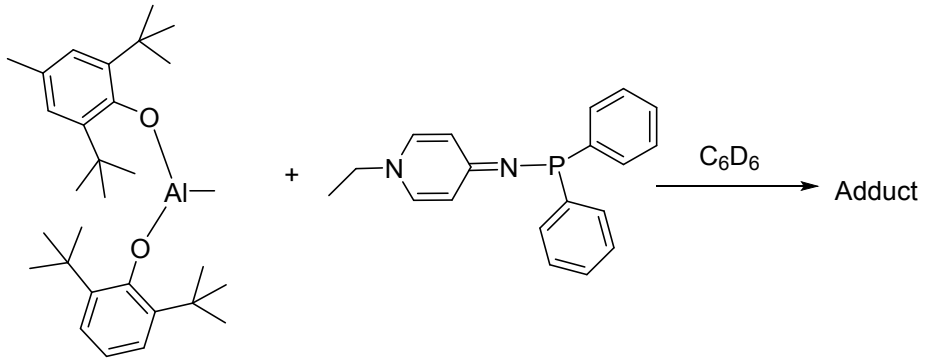

A NMR tube was charged with PyAP-Ph (9.2 mg, 0.03 mmol) and 0.3 mL of C_6D_6. A solution of $MeAl(BHT)_2$ (14 mg, 0.03 mmol) , 0.3 mL C_6D_6 was added to this tube via pipette at ambient temperature, and the mixture was allowed to react for 5 min before analyzed by NMR spectroscopy.

Formation of associated species was indicated by $^{31}P\{^{1}H\}$ NMR spectroscopy.

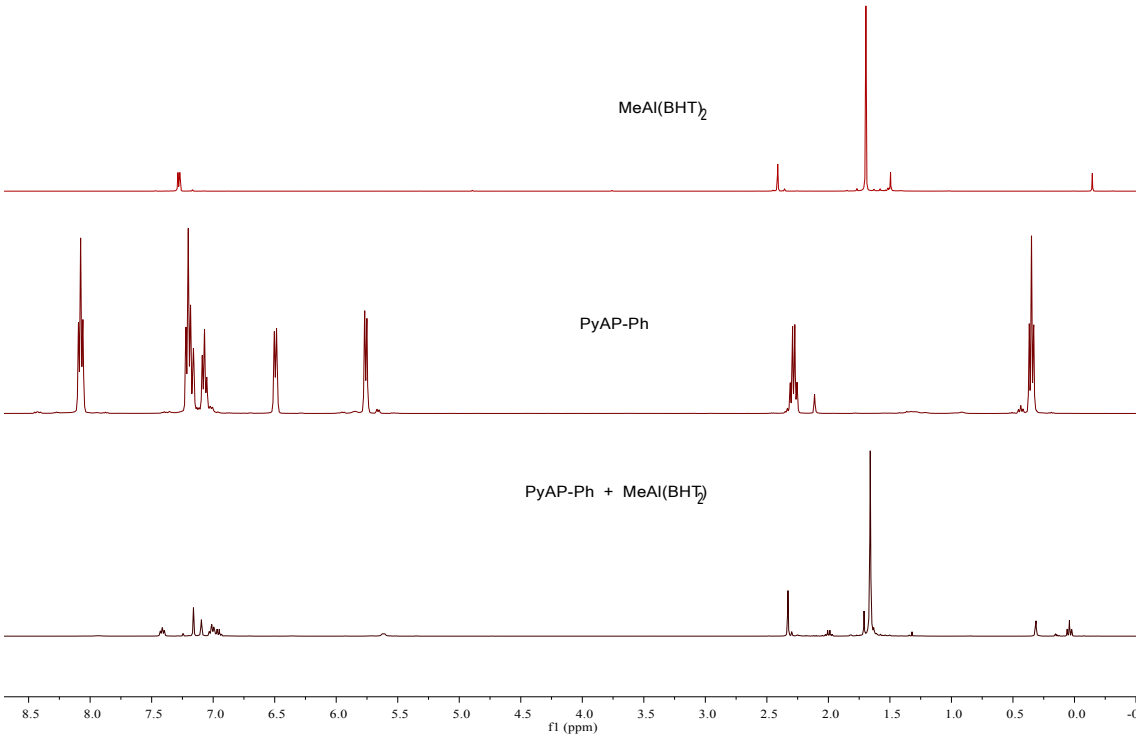

Figure S28. ^{1}H NMR spectrum for reaction of PyAP-Ph with $MeAl(BHT)_2$ (400 MHz, C_6D_6, 298 K)

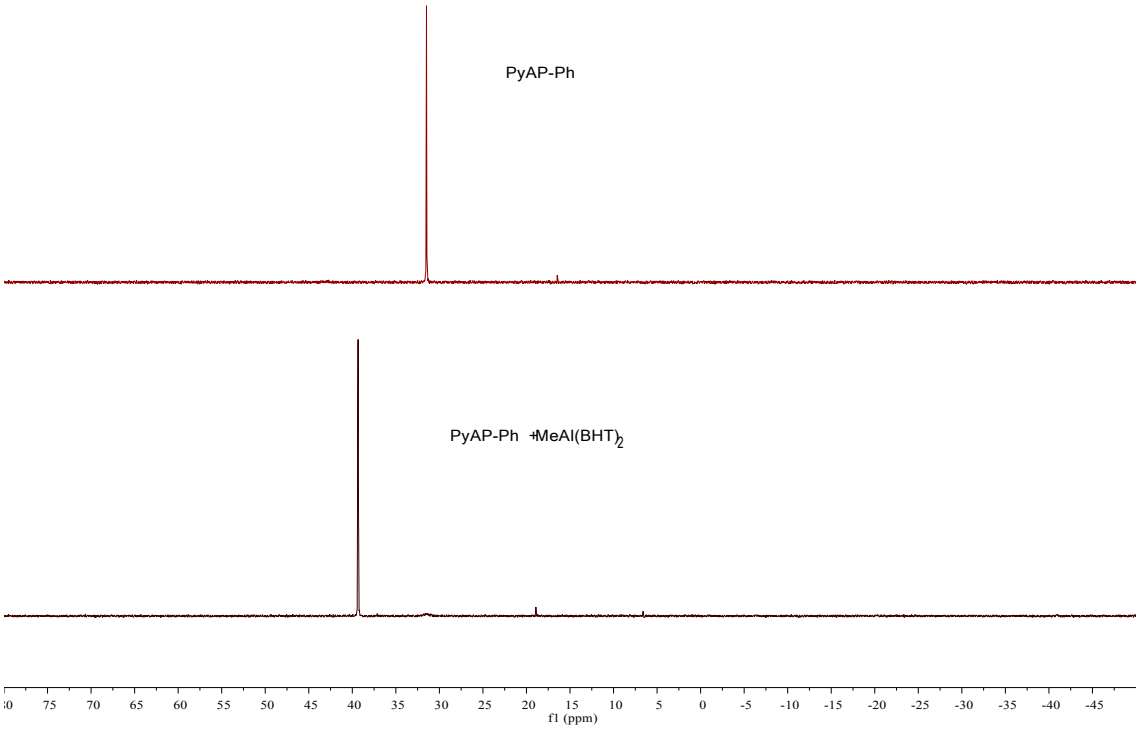

Figure S29. $^{31}P\{^{1}H\}$ NMR spectrum for reaction of PyAP-Ph with $MeAl(BHT)_2$ (162 MHz, C_6D_6, 298 K)

2.10 Stoichiometric NMR Reaction of PyAP-^{t}Bu with $Al(C_6F_5)_3$·MMA in a 1:1 molar ratio

In an argon-filled glovebox, a NMR tube was charged with 10.7 mg (0.04 mmol) of PyAP-^{t}Bu and 0.3 mL of C_6D_6. A 0.3 mL of C_6D_6 solution of $Al(C_6F_5)_3$ (22.9mg, 0.04 mmol) and 4.2 uL MMA (0.04 mmol) were slowly added to this tube via pipet at room temperature. The mixture was allowed to react for 5 min at room temperature before the NMR spectra were recorded. Zwitterionic enolaluminate was generated as two isomers (E/Z = 9:1). Only the major isomer was analyzed.

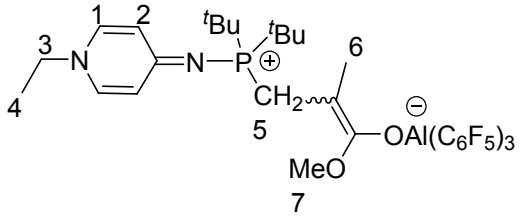

^{1}H NMR (400 MHz, C_6D_6, 298 K) δ (ppm) = 6.20 (m, 4H, 1-H, 2-H) , 3.45 (s, 3H, 7-H) , 2.56 (d, $^2J_{PH}$ = 7.0 Hz, 2H, 5-H), 2.49 (q, $^3J_{HH}$ = 7.3 Hz, 2H, 3-H), 1.43 (s, 3H, 6-H), 0.74

(d, $^3J_{PH}$ = 14.2 Hz, 18H, ^{t}Bu), 0.38 (t, $^3J_{HH}$ = 7.3 Hz, 3H, 4-H). ^{31}P {^{1}H} NMR (162 MHz, C_6D_6, 298 K) δ (ppm) = 45.9 (s).

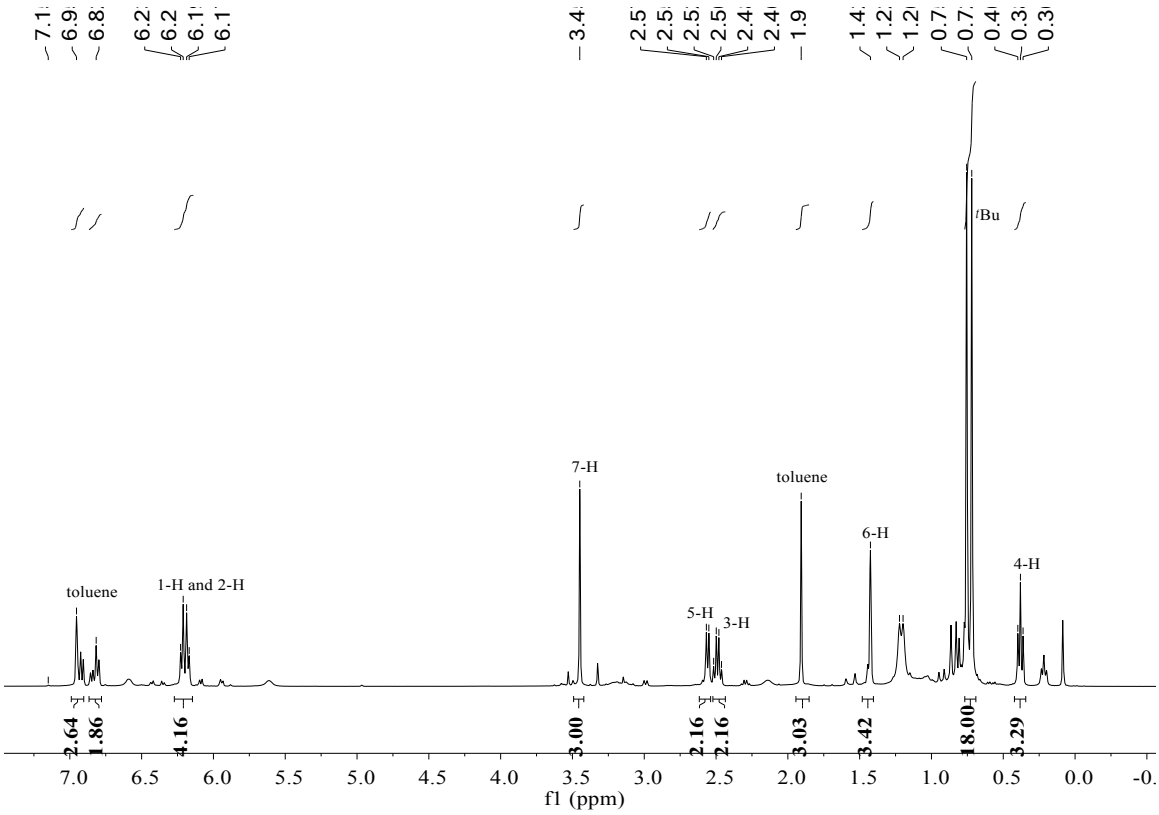

Figure S30. ^{1}H NMR spectrum for reaction of PyAP-^{t}Bu with Al(C_6F_5)$_3$·MMA (400 MHz, C_6D_6, 298 K) (9:1 mixture of isomer, only the major isomer was marked for clarity).

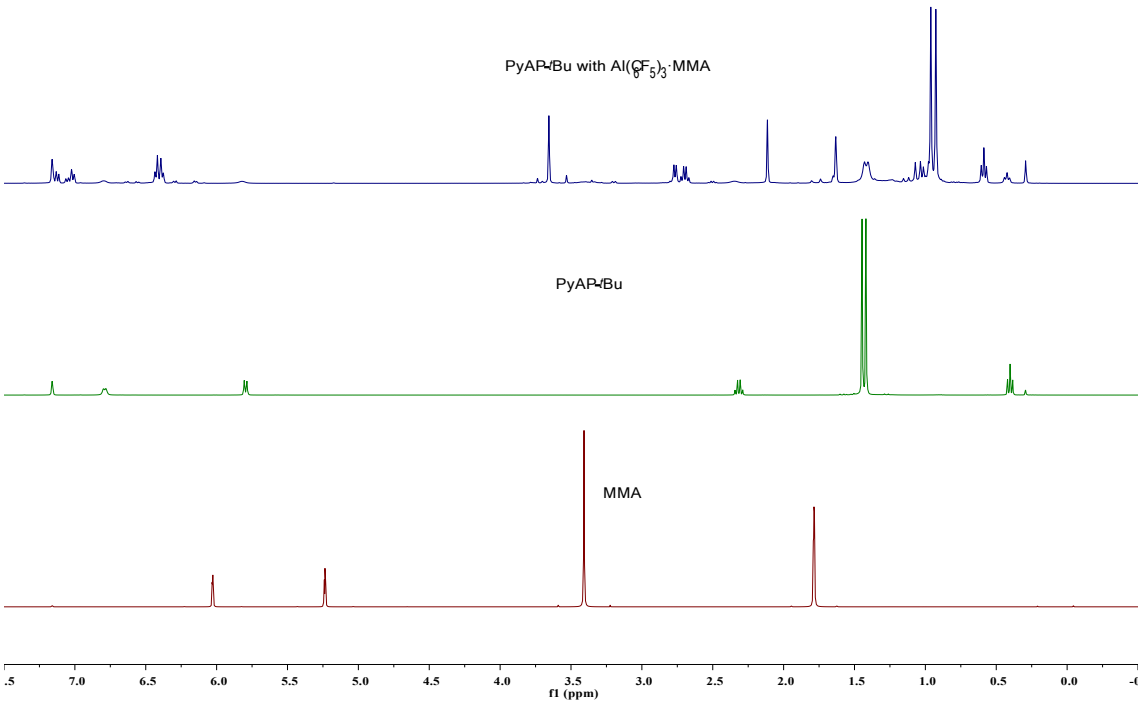

Figure S31. Stacked ^{1}H NMR spectra for reaction of PyAP-*t*Bu with $Al(C_6F_5)_3 \cdot MMA$ (400 MHz, C_6D_6, 298 K)

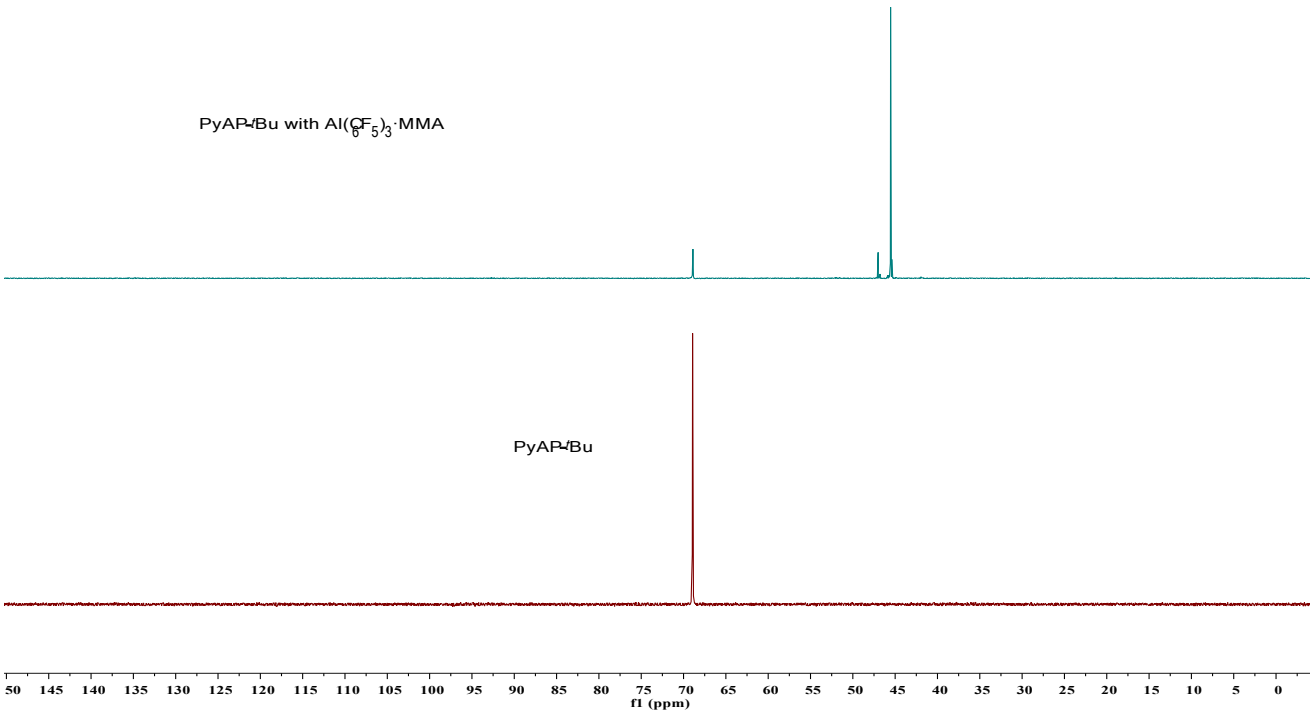

Figure S32. $^{31}P\{^{1}H\}$ NMR spectrum for reaction of PyAP-^{t}Bu with $Al(C_6F_5)_3$·MMA (162 MHz, C_6D_6, 298 K)

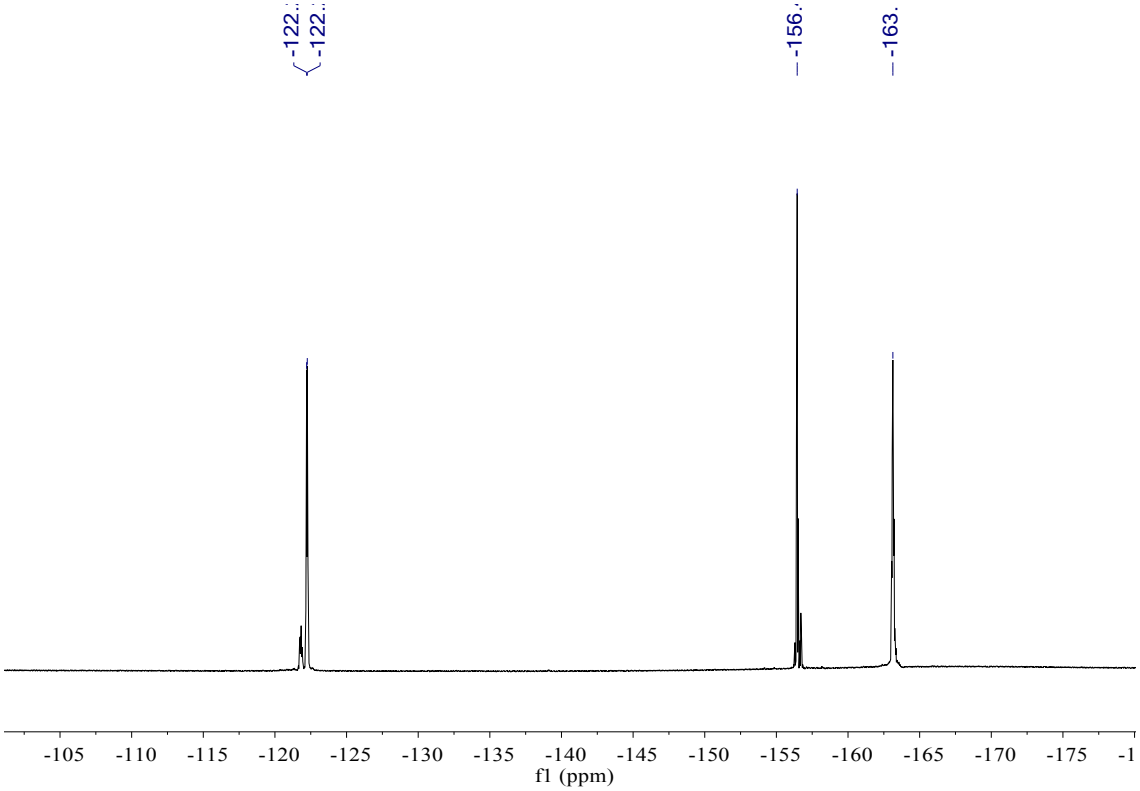

Figure S33. $^{19}F\{^{1}H\}$ NMR spectrum for reaction of PyAP-^{t}Bu with $Al(C_6F_5)_3$ (376 MHz, C_6D_6, 298 K)

2.11 Stoichiometric NMR Reaction of PyAP-Cy with $MeAl(BHT)_2$ ·MMA in a 1:1 ratio

In an argon-filled glovebox, a NMR tube was charged with 12.7 mg (0.04 mmol) of PyAP-Cy and 0.3 mL of C_6D_6. A 0.3 mL C_6D_6 solution of $MeAl(BHT)_2$ (18.7 mg, 0.04 mmol) and 4.2 uL MMA (0.04 mmol) were slowly added to this tube via pipet at room temperature. The mixture was allowed to react for 5 min at room temperature before the NMR spectra were recorded. Zwitterionic enolaluminate was generated as two isomers (E/Z = 9:1). Only the major isomer was analyzed.

^{1}H NMR (400 MHz, C_6D_6, 298 K) δ (ppm) = 7.26 (s, 4H, BHT-phenyl), 6.53 (d, 2H, $^{3}J_{HH}$ = 7.3 Hz, 1-H), 6.08 (d, 2H, $^{3}J_{HH}$ = 7.3 Hz, 2-H), 3.61 (s, 3H, 7-H) , 2.52 (q, $^{3}J_{HH}$ = 7.3 Hz, 2H, 3-H), 2.37 (d, $^{2}J_{PH}$ = 7.0 Hz, 2H, 5-H), 2.31 (s, 6H, BHT-Me), 1.85 (s, 39H, BHT-^{t}Bu and 6-H), 1.00-1.60 (m, 22H, Cy), 0.45 (t, $^{3}J_{HH}$ = 7.3 Hz, 3H, 4-H), 0.27 (s, 3H, Al-Me).

^{31}P $\{^{1}H\}$ NMR (162 MHz, C_6D_6, 298 K) δ (ppm) = 36.8 (s).

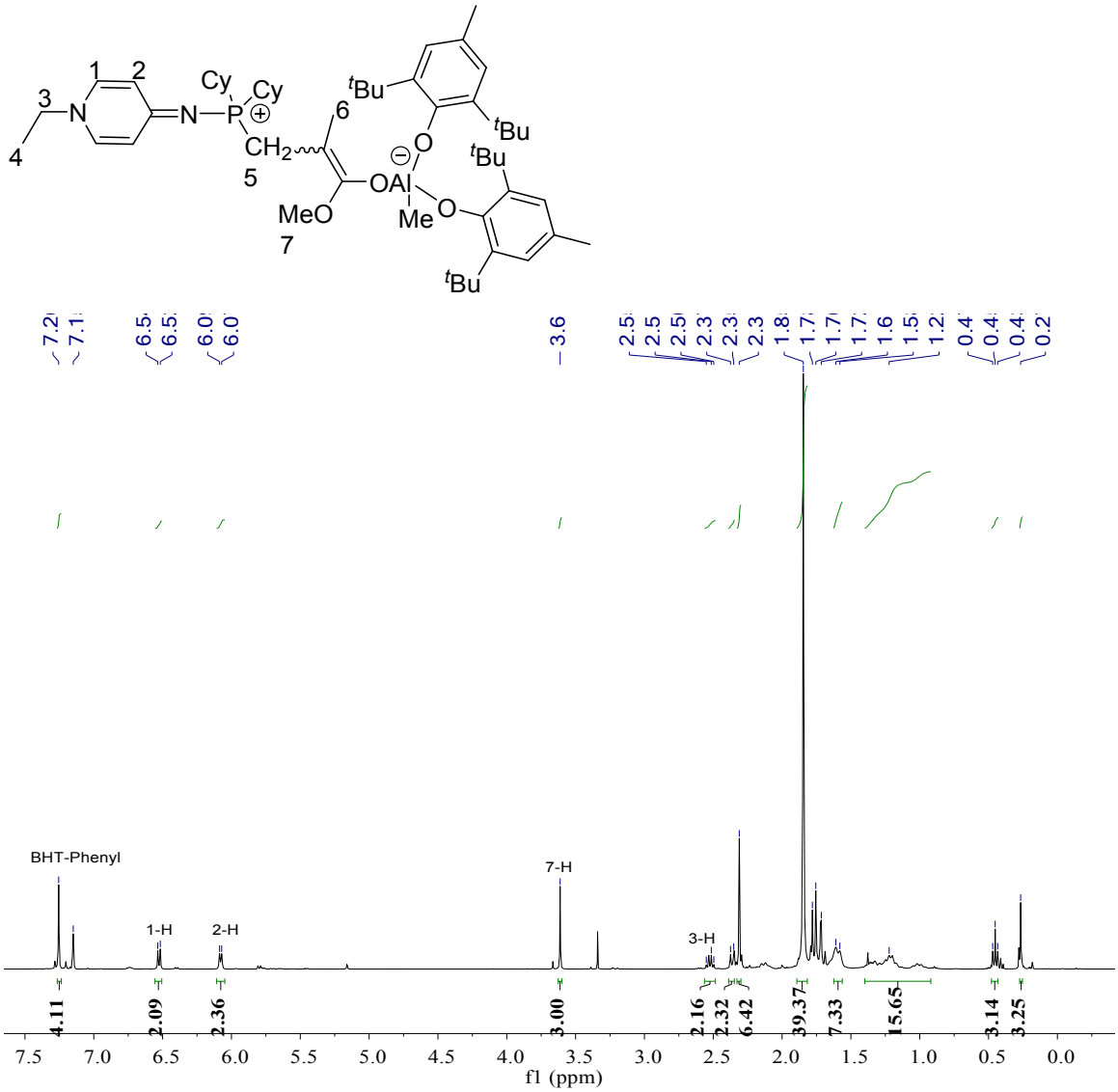

Figure S34. ^{1}H NMR spectrum for reaction of PyAP-Cy with $MeAl(BHT)_2$·MMA (400 MHz, C_6D_6, 298 K) (9:1 mixture of isomer, only the major isomer was marked for clarity).

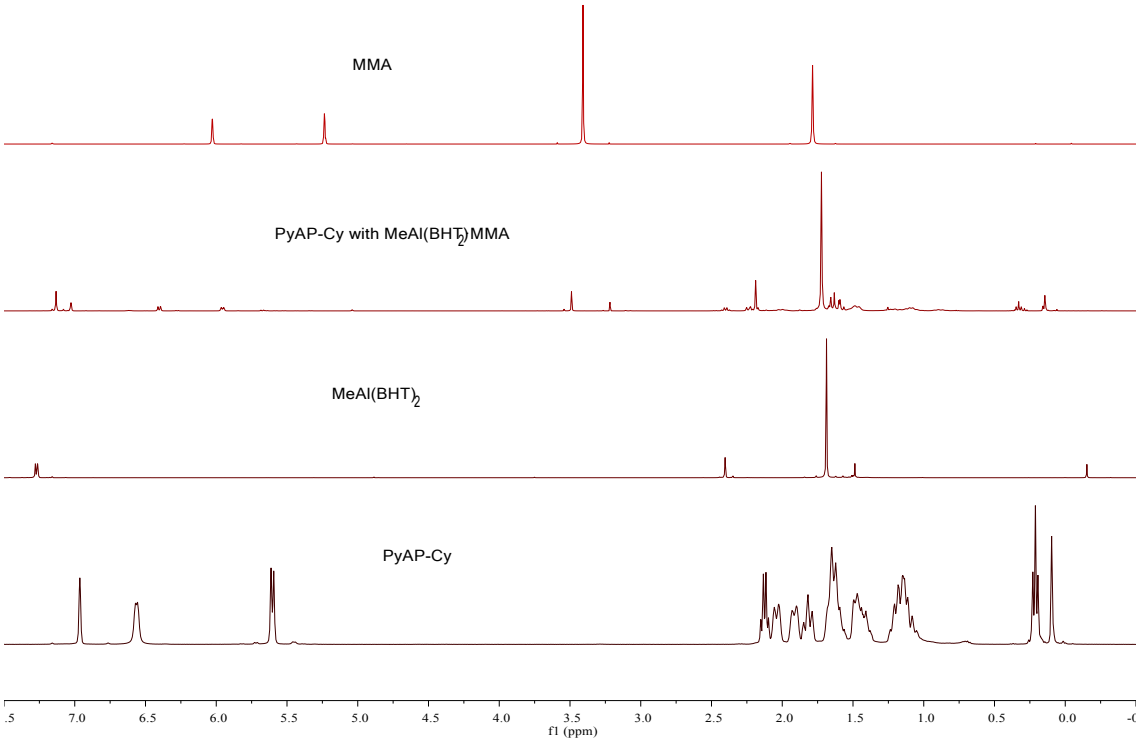

Figure S35. Stacked ^{1}H NMR spectra for reaction of PyAP-Cy with MeAl(BHT)$_2$·MMA (400 MHz, C_6D_6, 298 K)

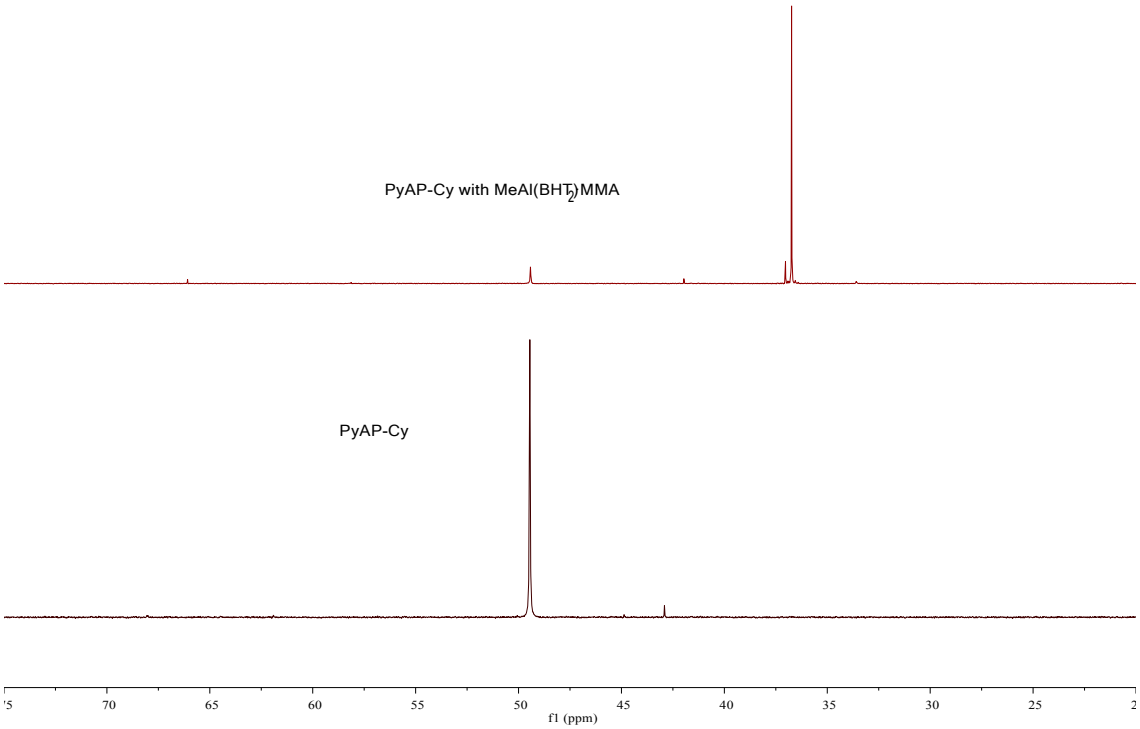

Figure S36. $^{31}P\{^{1}H\}$ NMR spectrum for reaction of PyAP-Cy with $MeAl(BHT)_2 \cdot MMA$ (162 MHz, C_6D_6, 298 K)

2.12 Stoichiometric NMR Reaction of PyAP-^{t}Bu with $MeAl(BHT)_2 \cdot MMA$ in a 1:1 molar ratio

In an argon-filled glovebox, a NMR tube was charged with 10.7 mg (0.04 mmol) of PyAP-^{t}Bu and 0.3 mL of C_6D_6. A 0.3 mL C_6D_6 solution of $MeAl(BHT)_2$ (18.7 mg, 0.04 mmol) and 4.2 uL MMA (0.04 mmol) were slowly added to this tube via pipet at room temperature. The mixture was allowed to react for 5 min at room temperature before the NMR spectra were recorded. Zwitterionic enolaluminate was generated as two isomers (E/Z = 100:4). Only the major isomer was analyzed. Suitable singles crystals of INT1 were obtained from its toluene solution at -35℃ for 2 days.

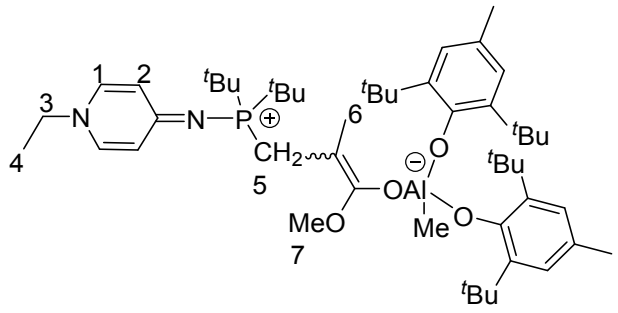

INT1

^{1}H NMR (400 MHz, C_6D_6, 298 K) δ (ppm) = 7.24 (s, 4H, BHT-phenyl), 6.49 (d, 2H, $^{3}J_{HH}$ = 7.3 Hz, 1-H), 6.12 (d, 2H, $^{3}J_{HH}$ = 7.3 Hz, 2-H), 3.71 (s, 3H, 7-H) , 2.80 (d, $^{2}J_{PH}$ = 7.0 Hz, 2H, 5-H), 2.58 (q, $^{3}J_{HH}$ = 7.3 Hz, 2H, 3-H), 2.30 (s, 6H, BHT-Me), 1.83 (s, 36H, BHT-^{t}Bu), 1.74 (s, 3H, 6-H), 1.00 (d, $^{3}J_{PH}$ = 14.1 Hz, 18H, ^{t}Bu), 0.54 (t, $^{3}J_{HH}$ = 7.3 Hz, 3H, 4-H), 0.30 (s, 3H, Al-Me). ^{31}P {^{1}H} NMR (162 MHz, C_6D_6, 298 K) δ (ppm) = 36.8 (s).

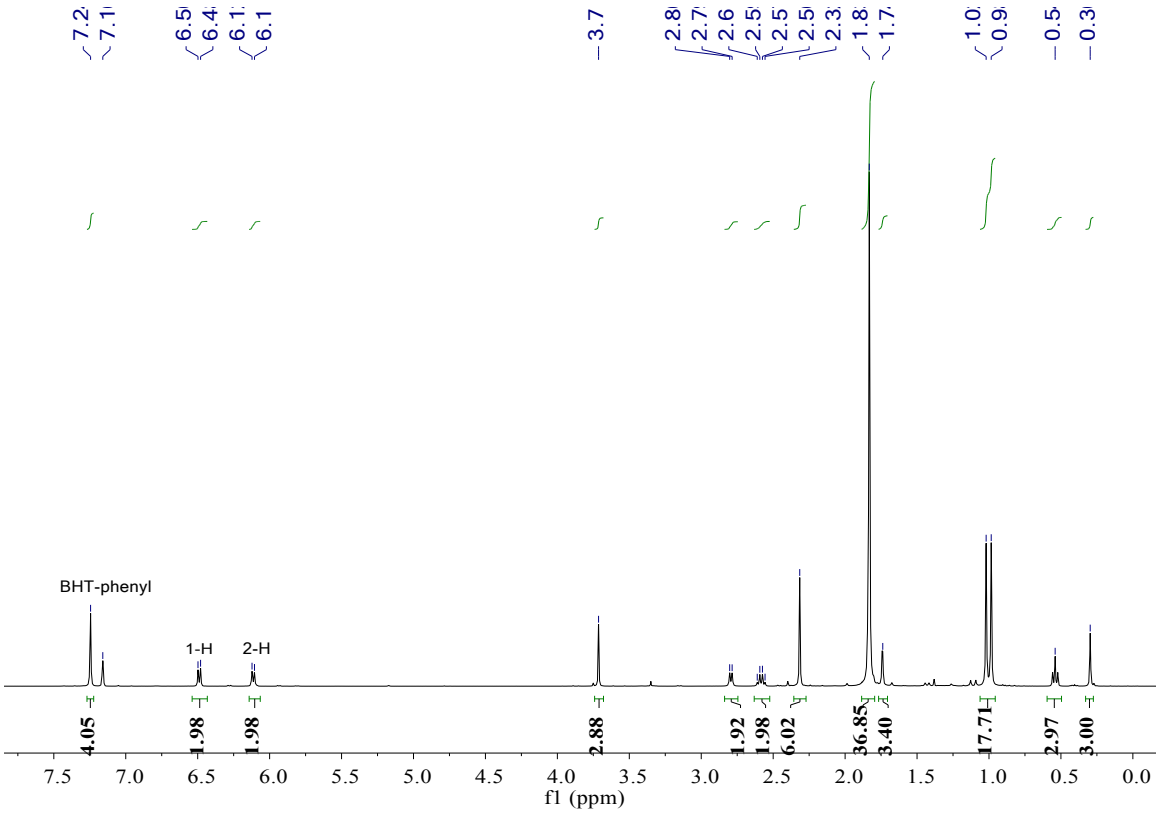

Figure S37. ^{1}H NMR spectrum for reaction of PyAP-^{t}Bu with MeAl(BHT)$_2$·MMA (400 MHz, C_6D_6, 298 K) (100:4 mixture of isomer, only the major isomer was marked for clarity).

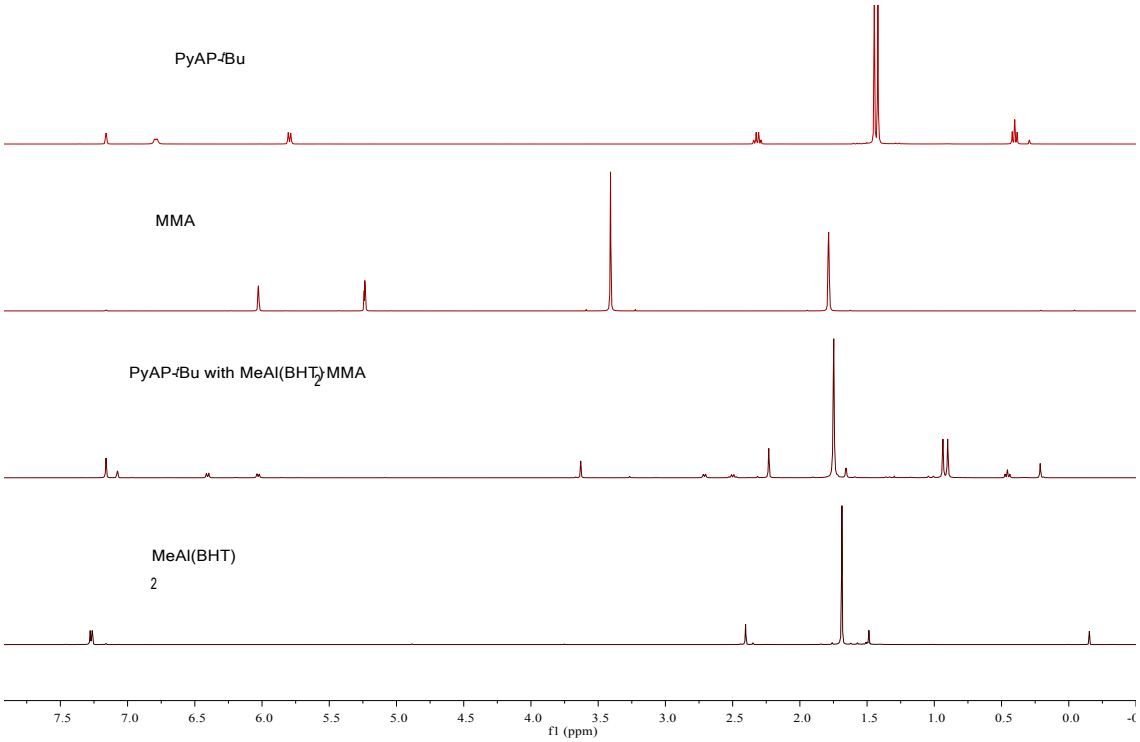

Figure S38. Stacked ^{1}H NMR spectra for reaction of PyAP-*t*Bu with MeAl(BHT)$_2$·MMA (400 MHz, C_6D_6, 298 K)

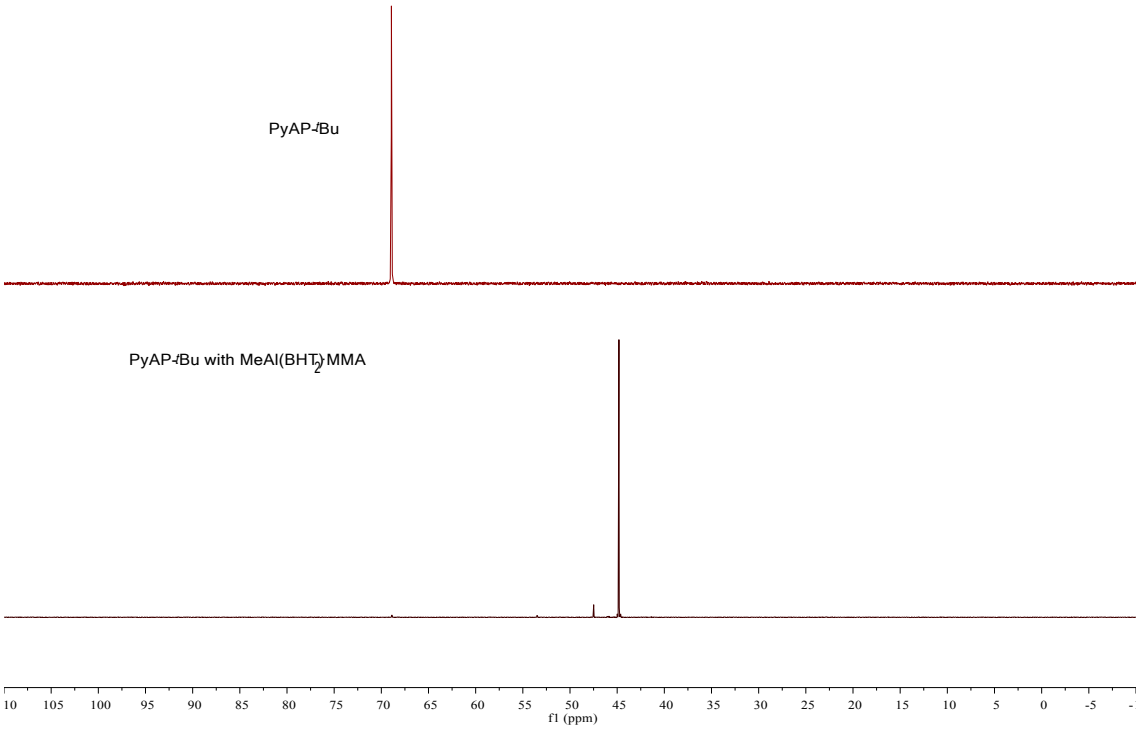

Figure S39. $^{31}P\{^{1}H\}$ NMR spectrum for reaction of PyAP-^{t}Bu with MeAl(BHT)$_2$·MMA (162 MHz, C_6D_6, 298 K)

2.13 Stoichiometric NMR Reaction of PyAP-^{i}Pr with MeAl(BHT)$_2$ ·MMA in a 1:1 molar ratio

In an argon-filled glovebox, a NMR tube was charged with 9.5 mg (0.04 mmol) of PyAP-^{i}Pr and 0.3 mL of C_6D_6. A 0.3 mL C_6D_6 solution of MeAl(BHT)$_2$ (18.7 mg, 0.04 mmol) and 4.2 uL MMA (0.04 mmol) were slowly added to this tube via pipet at room temperature. The mixture was allowed to react for 5 min at room temperature before the NMR spectra were recorded. Zwitterionic enolaluminate was generated as two isomers (E/Z = 100:8). Only the major isomer was analyzed.

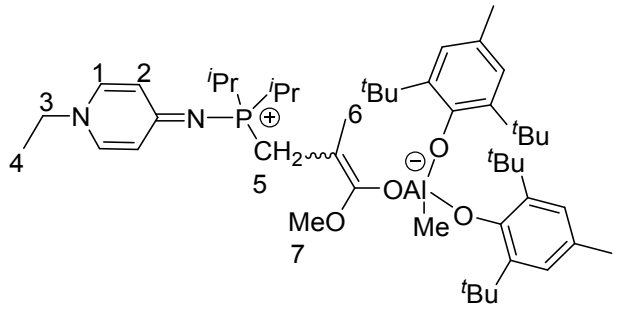

^{1}H NMR (400 MHz, C_6D_6, 298 K) δ (ppm) = 7.25 (s, 4H, BHT-phenyl), 6.43 (d, 2H, $^{3}J_{HH}$ = 7.3 Hz, 1-H), 5.95 (d, 2H, $^{3}J_{HH}$ = 6.3 Hz, 2-H), 3.59 (s, 3H, 7-H) , 2.55 (q, $^{3}J_{HH}$ = 7.3 Hz, 2H, 3-H), 2.36 (d, $^{2}J_{PH}$ = 9.1 Hz, 2H, 5-H), 2.31 (s, 6H, BHT-Me), 2.13 (m, 2H, CH of ^{i}Pr), 1.83 (s, 36H, BHT-^{t}Bu), 1.77 (s, 3H, 6-H), 0.91 (dt, $^{3}J_{PH}$ = 14.1 Hz, $^{3}J_{PH}$ =7.5 Hz, 12H, CH_3 of ^{i}Pr), 0.46 (t, $^{3}J_{HH}$ = 7.3 Hz, 3H, 4-H), 0.26 (s, 3H, Al-Me). CH of ^{i}Pr was not assigned due to the overlapping. ^{31}P {^{1}H} NMR (162 MHz, C_6D_6, 298 K) δ (ppm) = 42.5 (s).

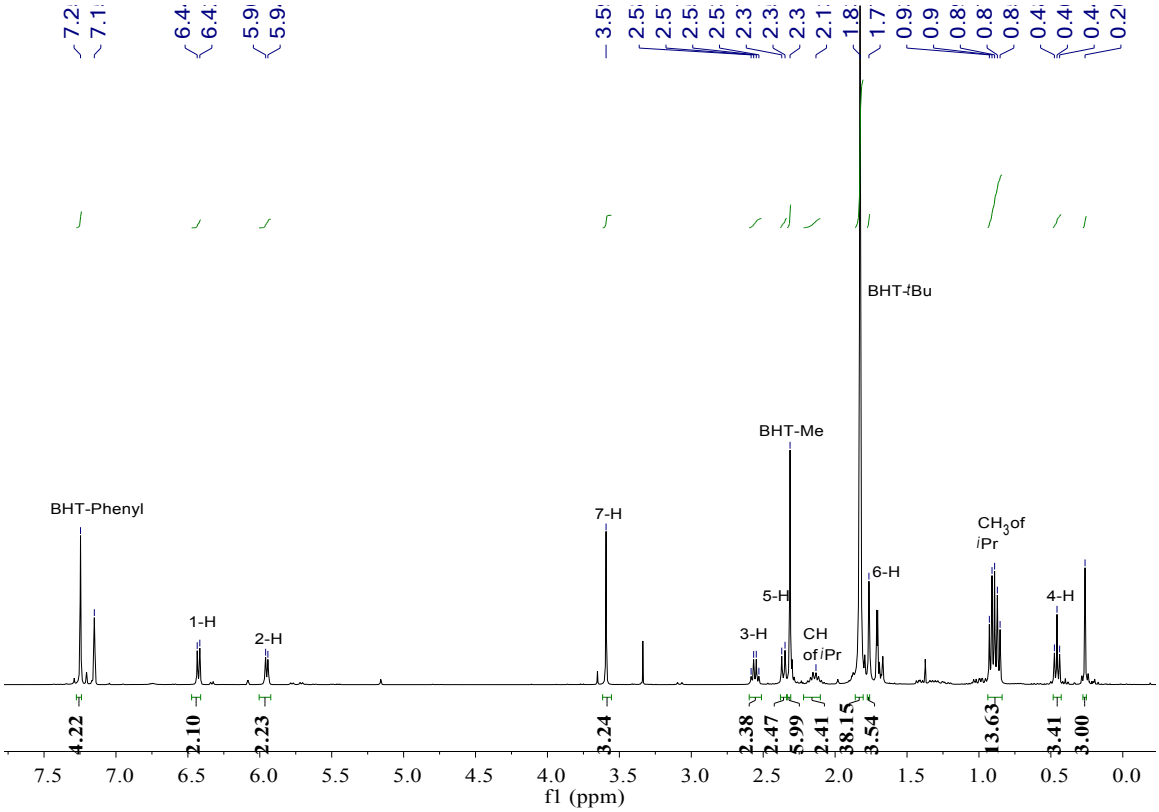

Figure S40. ^{1}H NMR spectrum for reaction of PyAP-^{i}Pr with MeAl(BHT)$_2$·MMA (400 MHz, C_6D_6, 298 K) (100:8 mixture of isomer, only the major isomer was marked for clarity).

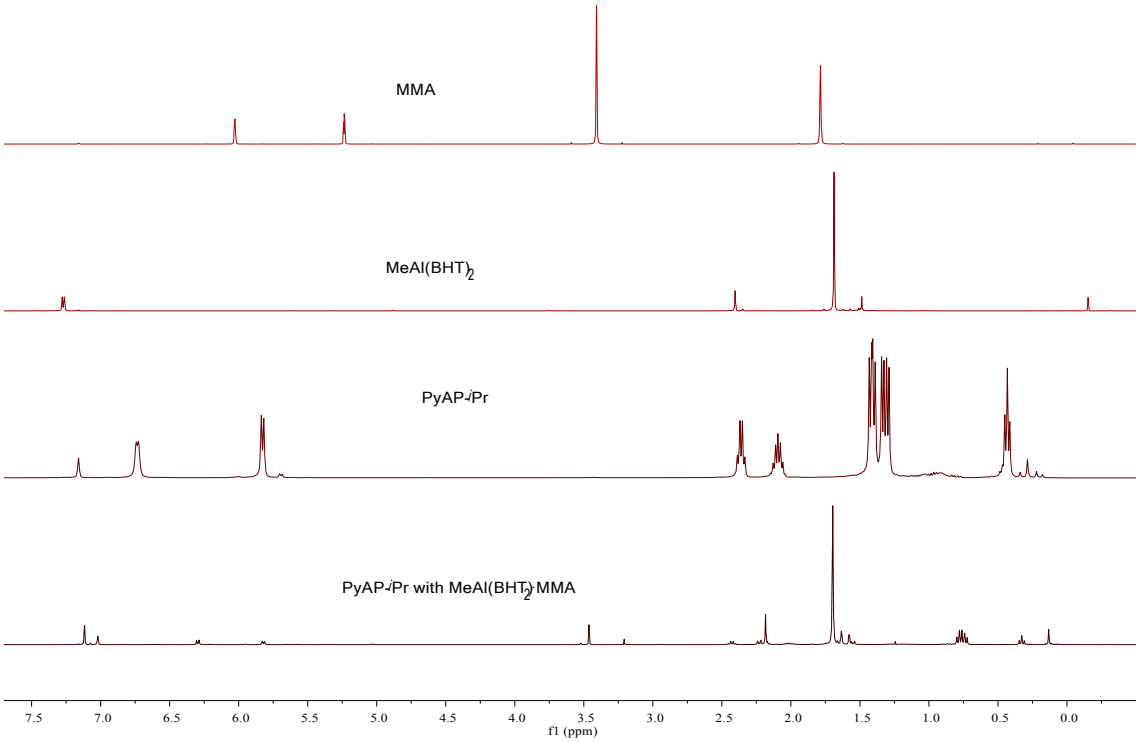

Figure S41. Stacked ^{1}H NMR spectra for reaction of PyAP-*i*Pr with MeAl(BHT)$_2$·MMA (400 MHz, C_6D_6, 298 K)

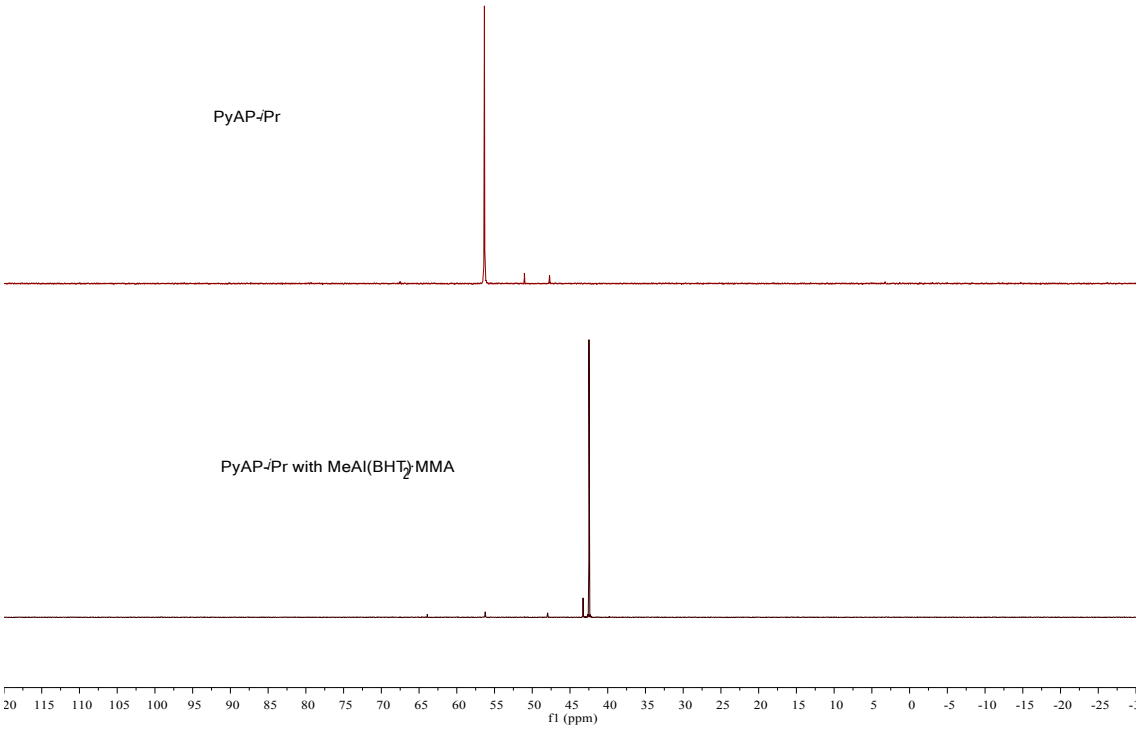

Figure S42. $^{31}P\{^{1}H\}$ NMR spectrum for reaction of PyAP-*i*Pr with MeAl(BHT)$_2$·MMA (162 MHz, C_6D_6, 298 K)

2.14 Stoichiometric NMR Reaction of PyAP-PPh with MeAl(BHT)$_2$·MMA in a 1:1 molar ratio

In an argon-filled glovebox, a NMR tube was charged with 12.3 mg (0.04 mmol) of PyAP-PPh and 0.3 mL of C_6D_6. A 0.3 mL C_6D_6 solution of MeAl(BHT)$_2$ (18.7 mg, 0.04 mmol) and 4.2 uL MMA (0.04 mmol) were slowly added to this tube via pipet at room temperature. The mixture was allowed to react for 5 min at room temperature before the NMR spectra were recorded. Zwitterionic enolaluminate was generated as two isomers (E/Z = 10:6). Only the major isomer was analyzed.

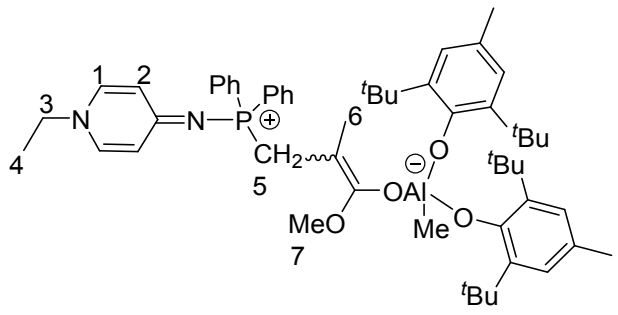

^{1}H NMR (400 MHz, C_6D_6, 298 K) δ (ppm) = 7.25 (s, 4H, BHT-phenyl), 7.05 (m, 10H, Ph), 6.38 (d, 2H, $^{3}J_{HH}$ = 7.3 Hz, 1-H), 6.01 (d, 2H, $^{3}J_{HH}$ = 6.3 Hz, 2-H), 3.42 (s, 3H, 7-H) , 2.53 (q, $^{3}J_{HH}$ = 7.3 Hz, 2H, 3-H), 2.32 (d, $^{2}J_{PH}$ = 9.1 Hz, 2H, 5-H), 2.32 (s, 6H, BHT-Me), 1.79 (s, 39H, BHT-^{t}Bu and 6-H), 0.42 (t, $^{3}J_{HH}$ = 7.3 Hz, 3H, 4-H), 0.10 (s, 3H, Al-Me). ^{31}P {^{1}H} NMR (162 MHz, C_6D_6, 298 K) δ (ppm) = 17.1 (s).

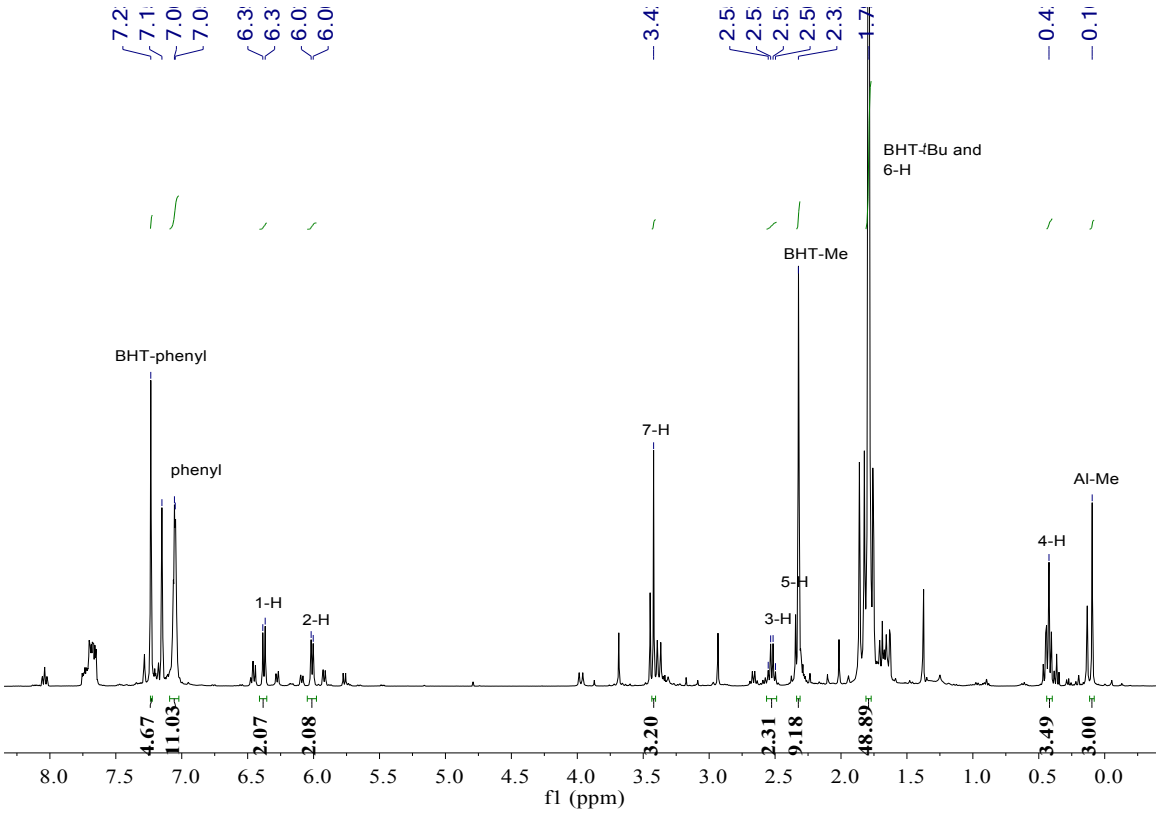

Figure S43. ^{1}H NMR spectrum for reaction of PyAP-PPh with MeAl(BHT)$_2$·MMA (400 MHz, C_6D_6, 298 K) (10:6 mixture of isomer, only the major isomer was marked for clarity).

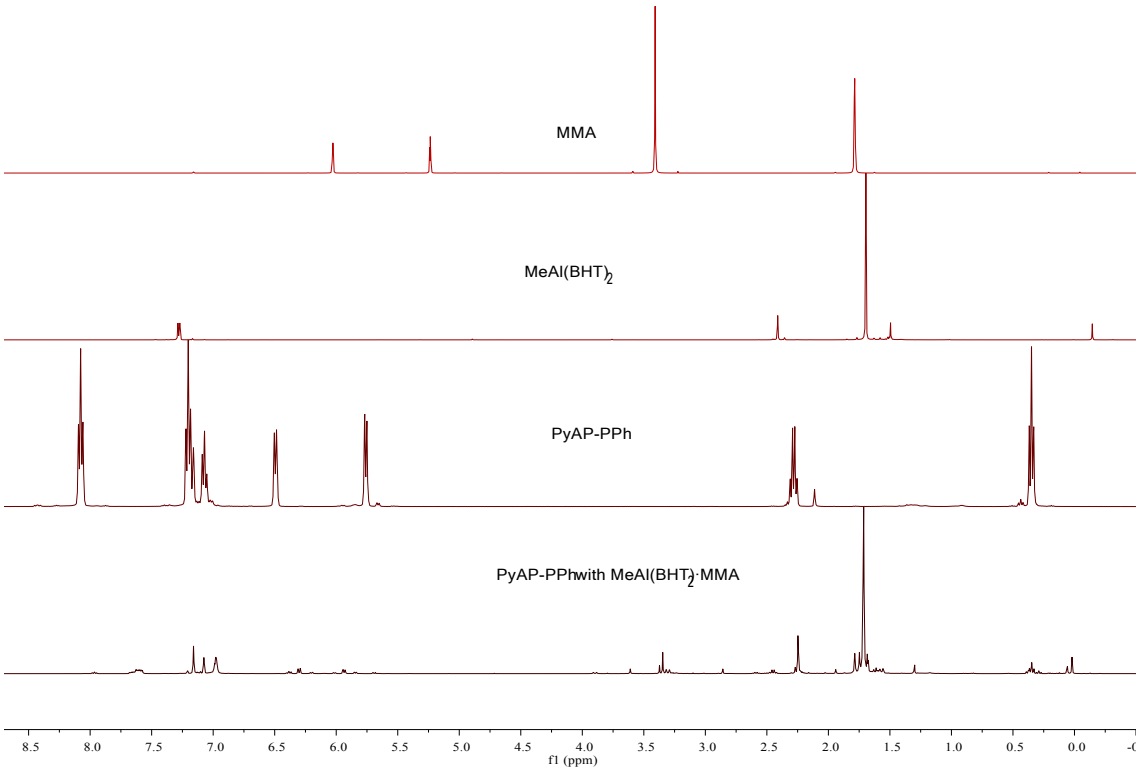

Figure S44. Stacked ^{1}H NMR spectra for reaction of PyAP-PPh with $MeAl(BHT)_2 \cdot MMA$ (400 MHz, C_6D_6, 298 K)

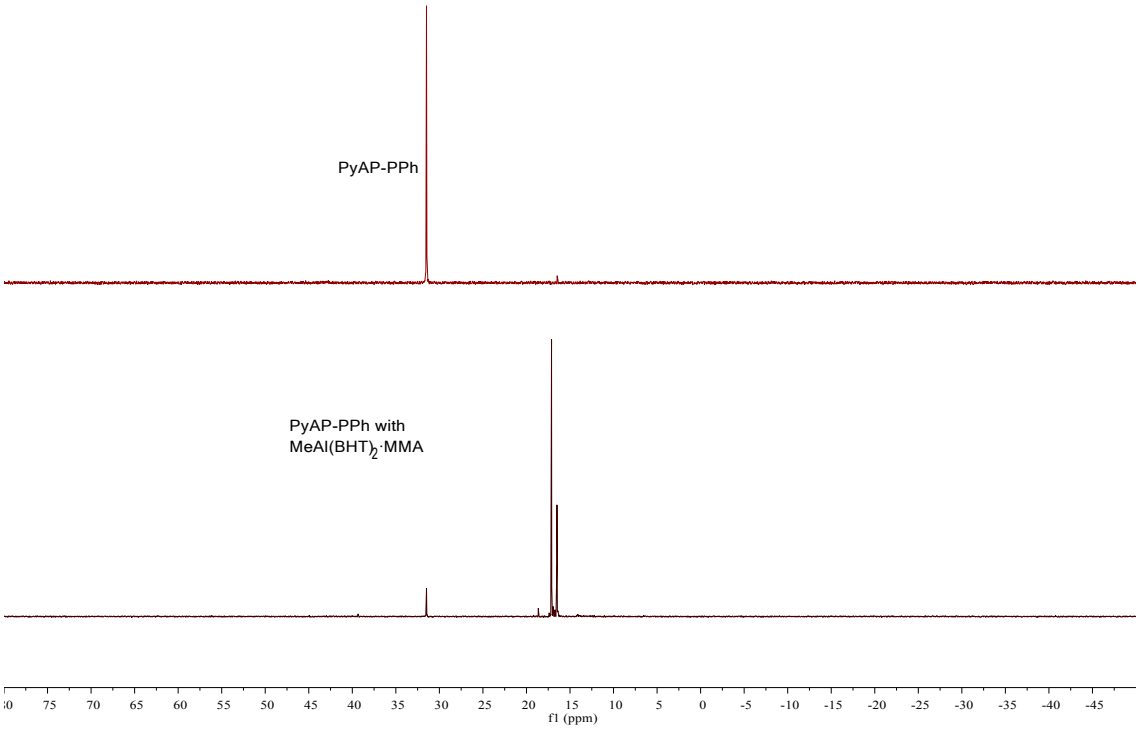

Figure S45. $^{31}P\{^{1}H\}$ NMR spectrum for reaction of PyAP-PPh with $MeAl(BHT)_2$·MMA (162 MHz, C_6D_6, 298 K)

2.15 Stoichiometric NMR Reaction of PyAP-Cy with $^{i}BuAl(BHT)_2$·MMA in a 1:1 molar ratio

In an argon-filled glovebox, a NMR tube was charged with 12.7 mg (0.04 mmol) of PyAP-Cy and 0.3 mL of C_6D_6. A 0.3 mL C_6D_6 solution of $^{i}BuAl(BHT)_2$ (20.9mg, 0.04 mmol) and 4.2 uL MMA (0.04 mmol) were slowly added to this tube via pipet at room temperature. The mixture was allowed to react for 5 min at room temperature before the NMR spectra were recorded. Zwitterionic enolaluminate was generated as two isomers (E/Z = 5:1). Only the major isomer was analyzed.

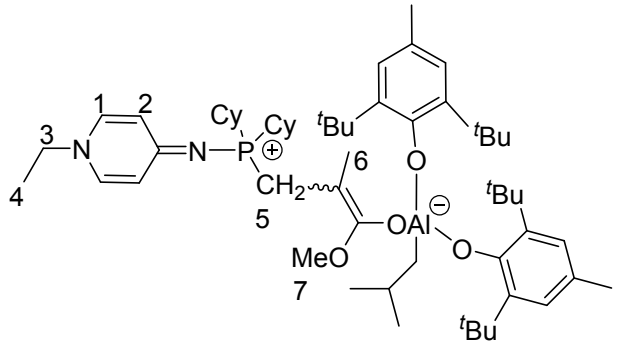

^{1}H NMR (400 MHz, C_6D_6, 298 K) δ (ppm) = 7.31 (s, 4H, BHT-phenyl), 6.50 (d, 2H, $^{3}J_{HH}$ = 7.3 Hz, 1-H), 6.17 (d, 2H, $^{3}J_{HH}$ = 7.3 Hz, 2-H), 3.61 (s, 3H, 7-H) , 2.58 (q, $^{3}J_{HH}$ = 7.3 Hz, 2H, 3-H), 2.42 (d, $^{2}J_{PH}$ = 7.0 Hz, 2H, 5-H), 2.33 (s, 6H, BHT-Me), 1.89, 1.85 (s, 39H, BHT-^{t}Bu and 6-H), 1.00-1.62 (m, 22H, Cy), 1.40 (d, $^{3}J_{HH}$ = 6.4 Hz, 6H, CH_3 of ^{i}Bu), 0.93 (d, $^{3}J_{HH}$ = 6.5 Hz, 2H, CH_2 of ^{i}Bu), 0.28 (t, $^{3}J_{HH}$ = 7.3 Hz, 3H, 4-H), CH of ^{i}Bu was not assigned due to the overlapping. ^{31}P {^{1}H} NMR (162 MHz, C_6D_6, 298 K) δ (ppm) = 36.6 (s).

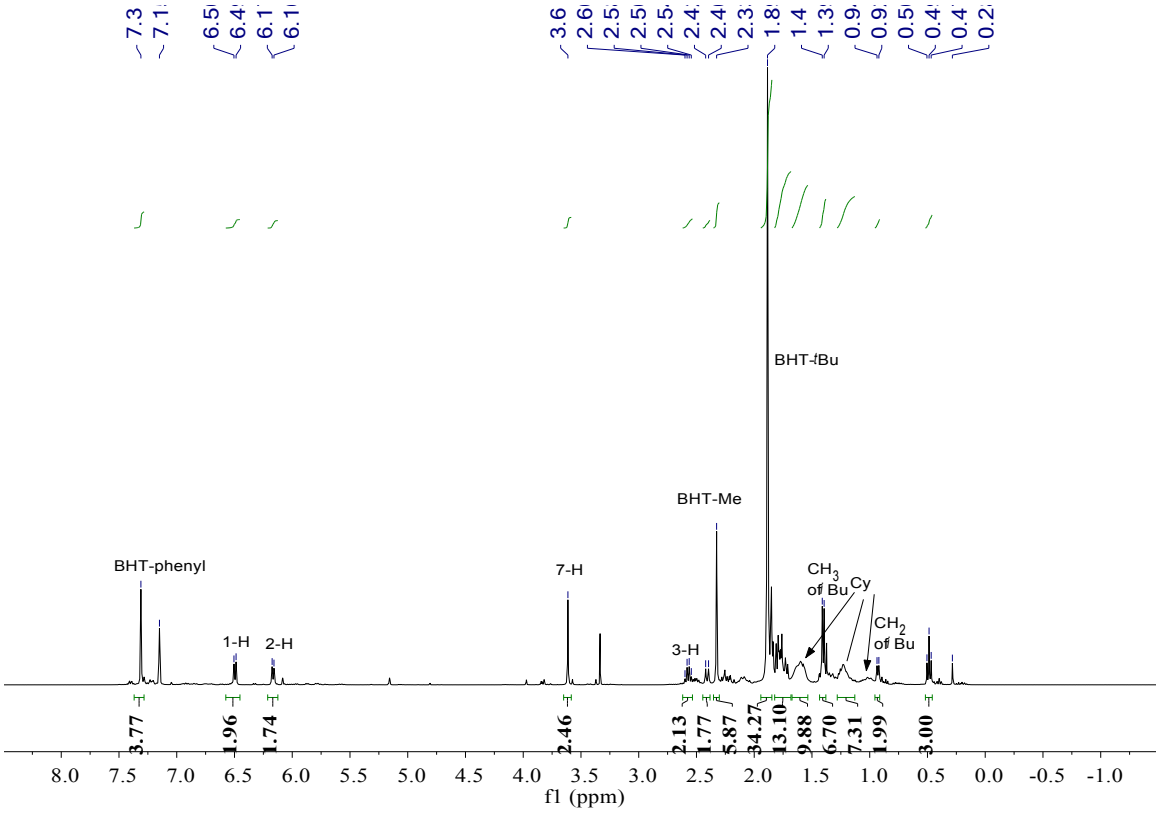

Figure S46. ^{1}H NMR spectrum for reaction of PyAP-Cy with ^{i}BuAl(BHT)$_2$·MMA (400 MHz, C_6D_6, 298 K) (5:1 mixture of isomer, only the major isomer was marked for clarity).

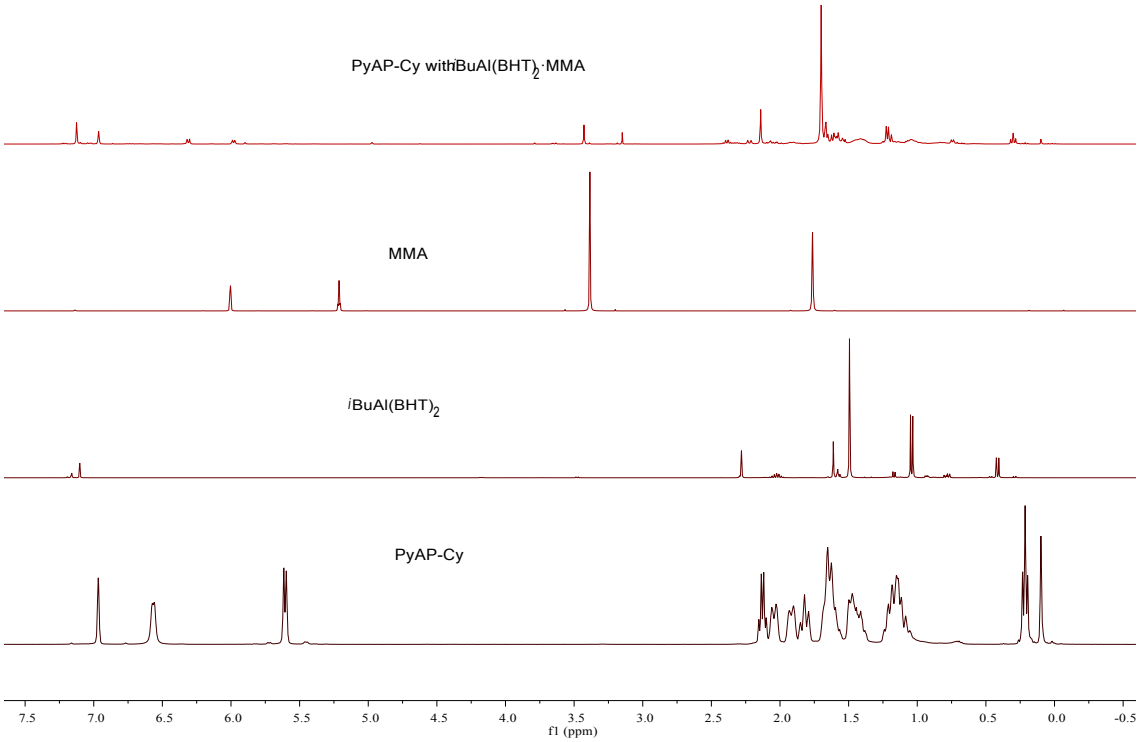

Figure S47. Stacked ^{1}H NMR spectra for reaction of PyAP-Cy with ^{i}BuAl(BHT)$_2$·MMA (400 MHz, C_6D_6, 298 K)

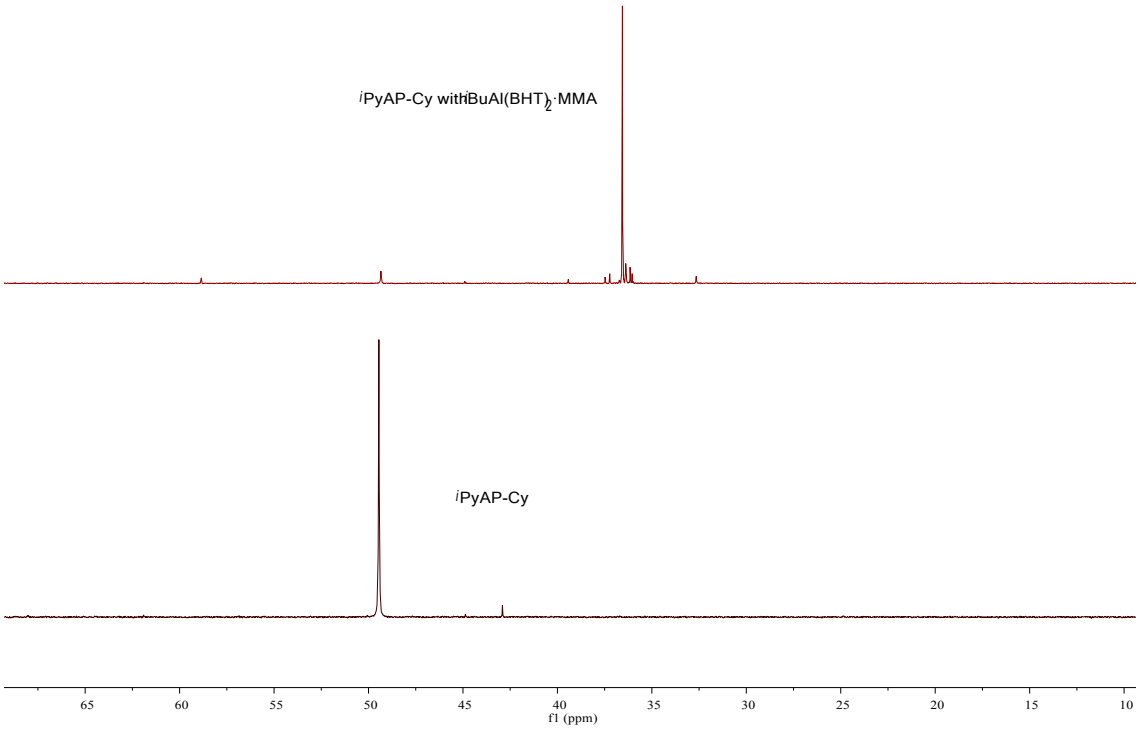

Figure S48. $^{31}P\{^{1}H\}$ NMR spectrum for reaction of PyAP-Cy with $^{i}BuAl(BHT)_2$·MMA (162 MHz, C_6D_6, 298 K)

2.16 Stoichiometric NMR Reaction of PyAP-^{t}Bu with ^{i}BuAl(BHT)$_2$·MMA in a 1:1 molar ratio

In an argon-filled glovebox, a NMR tube was charged with 10.7 mg (0.04 mmol) of PyAP-^{t}Bu and 0.3 mL of C_6D_6. A 0.3 mL C_6D_6 solution of $^{i}BuAl(BHT)_2$ (20.9mg, 0.04 mmol) and 4.2 uL MMA (0.04 mmol) were slowly added to this tube via pipet at room temperature. The mixture was allowed to react for 5 min at room temperature before the NMR spectra were recorded. Zwitterionic enolaluminate was generated as two isomers (E/Z = 8:2). Only the major isomer was analyzed.

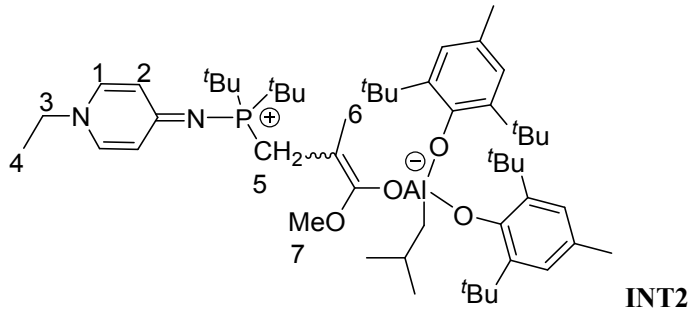

INT2

^{1}H NMR (400 MHz, C_6D_6, 298 K) δ (ppm) = 7.29 (s, 4H, BHT-phenyl), 6.45 (d, 2H, $^{3}J_{HH}$ = 7.3 Hz, 1-H), 6.22 (d, 2H, $^{3}J_{HH}$ = 7.3 Hz, 2-H), 3.71 (s, 3H, 7-H) , 2.85 (d, $^{2}J_{PH}$ = 7.0 Hz, 2H, 5-H), 2.60 (q, $^{3}J_{HH}$ = 7.3 Hz, 2H, 3-H), 2.32 (s, 6H, BHT-Me), 1.90 (s, 3H, 6-H), 1.87 (s, 36H, BHT-^{t}Bu), 1.37 (d, $^{3}J_{HH}$ = 6.4 Hz, 6H, CH_3 of ^{i}Bu), 1.00 (d, $^{3}J_{PH}$ = 14.1 Hz, 18H, ^{t}Bu), 0.54 (t, $^{3}J_{HH}$ = 7.3 Hz, 3H, 4-H), CH_2, CH of ^{i}Bu were not assigned due to the overlapping. ^{31}P {^{1}H} NMR (162 MHz, C_6D_6, 298 K) δ (ppm) = 44.8 (s).

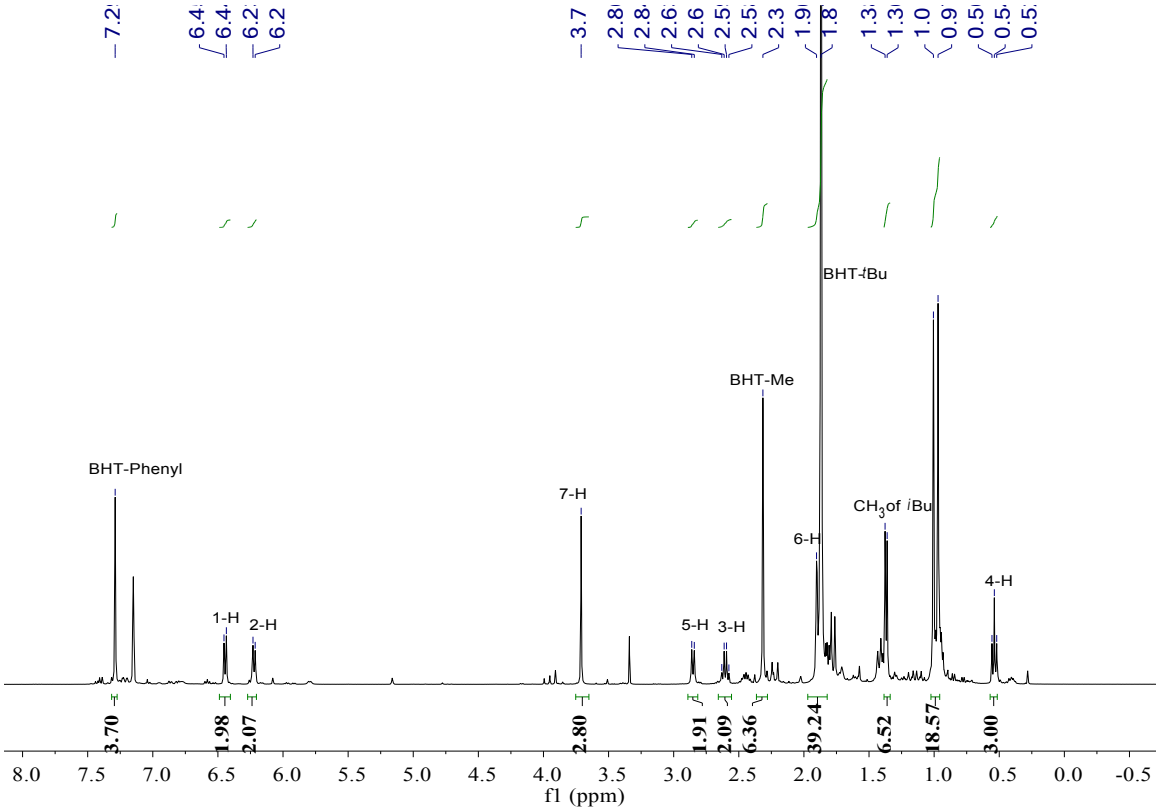

Figure S49. ^{1}H NMR spectrum for reaction of PyAP-^{t}Bu with ^{i}BuAl(BHT)$_2$ (400 MHz, C_6D_6, 298 K) (5:1 mixture of isomer, only the major isomer was marked for clarity).

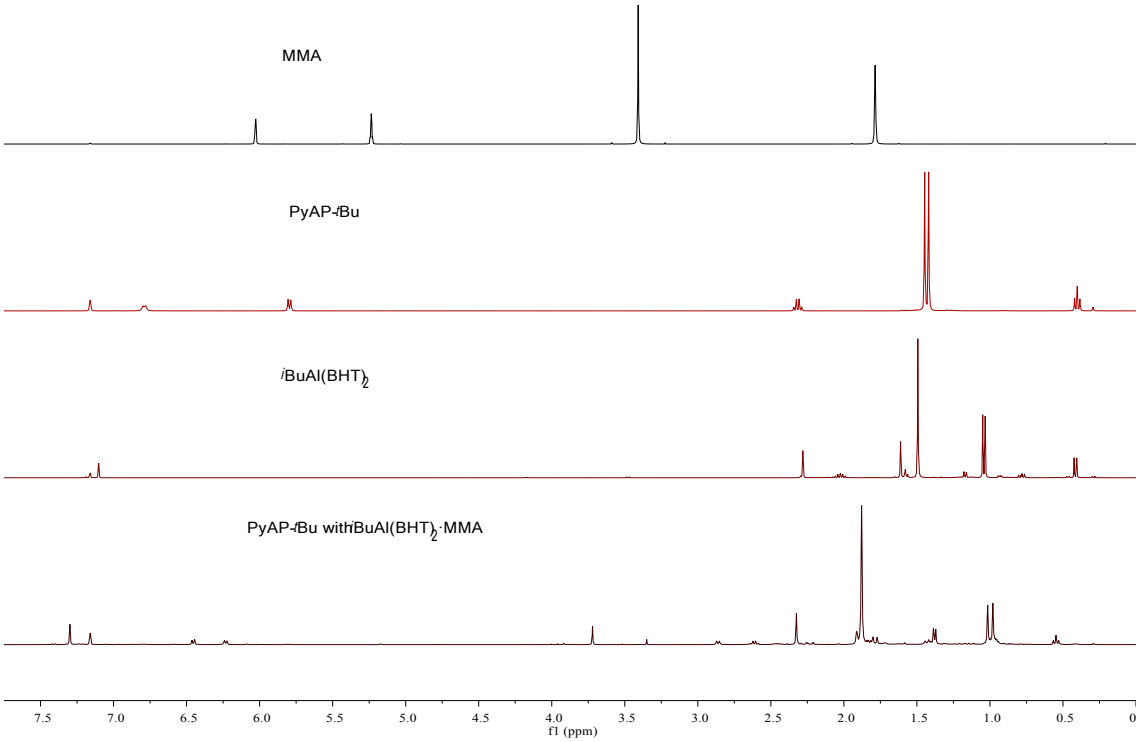

Figure S50. Stacked ^{1}H NMR spectra for reaction of PyAP-^{t}Bu with ^{i}BuAl(BHT)$_2$·MMA (400 MHz, C_6D_6, 298 K)

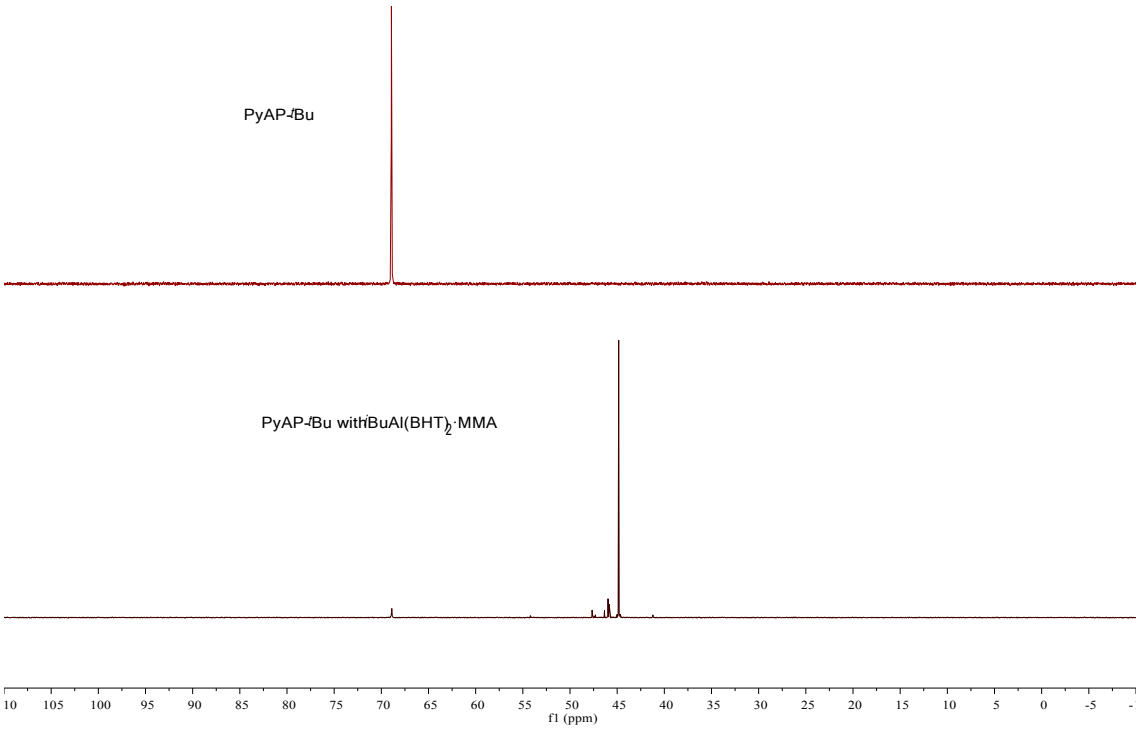

Figure S51. $^{31}P\{^{1}H\}$ NMR spectrum for reaction of PyAP-^{t}Bu with ^{i}BuAl(BHT)$_2$·MMA (162 MHz, C_6D_6, 298 K)

2.17 Stoichiometric NMR Reaction of PyAP-^{i}Pr with ^{i}BuAl(BHT)$_2$ ·MMA in a 1:1 molar ratio

In an argon-filled glovebox, a NMR tube was charged with 9.5 mg (0.04 mmol) of PyAP-^{i}Pr and 0.3 mL of C_6D_6. A 0.3 mL C_6D_6 solution of ^{i}BuAl(BHT)$_2$ (20.9 mg, 0.04 mmol) and 4.2 uL MMA (0.04 mmol) were slowly added to this tube via pipet at room temperature. The mixture was allowed to react for 5 min at room temperature before the NMR spectra were recorded. Zwitterionic enolaluminate was generated as two isomers (E/Z = 10:1). Only the major isomer was analyzed.

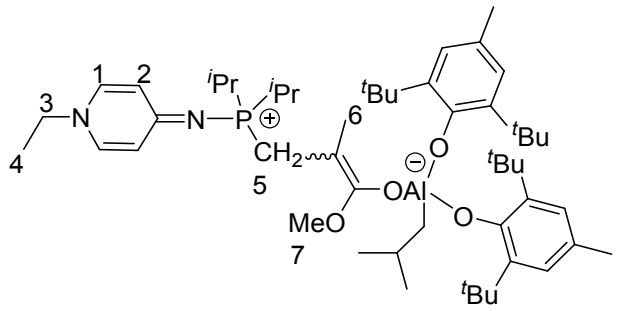

^{1}H NMR (400 MHz, C_6D_6, 298 K) δ (ppm) = 7.31 (s, 4H, BHT-phenyl), 6.41 (d, 2H, $^{3}J_{HH}$ = 7.3 Hz, 1-H), 6.12 (d, 2H, $^{3}J_{HH}$ = 6.3 Hz, 2-H), 3.61 (s, 3H, 7-H) , 2.60 (q, $^{3}J_{HH}$ = 7.3 Hz, 2H, 3-H), 2.39 (d, $^{2}J_{PH}$ = 9.1 Hz, 2H, 5-H), 2.32 (s, 6H, BHT-Me), 2.13 (m, 2H, CH of ^{i}Pr), 1.87 (s, 36H, BHT-^{t}Bu), 1.82 (s, 3H, 6-H), 1.37 (m, 7H, CH_3 and CH of ^{i}Bu), 0.90 (m, 16H, ^{i}Pr and CH_2 of ^{i}Bu), 0.51 (t, $^{3}J_{HH}$ = 7.3 Hz, 3H, 4-H). $^{31}P\{^{1}H\}$ NMR (162 MHz, C_6D_6, 298 K) δ (ppm) = 42.5 (s).

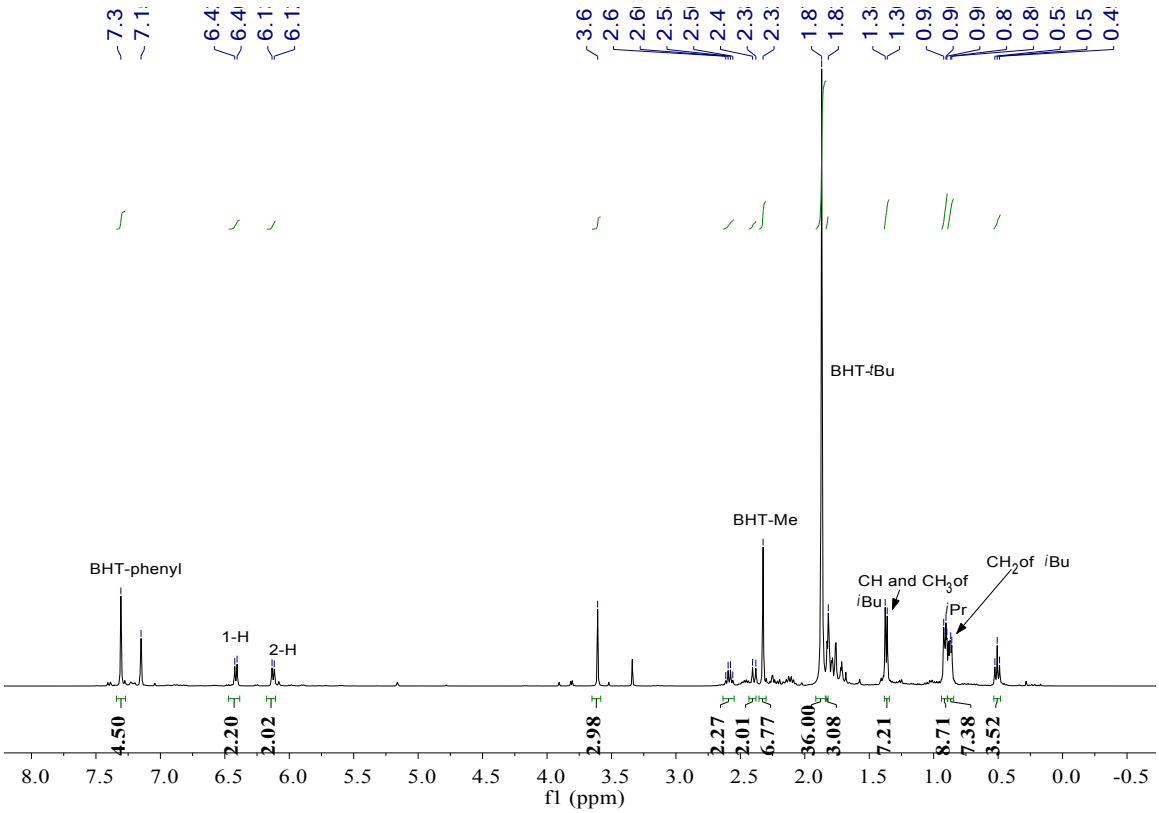

Figure S52. ^{1}H NMR spectrum for reaction of PyAP-^{i}Pr with ^{i}BuAl(BHT)$_2$·MMA (400 MHz, C_6D_6, 298 K) (10:1 mixture of isomer, only the major isomer was marked for clarity).

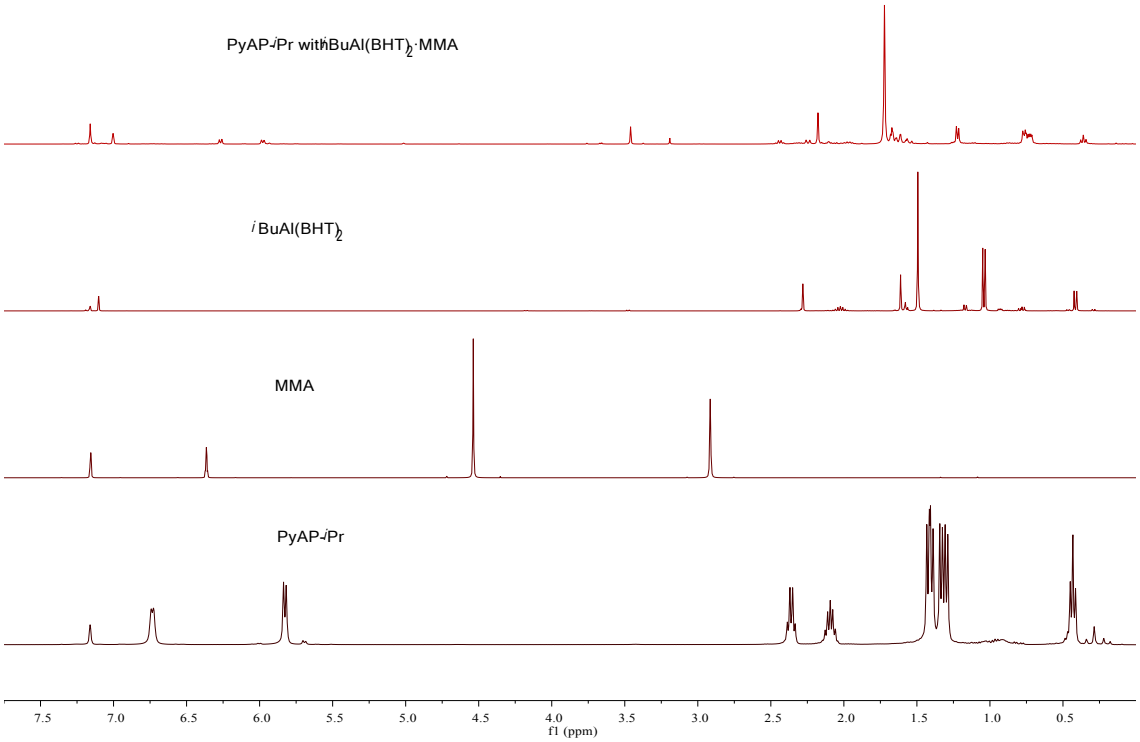

Figure S53. Stacked ^{1}H NMR spectra for reaction of PyAP-*i*Pr with ^{i}BuAl(BHT)$_2$·MMA (400 MHz, C_6D_6, 298 K)

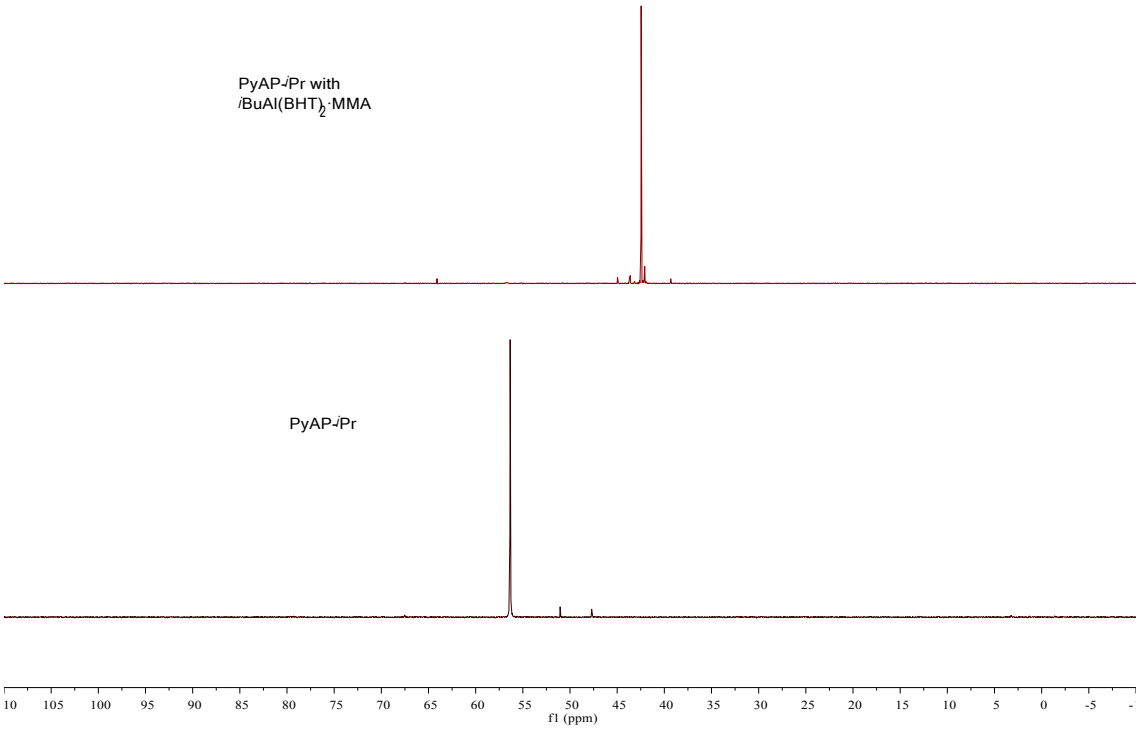

Figure S54. $^{31}P\{^{1}H\}$ NMR spectrum for reaction of PyAP-^{i}Pr with ^{i}BuAl(BHT)$_2$·MMA (162 MHz, C_6D_6, 298 K)

2.18 Stoichiometric NMR Reaction of PyAP-Ph with ^{i}BuAl(BHT)$_2$·MMA in a 1:1 molar ratio

In an argon-filled glovebox, a NMR tube was charged with 12.3 mg (0.04 mmol) of P^{i}Ph$_2$ and 0.3 mL of C_6D_6. A 0.3 mL C_6D_6 solution of ^{i}BuAl(BHT)$_2$ (20.9 mg, 0.04 mmol) and 4.2 uL MMA (0.04 mmol) were slowly added to this tube via pipet at room temperature. The mixture was allowed to react for 5 min at room temperature before the NMR spectra were recorded. Zwitterionic enolaluminate was generated as two isomers (E/Z = 5:3). Only the major isomer was analyzed.

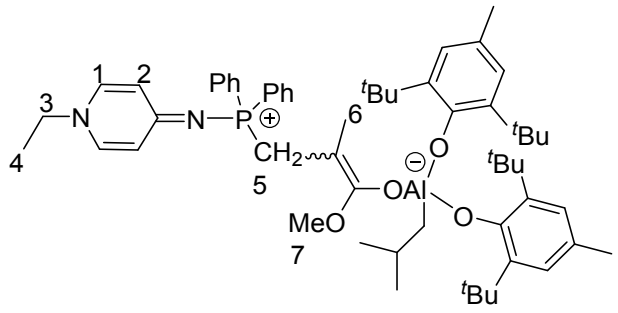

^{1}H NMR (400 MHz, C_6D_6, 298 K) δ (ppm) = 7.26 (s, 4H, BHT-phenyl), 7.06 (m, 10H, Ph), 6.33 (d, 2H, $^{3}J_{HH}$ = 7.3 Hz, 1-H), 6.07 (d, 2H, $^{3}J_{HH}$ = 6.3 Hz, 2-H), 3.40 (s, 3H, 7-H) , 2.53 (q, $^{3}J_{HH}$ = 7.3 Hz, 2H, 3-H), 2.31 (s, 6H, BHT-Me), 2.26 (d, $^{2}J_{PH}$ = 9.1 Hz, 2H, 5-H), 1.84 (s, 39H, BHT-^{t}Bu), 1.72 (s, 3H, 6-H), 1.30 (m, 7H, CH and CH_3 of ^{i}Bu), 0.48 (t, $^{3}J_{HH}$ = 7.3 Hz, 3H, 4-H), CH_2 of ^{i}Bu were not assigned due to the overlapping.^{31}P {^{1}H} NMR (162 MHz, C_6D_6, 298 K) δ (ppm) = 13.4 (s).

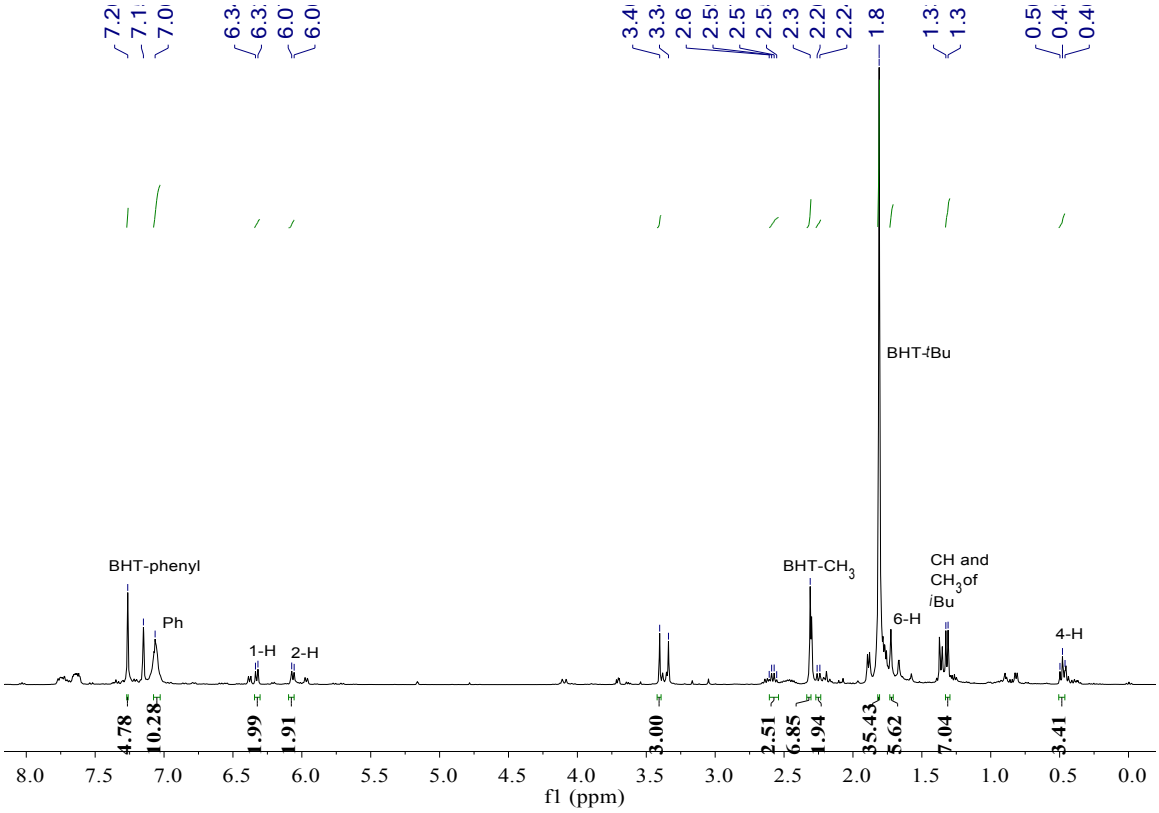

Figure S55. ^{1}H NMR spectrum for reaction of PyAP-Ph with ^{i}BuAl(BHT)$_2$·MMA (400 MHz, C_6D_6, 298 K) (5:3 mixture of isomer, only the major isomer was marked for clarity).

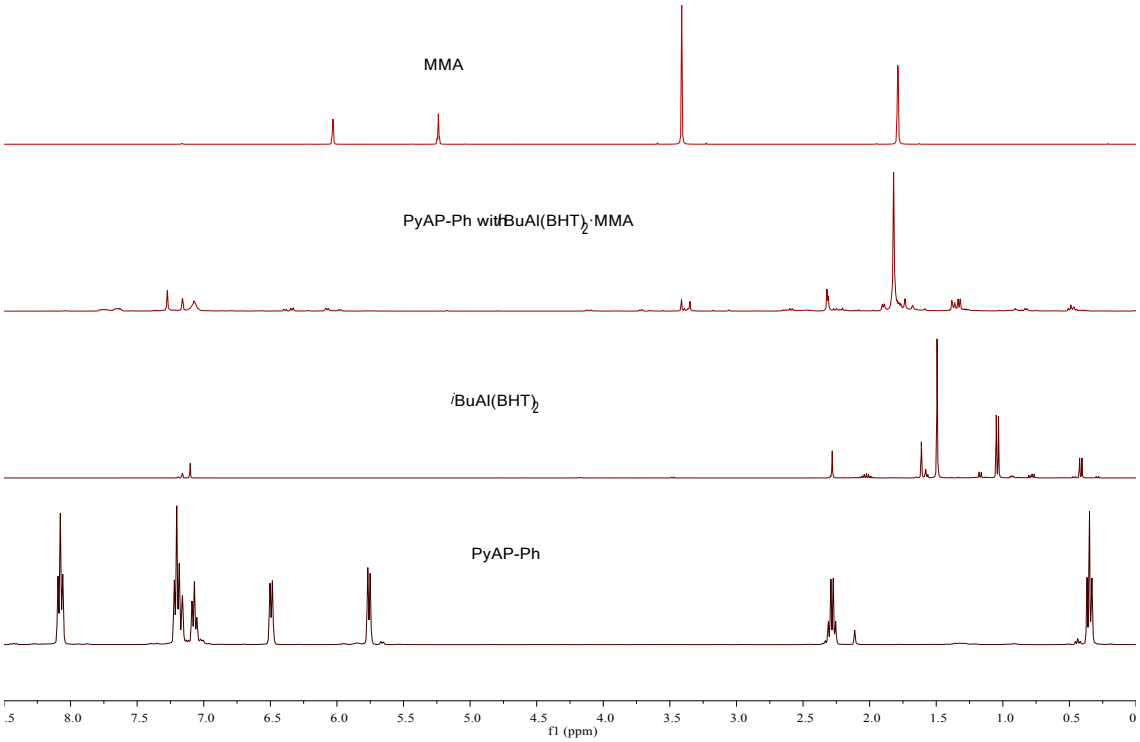

Figure S56. Stacked ^{1}H NMR spectra for reaction of PyAP-Ph with ^{i}BuAl(BHT)$_2$·MMA (400 MHz, C_6D_6, 298 K)

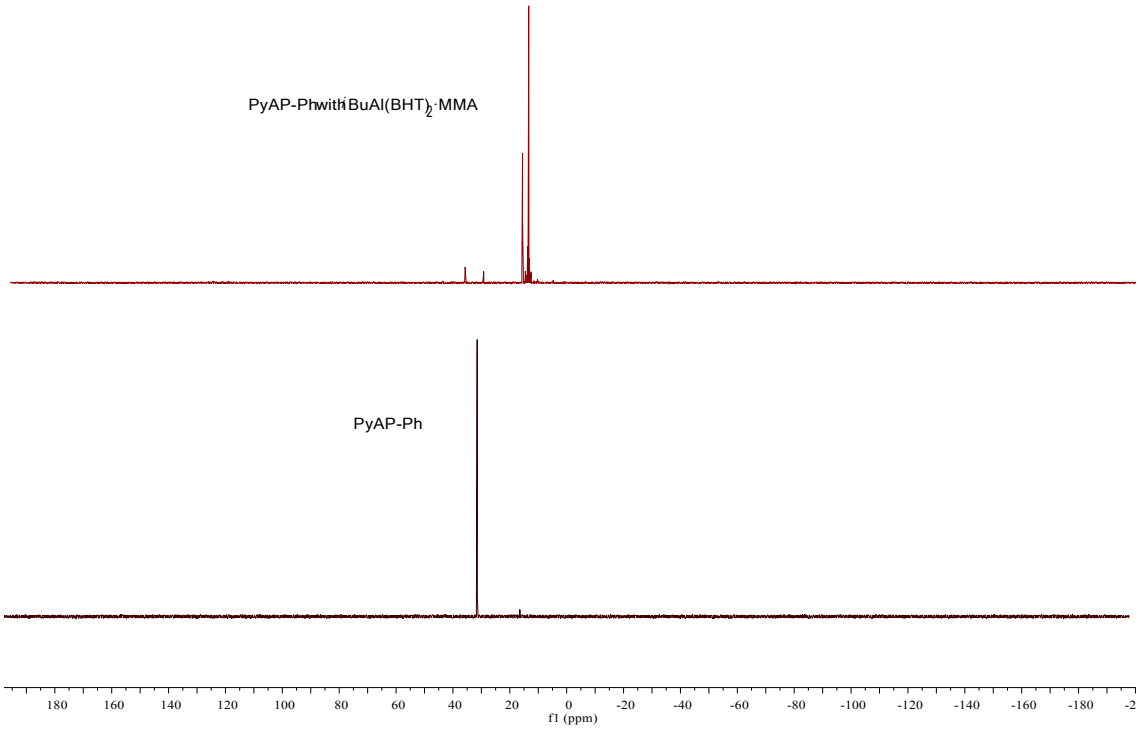

Figure S57. $^{31}P\{^{1}H\}$ NMR spectrum for reaction of PyAP-Ph with $^{i}BuAl(BHT)_2 \cdot MMA$ (162 MHz, C_6D_6, 298 K)

3. Additional Polymerization Data

Table S1 Control Experiments of MMA Polymerization Catalyzed by PyAPs

Run[a]	LB	Conv.[b] (%)	M_n[c] ($g \cdot mol^{-1}$)	$M_{n(calcd)}$ ($g \cdot mol^{-1}$)	Đ (M_w/M_n)
1	PyAP-^{t}Bu	0	-	-	-
2	PyAP-Cy	0	-	-	-
3	PyAP-^{i}Pr	0	-	-	-
4	PyAP-Ph	0	-	-	-

[a]Condition: The polymerization was carried out at ambient temperature in 4.6 mL of toluene using the following procedure: for a 200 MMA/1 LB molar ratio, $[MMA]_0$ =

0.941 M (4.8 mmol) and $[LB]_0$ = 9.4 mM (0.048 mmol).

Table S2 Different Procedures in MMA Polymerization Catalyzed by PyAP-*i*Pr and Organoaluminium Lewis Acids

Run[a]	LB : LA:M	Conv.[b] (%)	selectivity			M_n[c] (g·mol^{-1})	$M_{n(calcd)}$ (g·mol^{-1})	Đ (M_w/M_n)	I*[d] (%)
			rr	mr	mm				
1[e]	1 : 2MeAl(BHT)$_2$: 200	>99	64.9	31.8	3.3	35000	20262	1.18	58
2[f]	1 : 2MeAl(BHT)$_2$: 200	>99	67.1	29.5	3.4	45400	20262	1.30	45
3[e]	1 : 2^{t}BuAl(BHT)$_2$: 200	>99	67.6	29.1	3.3	31200	20262	1.21	65
4[f]	1 : 2^{t}BuAl(BHT)$_2$: 200	>99	67.6	29.1	3.3	39300	20262	1.20	52
5[e]	1 : 2^{i}Bu$_2$Al(BHT) : 200	>99	60.2	36.1	3.7	37900	20262	1.17	54
6[f]	1 : 2^{i}Bu$_2$Al(BHT) : 200	>99	61.7	34.6	3.7	39600	20262	1.21	51

[a]Condition: The polymerization was carried out at ambient temperature in 4.6 mL of toluene using the following procedure: for a 200 MMA/1 LB/2 LA ratio, $[MMA]_0$ = 0.941

M (4.8 mmol) and $[LA]_0$ =2 $[LB]_0$ = 9.4 mM (0.048 mmol). [b]Monomer conversions were measured by ^1H NMR. [c]M_n and Đ determined by GPC relative to PMMA standards in THF. [d]Initiation efficiency (I*)% = $M_{n(calcd)}/M_{n(exptl)} \times 100$, where $M_{n(calcd)}$ = $[M_W(MMA)]([MMA]_0/[I]_0)$(conversion) + M_W of chain end groups. e: procedure A: the LA and LB was premixed before the addition of MMA. f: procedure B: LA was premixed with MMA, followed by addition of LB.

Table S3 Low Molecular Weight PMMA Experiments Used for Maldi -TOF Measurements

Run[a]	LB : LA:M	Conv.[b] (%)	Maldi -TOF
1	1 PyAP-^{t}Bu : 2MeAl(BHT)$_2$: 25	>99	Linear chain end (controlled and living)
2	1 PyAP-^{t}Bu : 2^{i}BuAl(BHT)$_2$: 25	>99	Chain end capped with cyclization (controlled)
3	1 PyAP-^{t}Bu : 2^{i}Bu$_2$Al(BHT) : 25	>99	Both Chain end capped with cyclization (major) and linear chain end (minor)
4	1 PyAP-Cy : 2MeAl(BHT)$_2$: 25	>99	Both Chain end capped with cyclization (minor) and linear chain end (major)(not controlled)
5	1 PyAP-Cy : 2^{i}BuAl(BHT)$_2$: 25	>99	Both Chain end

			capped with cyclization (major) and linear chain end (minor)
6	1 PyAP-Cy : 2^{i}Bu$_2$Al(BHT) : 25	>99	Chain end capped with cyclization (major) and unidentified species (minor)
7	1 PyAP-^{i}Pr : 2MeAl(BHT)$_2$: 25	>99	Both Chain end capped with cyclization (minor) and linear chain end (major)
8	1 PyAP-^{i}Pr : 2^{i}BuAl(BHT)$_2$: 25	>99	Only chain end capped with cyclization was observed
9	1 PyAP-^{i}Pr : 2^{i}Bu$_2$Al(BHT) : 25	>99	Chain end capped with cyclization (major) and tiny amount of other species
10	1 PyAP-Ph : 2MeAl(BHT)$_2$: 25	>99	Only chain end capped with cyclization
11	1 PyAP-Ph : 2^{i}BuAl(BHT)$_2$: 25	>99	Chain end capped with cyclization

			(major) and unidentified species (minor)
12	1 PyAP-Ph : 2^{i}Bu$_2$Al(BHT) : 25	>99	Chain end capped with cyclization and unidentified species (minor)
13	1 PyAP-^{t}Bu: 2Al(C_6F_5)$_3$: 25	>99	Both Chain end capped with cyclization (major) and linear chain end (minor)

[a]Condition: The polymerization was carried out at ambient temperature in 0.6 mL of toluene using the following procedure: for a 25 MMA/1 LB/2 LA ratio, $[MMA]_0$ = 0.936 M (0.6 mmol) and $[LA]_0$ =2 $[LB]_0$ = 9.2 mM (0.048 mmol). [b]Monomer conversions measured by ^{1}H NMR. [c]M_n and Đ determined by GPC relative to PMMA standards in THF. [d]Initiation efficiency (I*)% = $M_{n(calcd)}/M_{n(exptl)}$ × 100, where $M_{n(calcd)}$ = $[M_W(MMA)]([MMA]_0/[I]_0)$(conversion) + M_W of chain end groups. A: procedure A. B: procedure B.

Table S4 MMA Polymerization by PyAP-^{t}Bu/ MeAl(BHT)$_2$ LP in a molar ratio of MMA/PyAP-^{t}Bu = 400/1

Run[a]	Time (min)	LB : LA:M	Conv.[b] (%)	M_n[c] (g·mol^{-1})	$M_{n(calcd)}$ (g·mol^{-1})	Đ (Mw/Mn)	I*[d](%)
1	1	1 PyAP-^{t}Bu : 2MeAl(BHT)$_2$: 400	18	8700	7475	1.10	86

2	2	1 PyAP-^{t}Bu : 2MeAl(BHT)$_2$: 400	25.9	10800	10639	1.22	99
3	3	1 PyAP-^{t}Bu : 2MeAl(BHT)$_2$: 400	33.8	14000	13803	1.12	99
4	4.5	1 PyAP-^{t}Bu : 2MeAl(BHT)$_2$: 400	39.1	16200	15925	1.13	98
5	6	1 PyAP-^{t}Bu : 2MeAl(BHT)$_2$: 400	46.8	19100	19009	1.20	100
6	8	1 PyAP-^{t}Bu : 2MeAl(BHT)$_2$: 400	57.1	21600	23134	1.25	107
7	10	1 PyAP-^{t}Bu : 2MeAl(BHT)$_2$: 400	63	25900	25497	1.15	98
8	12	1 PyAP-^{t}Bu : 2MeAl(BHT)$_2$: 400	70.6	29200	28540	1.17	98
9	15	1 PyAP-^{t}Bu : 2MeAl(BHT)$_2$: 400	88.9	32000	35869	1.16	112
10	20	1 PyAP-^{t}Bu : 2MeAl(BHT)$_2$	100	40700	40314	1.19	99

: 400

[a]Condition: The polymerization was carried out at ambient temperature in 9.2 mL of toluene using the following procedure: for a 400 MMA/1 LB/2 LA ratio, $[MMA]_0$ = 0.936 M (0.6 mmol) and $[LA]_0$ =2 $[LB]_0$ = 4.7mM (0.048 mmol). n.d.: not determined. [b]Monomer conversions measured by ^1H NMR. [c]M_n and Đ determined by GPC relative to PMMA standards in THF. [d]Initiation efficiency (I*)% = $M_{n(calcd)}/M_{n(exptl)} \times 100$, where $M_{n(calcd)} = [M_W(MMA)]([MMA]_0/[I]_0)(conversion) + M_W$ of chain end groups.

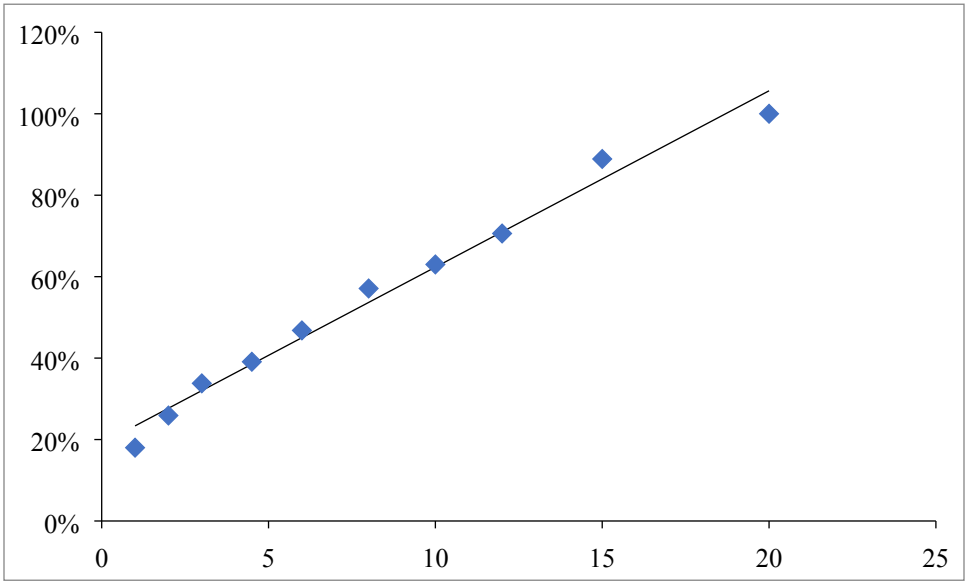

Figure S58. Plots of conversion of MMA vs time catalyzed by PyAP-^{t}Bu/MeAl(BHT)$_2$ at ambient temperature. Conditions: $[MMA]_0/[PyAP\text{-}^tBu]_0/ [MeAl(BHT)_2]_0$ = 400:1:2.

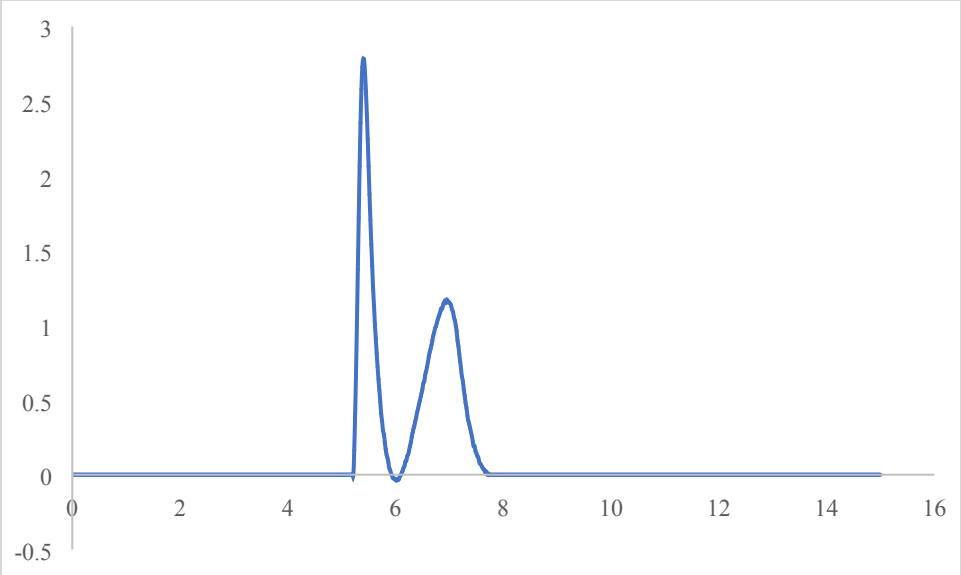

Figure S59. GPC traces of PMMA samples obtained by $[MMA]_0/[PyAP\text{-}^tBu]_0/ [MeAl(BHT)_2]_0$ = 3200:1:2.

Table S5 PyAP-^{t}Bu/ MeAl(BHT)$_2$ LP-catalyzed ^{t}BA Polymerization

Run[a]	LB : LA: M	Conv.[b] (%)	M_n[c] (g·mol^{-1})	Đ (M_w/M_n)
1	1 : 2 : 200	100	40600	1.30

[a]Condition: The polymerization was carried out at ambient temperature in 4.6 mL of toluene using the following procedure: for a 200 ^{t}BA /1 LB/2 LA ratio, $[^tBA]_0$ = 0.936 M (4.8 mmol) and $[LA]_0$ =2 $[LB]_0$ = 9.4mM (0.048 mmol). [b]Monomer conversions measured by ^{1}H NMR. [c]M_n and Đ determined by GPC relative to PMMA standards in THF.

Table S6 Copolymerization of MMA by PyAP-^{t}Bu/MeAl(BHT)$_2$ system

Run[a]	M1/M2/M3	Conv.[b] (%)	M_n[c] (g·mol^{-1})	Đ (M_w/M_n)
1	200MMA/200^{t}BA	MMA:>99 ^{t}BA:>99	22700 49500	1.20 1.50
2	200^{t}BA /200MMA	^{t}BA:>99	-	

MMA:0

[a]Condition: The polymerization was carried out at ambient temperature in 4.6 mL of toluene using the following procedure: for a 200 MMA /1 LB/2 LA ratio, $[MMA]_0$ = 0.936 M (4.8 mmol) and $[LA]_0$ =2 $[LB]_0$ = 9.4mM (0.048 mmol). The reaction mixture was stirred for 20 min, then a 200 ^{t}BA /1 LB/2 LA ratio, ^{t}BA (4.8 mmol) was added. n.d.: not determined. [b]Monomer conversions measured by ^{1}H NMR. [c]M_n and Đ determined by GPC relative to PMMA standards in THF. [d]Initiation efficiency (I*)% = $M_{n(calcd)}/M_{n(exptl)}$ × 100, where $M_{n(calcd)}$ = $[M_W(^tBA)]([^tBA]_0/[I]_0)$(conversion) + M_W of chain end groups.

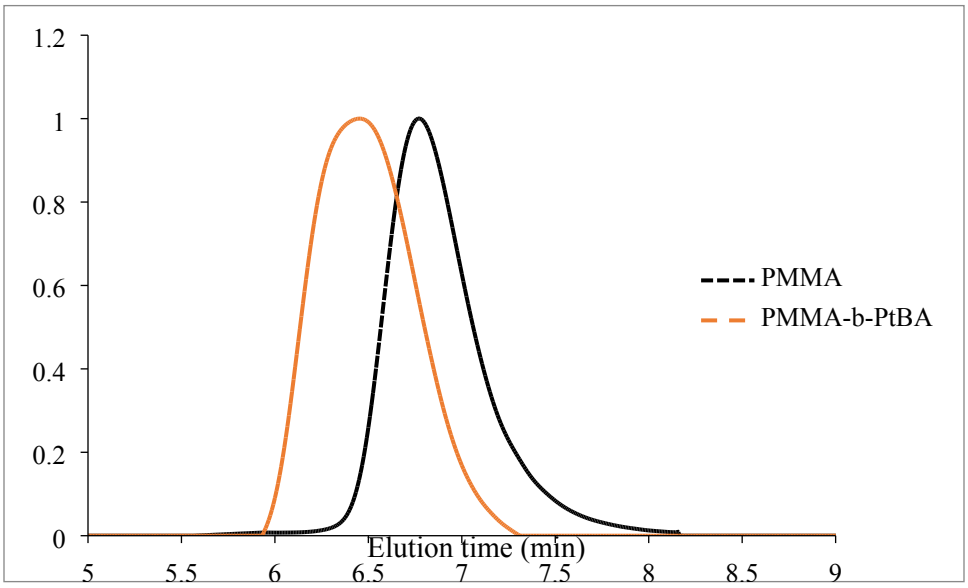

Figure S60 GPC traces of homopolymer (black), diblock copolymer (orange) produced from the sequential block copolymerization of MMA and ^{t}BA by PyAP-^{t}Bu/ MeAl(BHT)$_2$ in toluene at ambient temperature.

4 MALDI-TOF MS Spectra of Low M_W PMMA

MALDI-TOF MS spectra of low-M_W PMMA by PyAP-^{t}Bu/Al(C_6F_5)$_3$

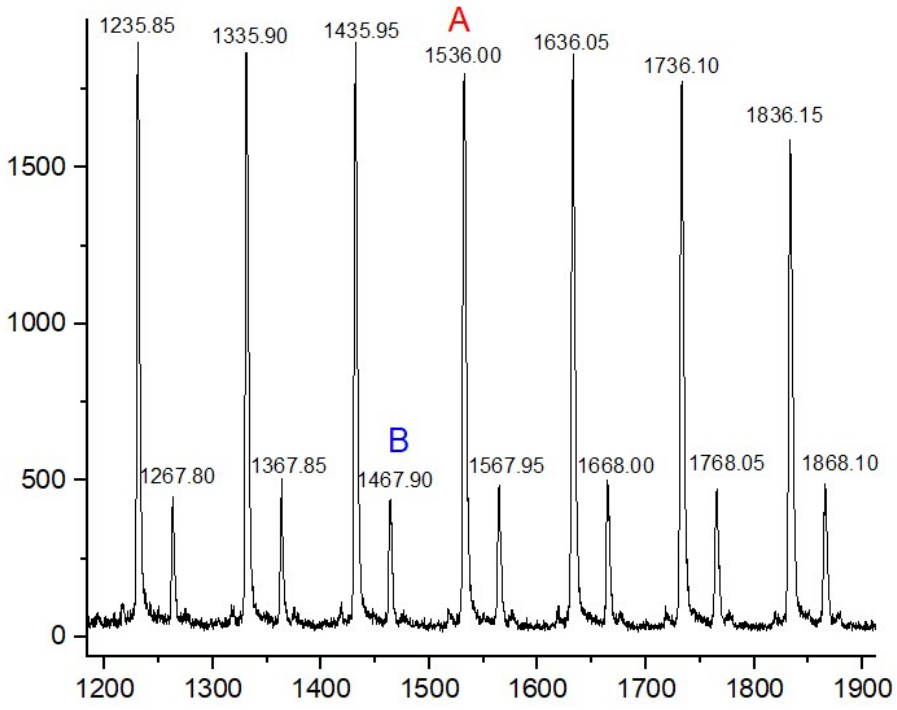

Figure S61. MALDI-TOF MS spectrum of the low-M_W PMMA sample produced by PyAP-^{t}Bu/Al(C_6F_5)$_3$ in toluene at ambient temperature

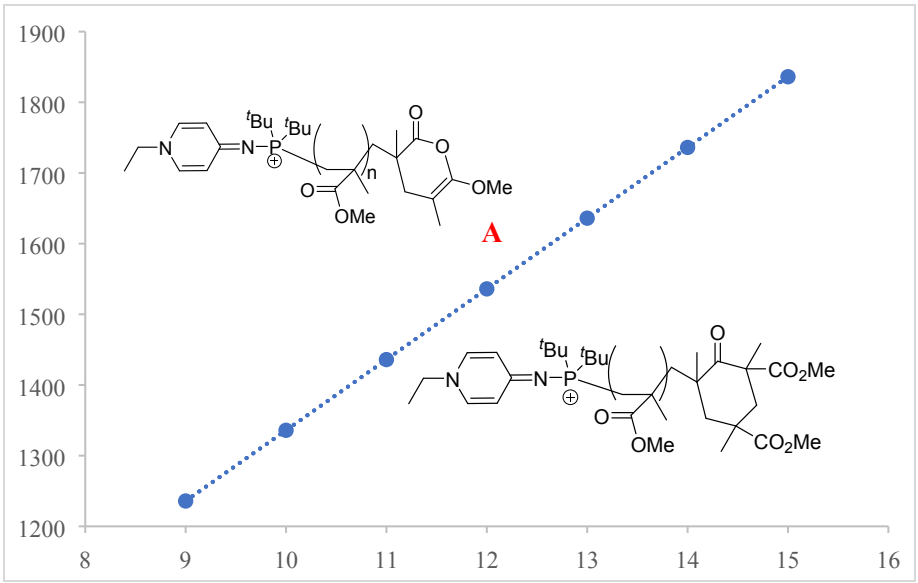

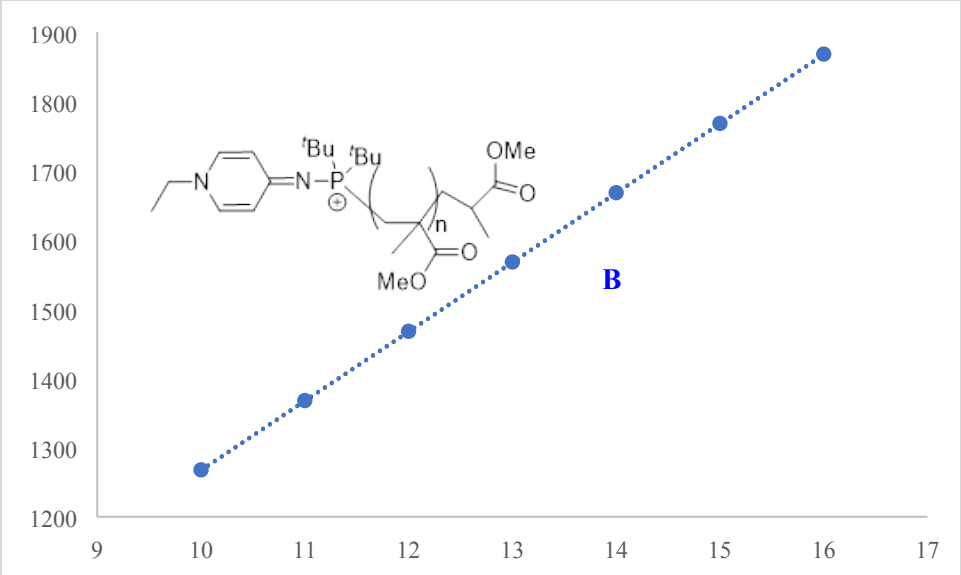

Figure S62. Plot of m/z values taken from Figure S61 vs the number of MMA repeat units (n) and the deduced corresponding polymer chain structure produced by PyAP-^{t}Bu/Al(C_6F_5)$_3$, upper: major peaks **A**, bottom: minor peaks **B**.

MALDI-TOF MS spectra of low-M_W PMMA by PyAP-^{t}Bu/MeAl(BHT)$_2$

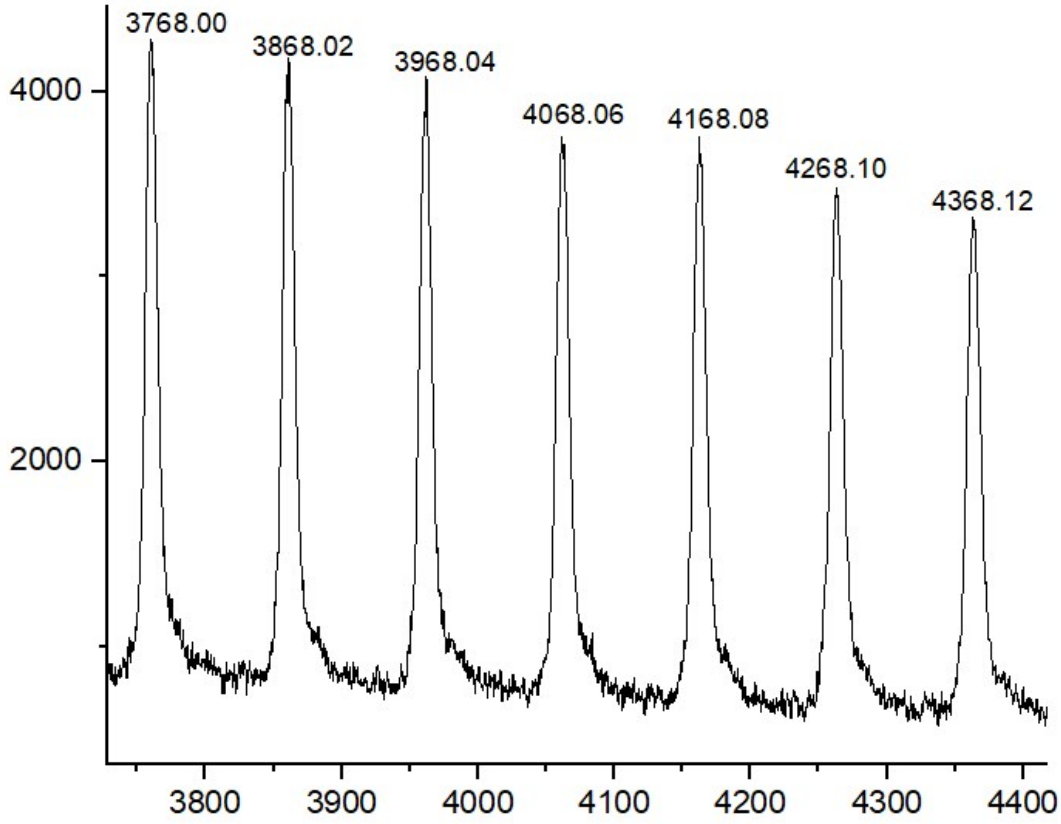

Figure S63. MALDI-TOF MS spectrum of the low-M_W PMMA sample produced by PyAP-^{t}Bu/MeAl(BHT)$_2$ in toluene at ambient temperature

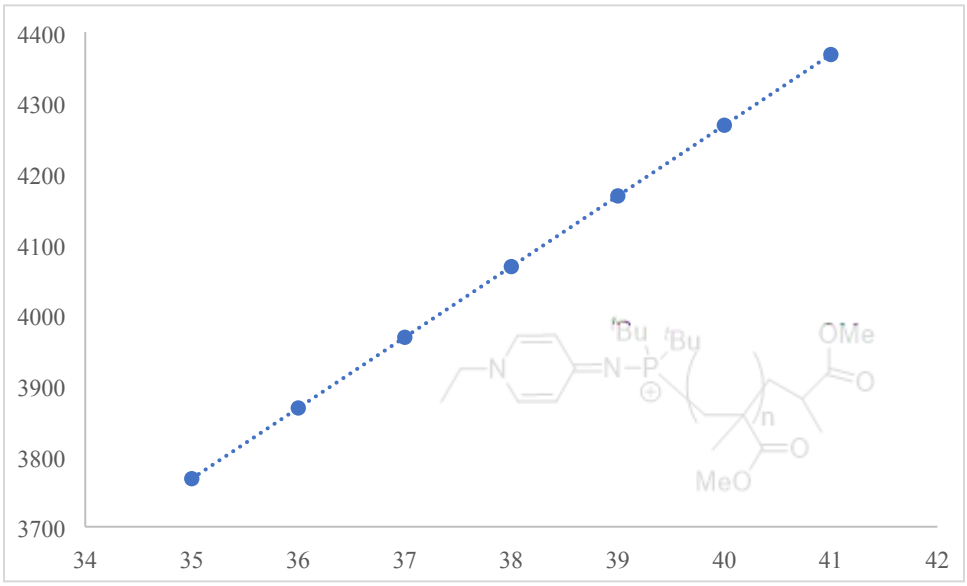

Figure S64. Plot of m/z values taken from Figure S63 vs the number of MMA repeat units (n) and the deduced corresponding polymer chain structure produced by PyAP-^{t}Bu/MeAl(BHT)$_2$.

MALDI-TOF MS spectra of low-M_W PMMA by PyAP-^{t}Bu/ ^{i}BuAl(BHT)$_2$

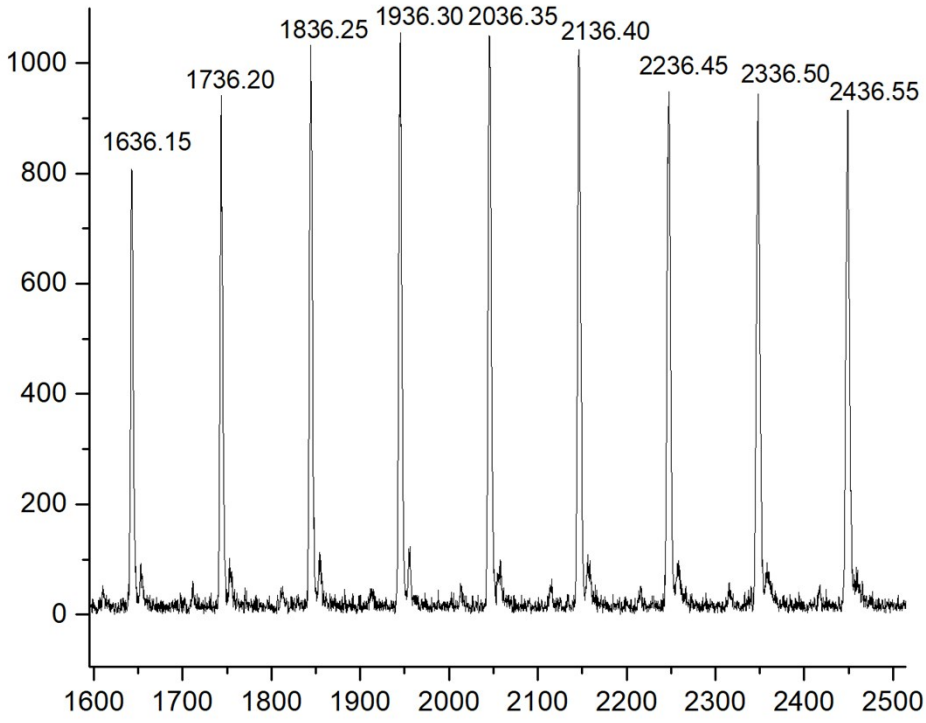

Figure S65. MALDI-TOF MS spectrum of the low-M_W PMMA sample produced by

PyAP-^{t}Bu/ ^{i}BuAl(BHT)$_2$ in toluene at ambient temperature

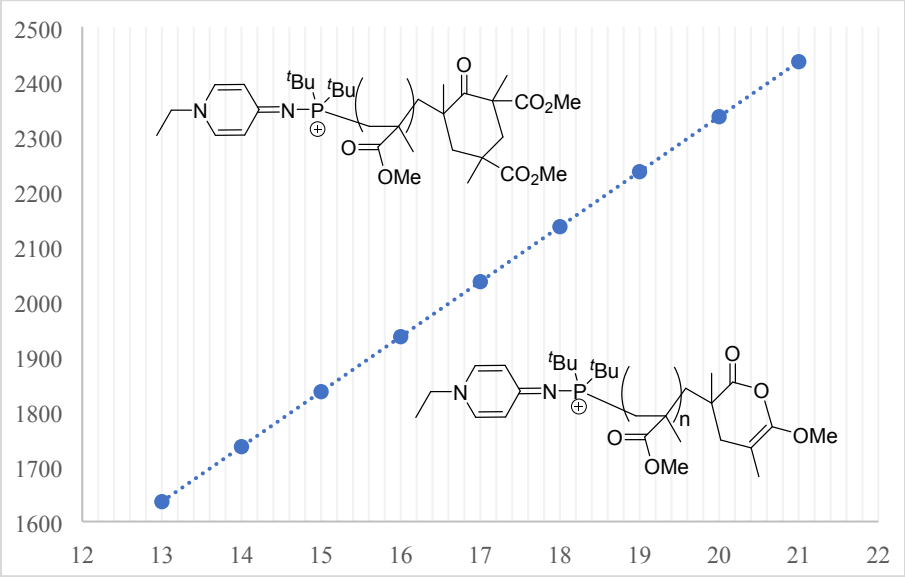

Figure S66. Plot of m/z values taken from Figure S65 vs the number of MMA repeat units (n) and the deduced corresponding polymer chain structure produced by PyAP-^{t}Bu/ ^{i}BuAl(BHT)$_2$.

MALDI-TOF MS spectra of low-M_W PMMA by PyAP-^{t}Bu/^{i}Bu$_2$AlBHT

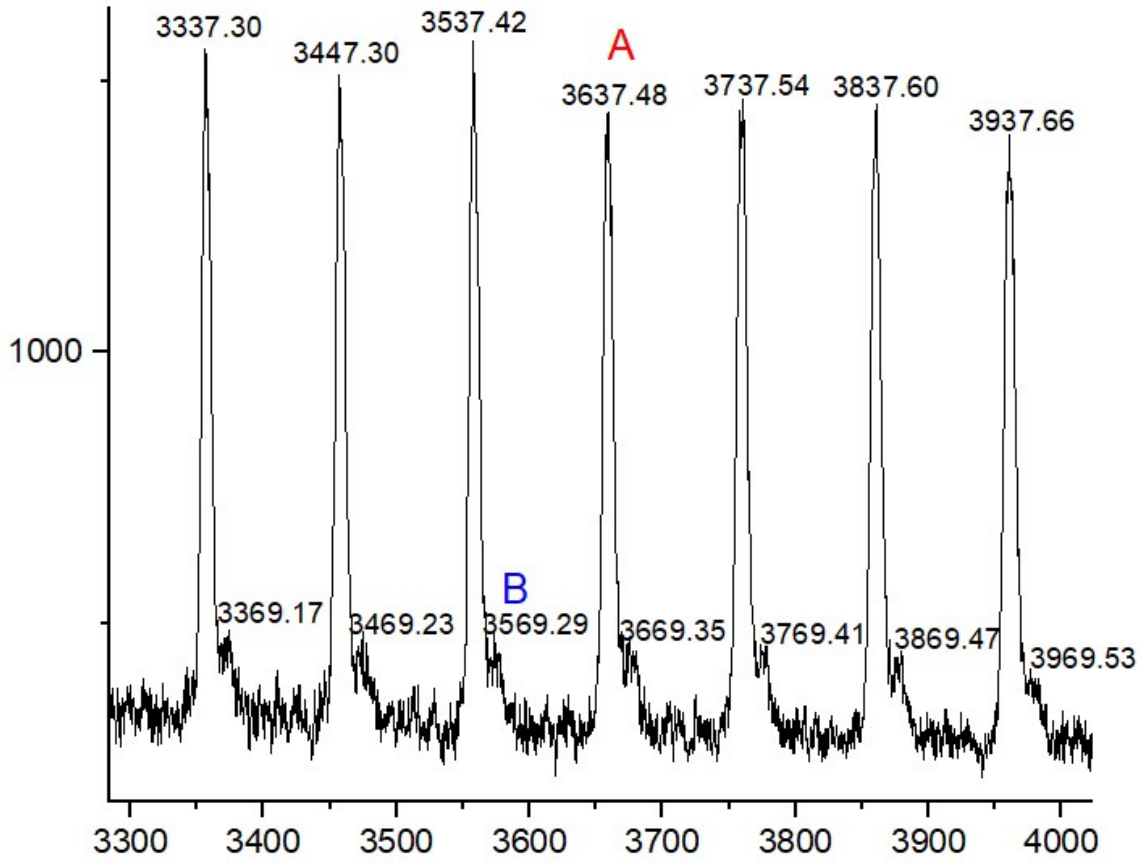

Figure S67. MALDI-TOF MS spectrum of the low-M_W PMMA sample produced by PyAP-^{t}Bu/^{i}Bu$_2$AlBHT in toluene at ambient temperature

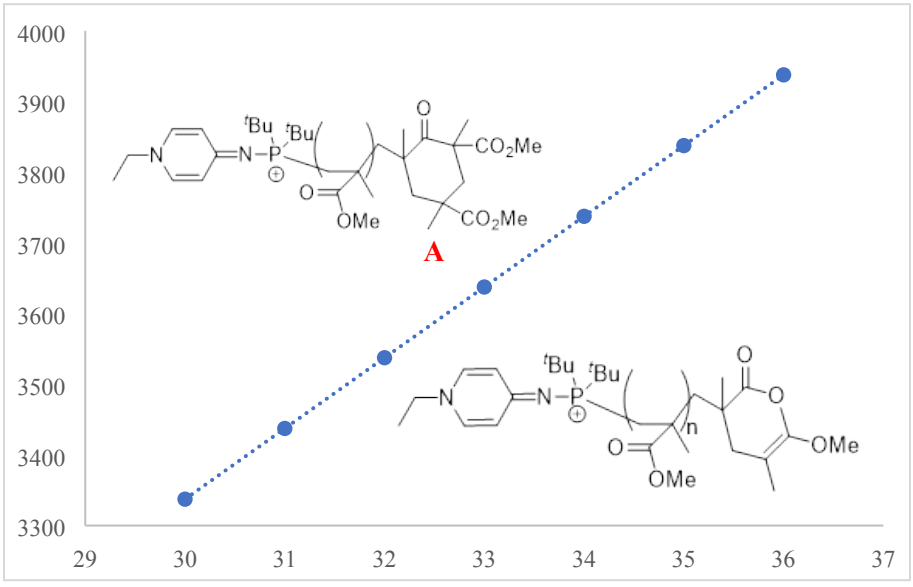

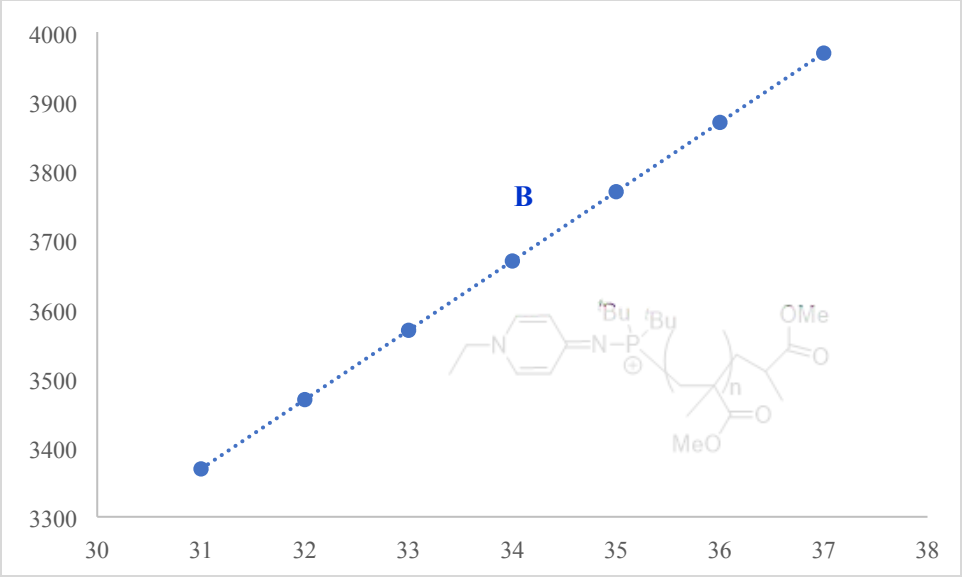

Figure S68. Plot of m/z values taken from Figure S67 vs the number of MMA repeat units (n) and the deduced corresponding polymer chain structure produced by PyAP-^{t}Bu/^{i}Bu$_2$AlBHT, upper: major peaks (**A**), bottom: minor peaks (**B**).

MALDI-TOF MS spectra of low-M_W PMMA by PyAP-Cy/MeAl(BHT)$_2$

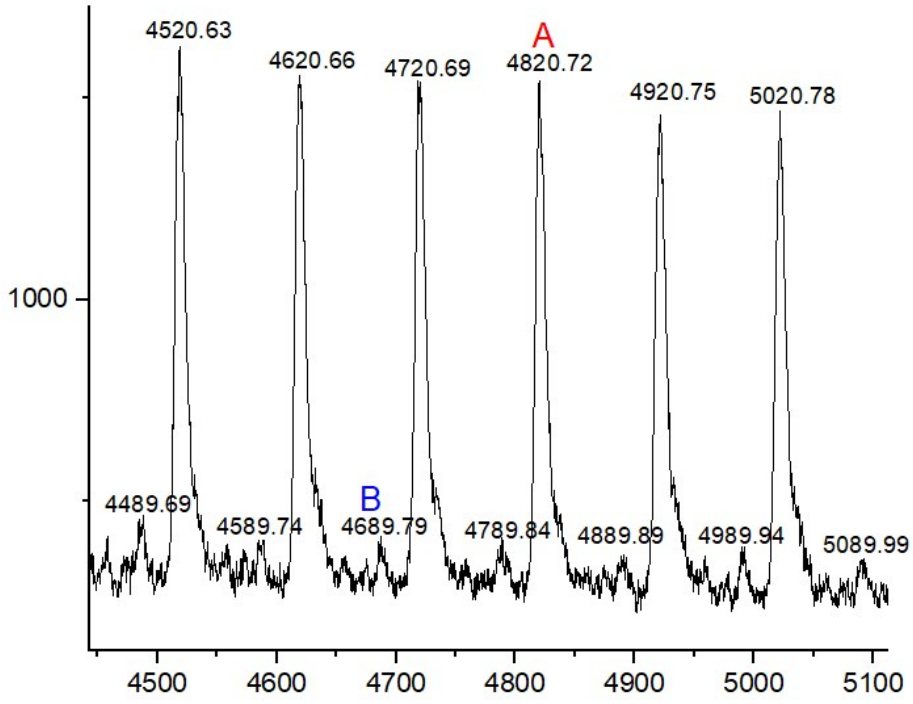

Figure S69. MALDI-TOF MS spectrum of the low-M_W PMMA sample produced by PyAP-Cy/MeAl(BHT)$_2$ in toluene at ambient temperature

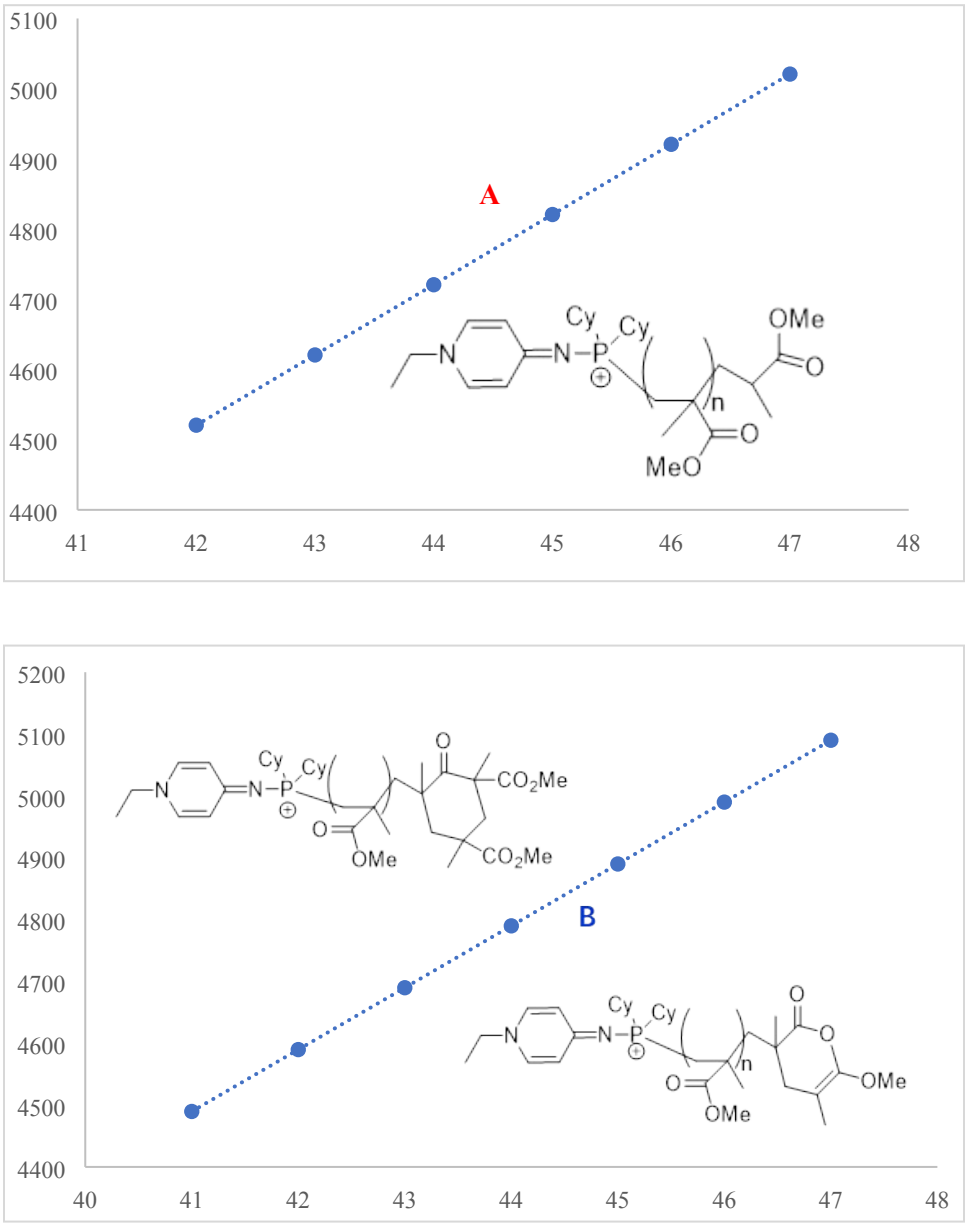

Figure S70. Plot of m/z values taken from Figure S69 vs the number of MMA repeat units (n) and the deduced corresponding polymer chain structure produced by PyAP-Cy/MeAl(BHT)$_2$, upper: major peaks (**A**), bottom: minor peaks (**B**).

MALDI-TOF MS spectra of low-M_W PMMA by PyAP-Cy/^{i}BuAl(BHT)$_2$

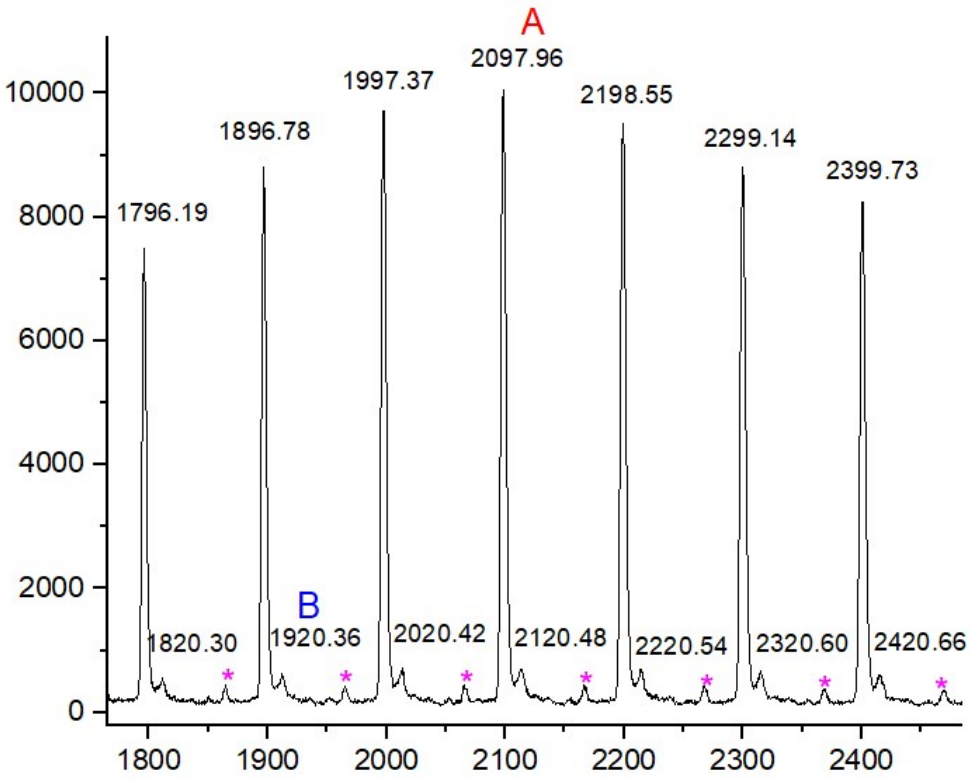

Figure S71. MALDI-TOF MS spectrum of the low-M_W PMMA sample produced by PyAP-Cy/^{i}BuAl(BHT)$_2$ in toluene at ambient temperature

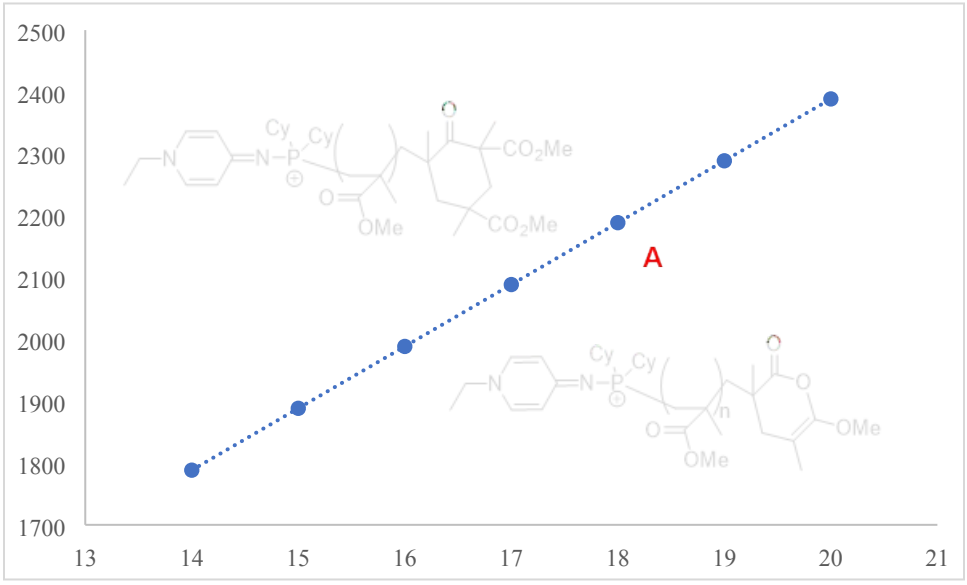

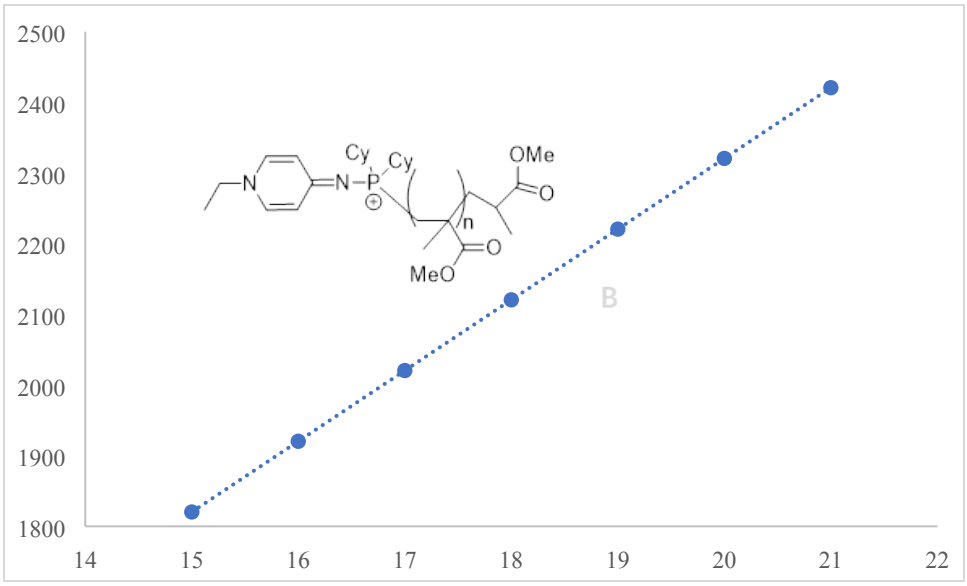

Pink(*): unidentified species

Figure S72. Plot of m/z values taken from Figure S71 vs the number of MMA repeat units (n) and the deduced corresponding polymer chain structure produced by PyAP-Cy/^{i}BuAl(BHT)$_2$, upper: major peaks (**A**), bottom: minor peaks (**B**).

MALDI-TOF MS spectra of low-M_W PMMA by PyAP-Cy/^{i}Bu$_2$Al(BHT)

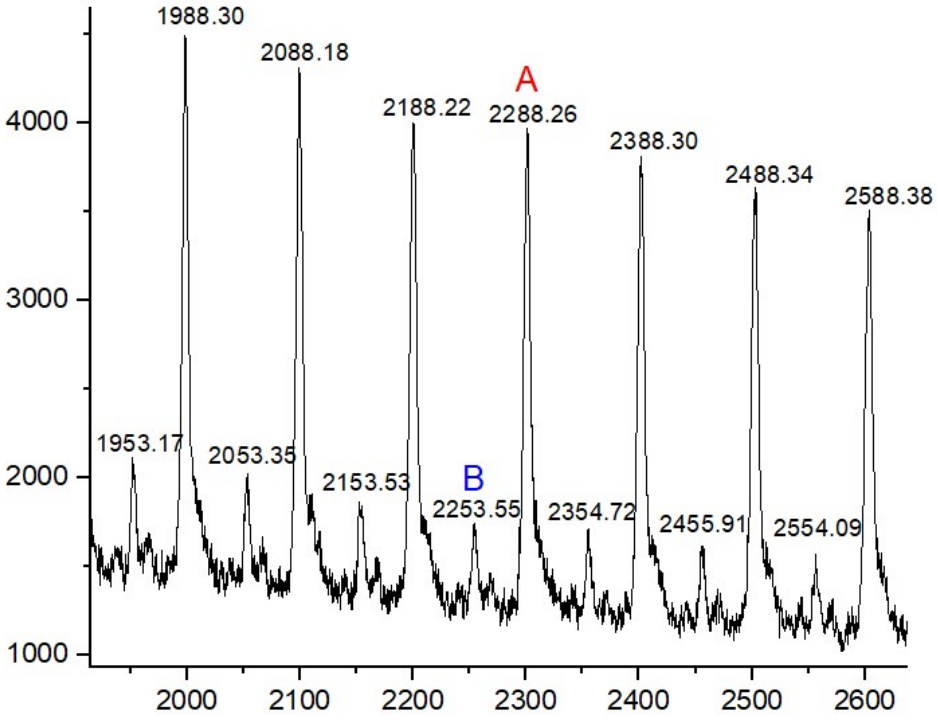

Figure S73. MALDI-TOF MS spectrum of the low-M_W PMMA sample produced by PyAP-Cy/^{i}Bu$_2$Al(BHT) in toluene at ambient temperature

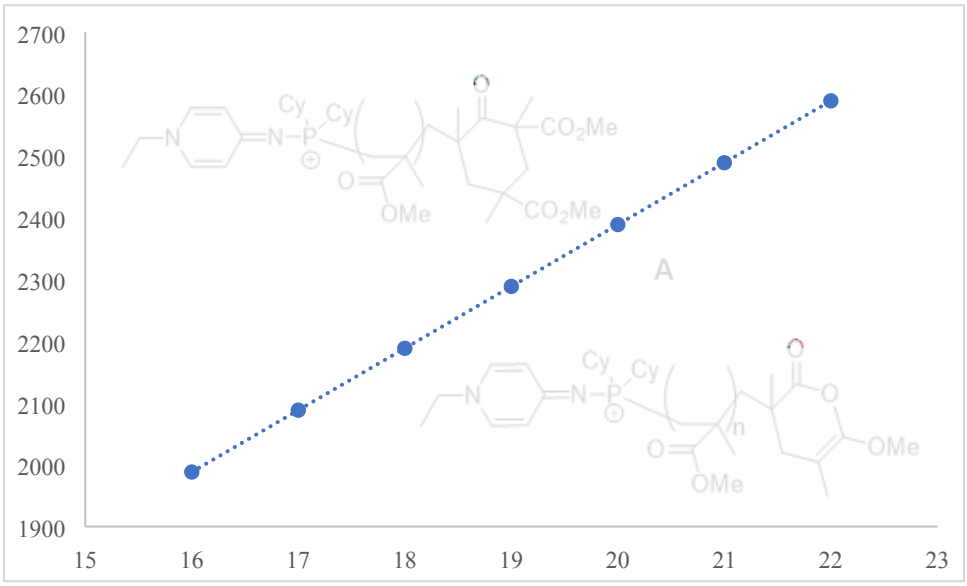

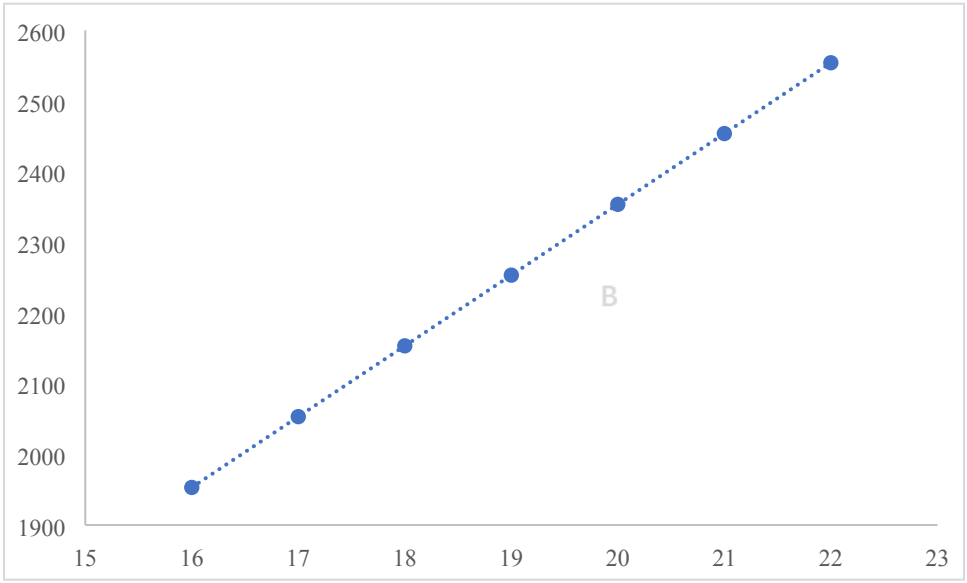

Figure S74. Plot of m/z values taken from Figure S73 vs the number of MMA repeat units (n) and the deduced corresponding polymer chain structure produced by PyAP-Cy/$^{i}Bu_2Al(BHT)$, upper: major peaks (**A**), bottom: minor peaks (**B**). Species B was not identified.

MALDI-TOF MS spectra of low-M_W PMMA by PyAP-^{i}Pr+$MeAl(BHT)_2$

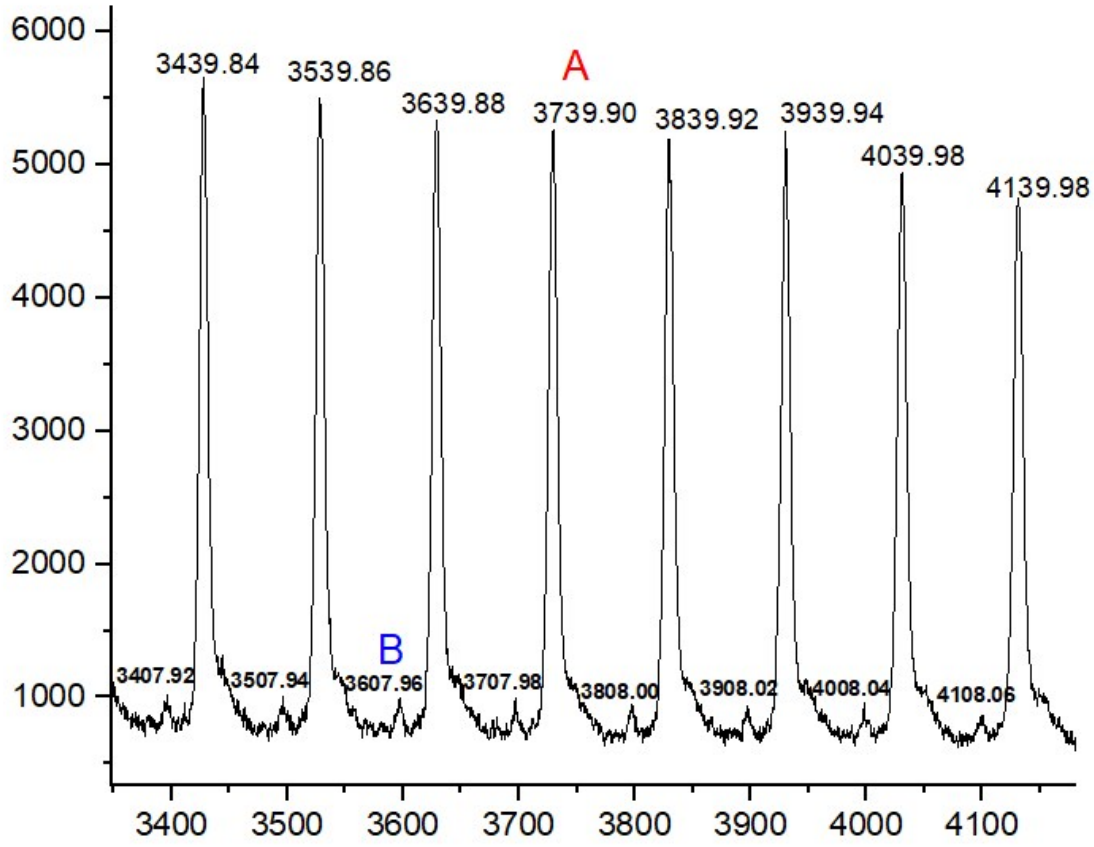

Figure S75. MALDI-TOF MS spectrum of the low-M_W PMMA sample produced by PyAP-^{i}Pr+MeAl(BHT)$_2$ in toluene at ambient temperature

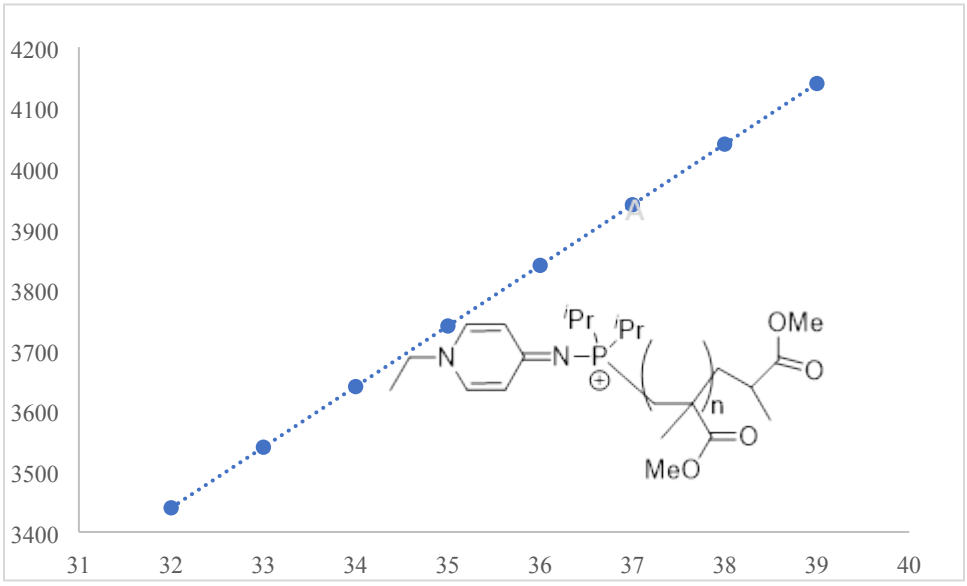

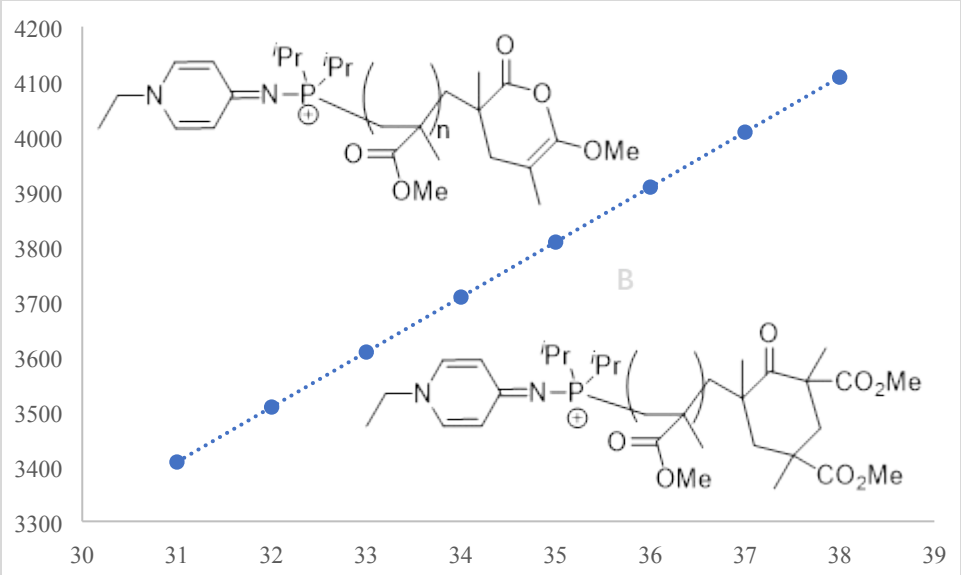

Figure S76. Plot of m/z values taken from Figure S75 vs the number of MMA repeat units (n) and the deduced corresponding polymer chain structure produced by PyAP-^{i}Pr+MeAl(BHT)$_2$, upper: major peaks (**A**), bottom: minor peaks (**B**).

MALDI-TOF MS spectra of low-M_W PMMA by PyAP-^{i}Pr+^{i}BuAl(BHT)$_2$

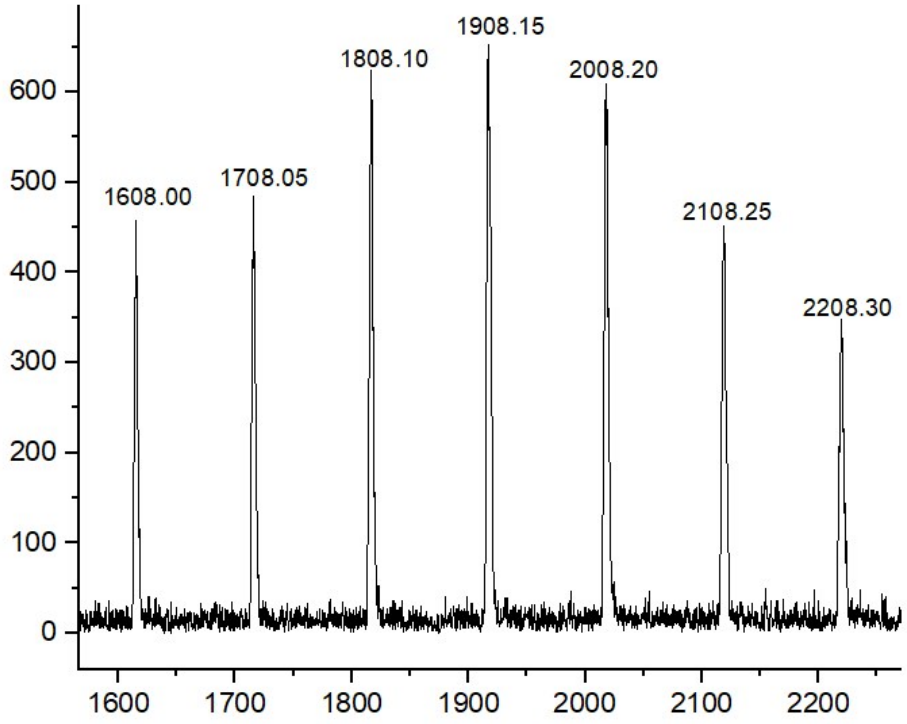

Figure S77. MALDI-TOF MS spectrum of the low-M_W PMMA sample produced by PyAP-^{i}Pr+^{i}BuAl(BHT)$_2$ in toluene at ambient temperature

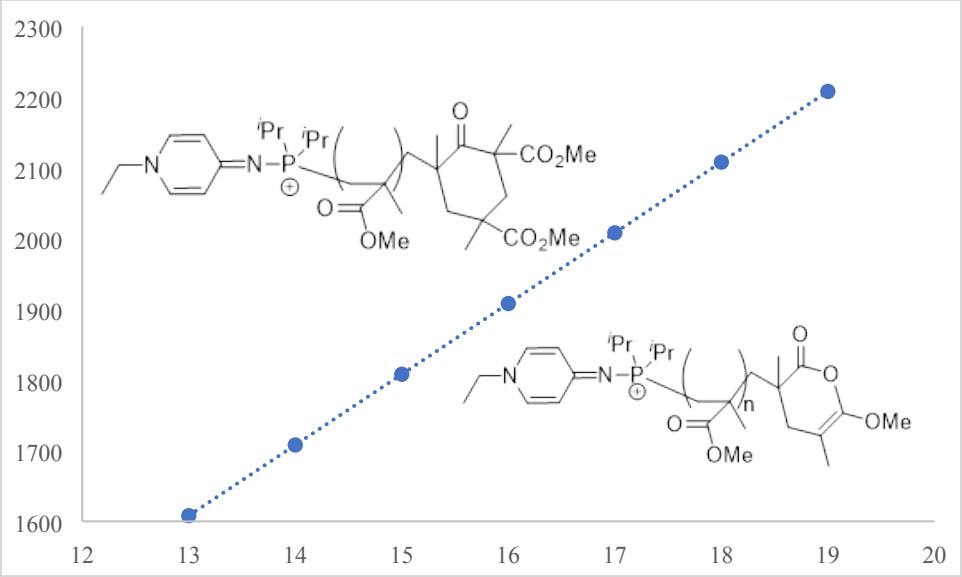

Figure S78. Plot of m/z values taken from Figure S77 vs the number of MMA repeat units (n) and the deduced corresponding polymer chain structure produced by PyAP-^{i}Pr+^{i}BuAl(BHT)$_2$

MALDI-TOF MS spectra of low-M_W PMMA by PyAP-^{i}Pr+^{i}Bu$_2$AlBHT

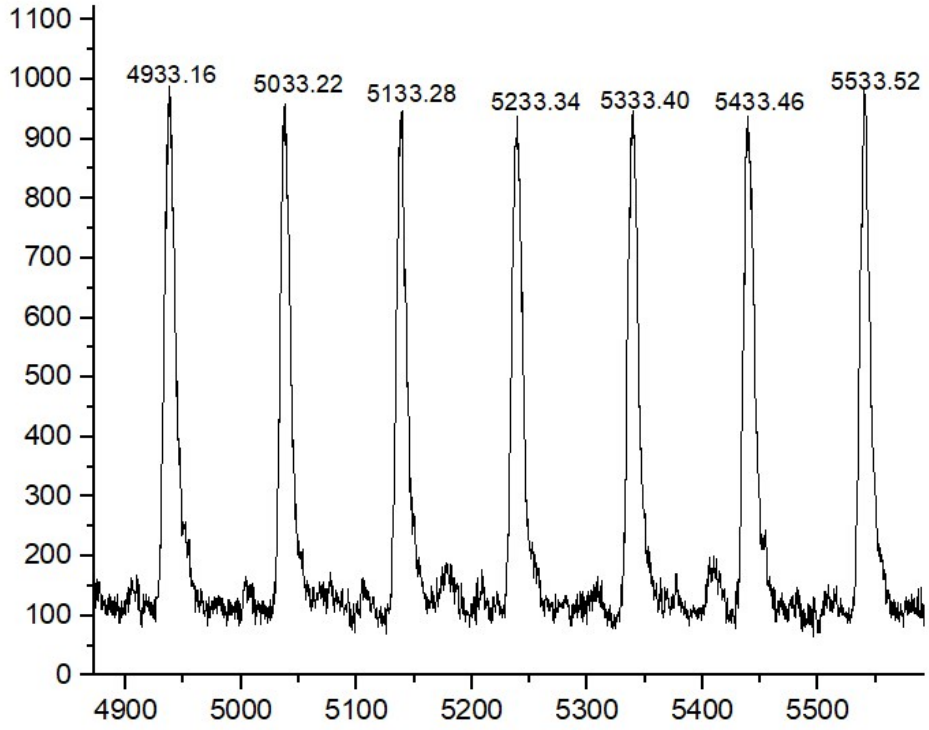

Figure S79. MALDI-TOF MS spectrum of the low-M_W PMMA sample produced by PyAP-^{i}Pr+^{i}Bu$_2$AlBHT in toluene at ambient temperature

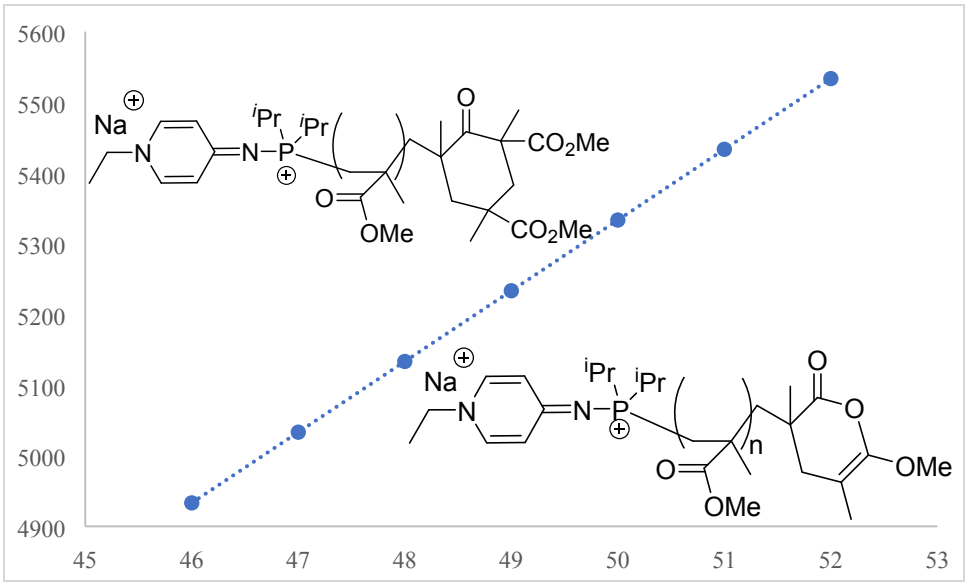

Figure S80. Plot of m/z values taken from Figure S79 vs the number of MMA repeat units (n) and the deduced corresponding polymer chain structure produced by PyAP-^{i}Pr+^{i}Bu$_2$AlBHT.

MALDI-TOF MS spectra of low-M_W PMMA by PyAP-Ph+MeAl(BHT)$_2$

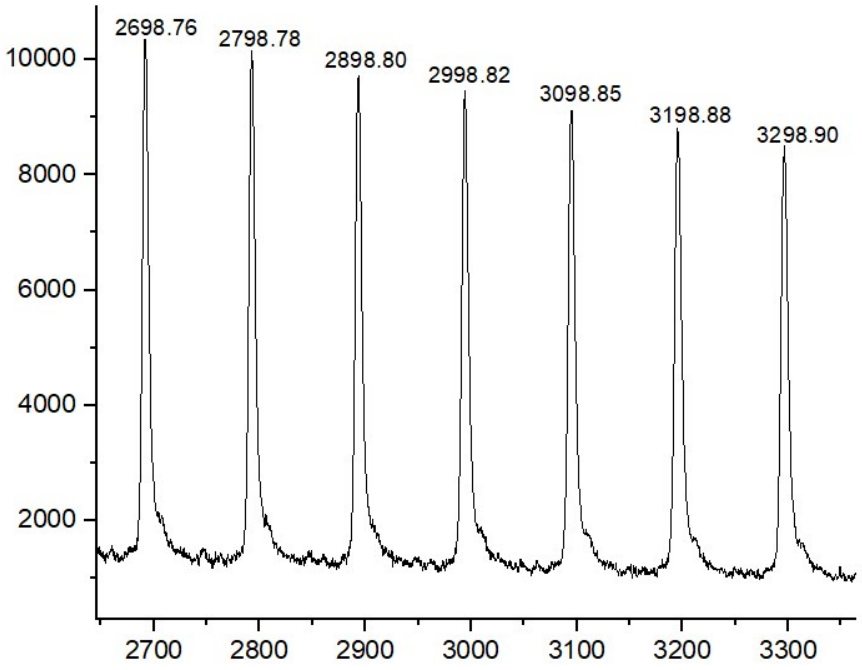

Figure S81. MALDI-TOF MS spectrum of the low-M_W PMMA sample produced by PyAP-Ph+MeAl(BHT)$_2$ in toluene at ambient temperature

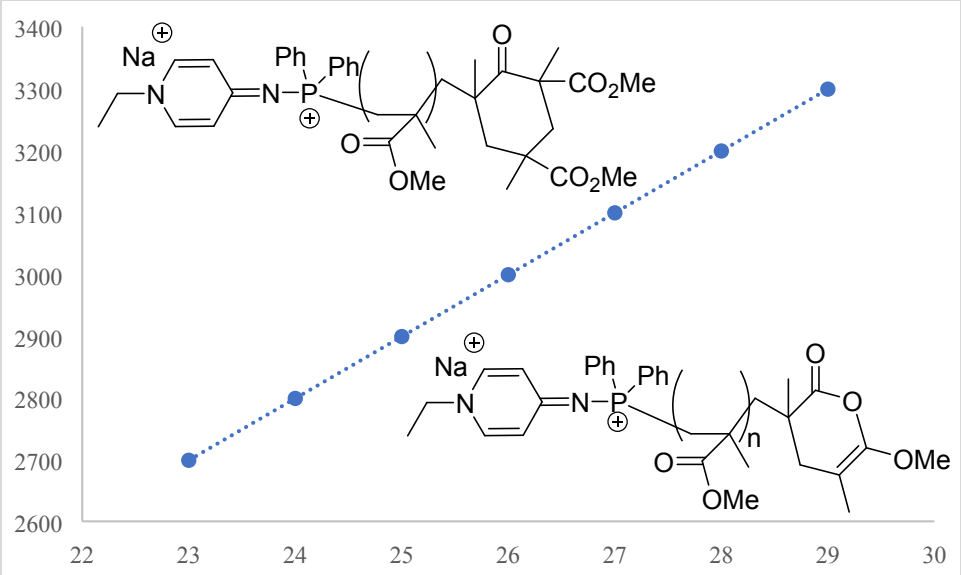

Figure S82. Plot of m/z values taken from Figure S81 vs the number of MMA repeat units (n) and the deduced corresponding polymer chain structure produced by PyAP-Ph+MeAl(BHT)$_2$

MALDI-TOF MS spectra of low-M$_W$ PMMA by PyAP-Ph+^{i}BuAl(BHT)$_2$

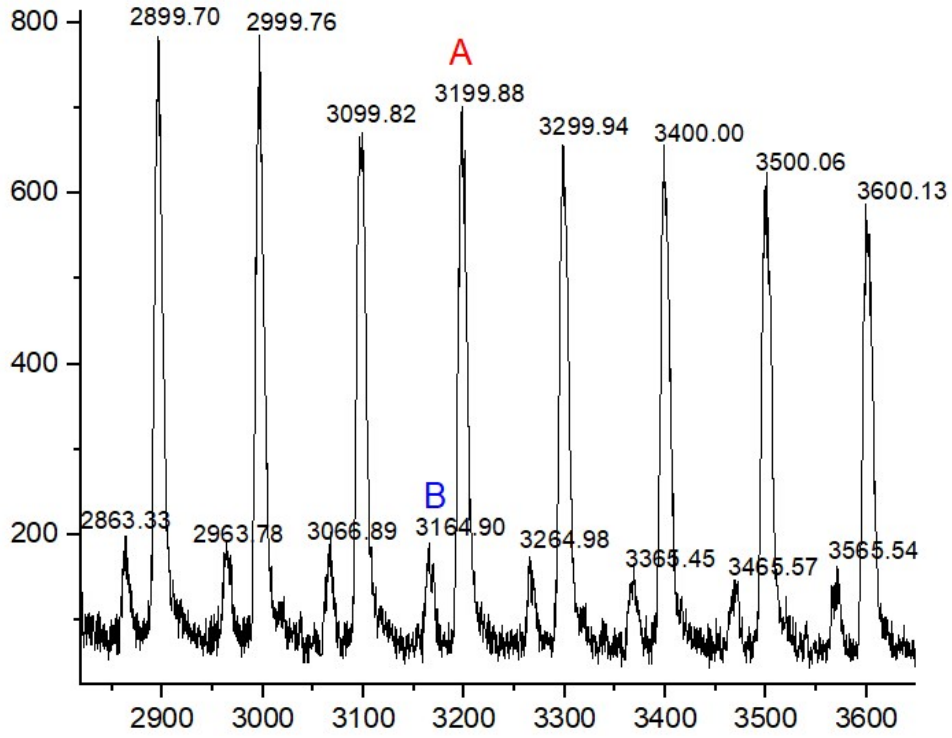

Figure S83. MALDI-TOF MS spectrum of the low-M$_W$ PMMA sample produced by

PyAP-Ph+^{i}BuAl(BHT)$_2$ in toluene at ambient temperature

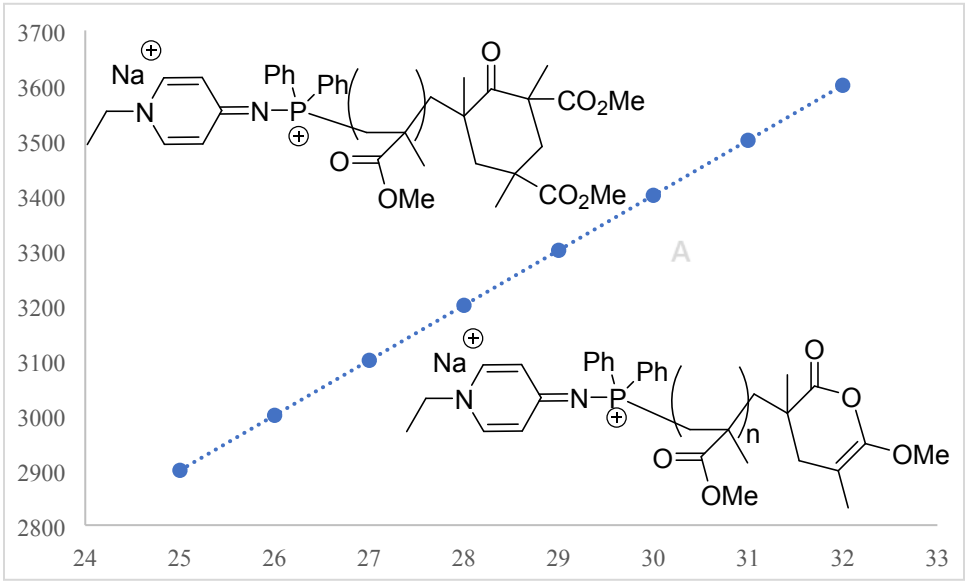

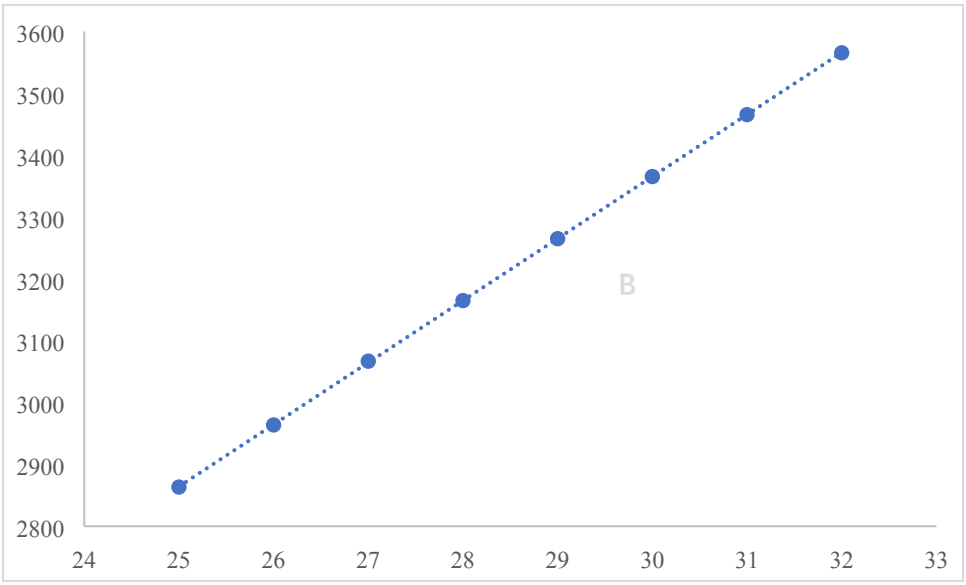

Figure S84. Plot of m/z values taken from Figure S83 vs the number of MMA repeat units (n) and the deduced corresponding polymer chain structure produced by PyAP-Ph+^{i}BuAl(BHT)$_2$, upper: major peaks (**A**), bottom: minor peaks (**B**). Species B was not identified.

MALDI-TOF MS spectra of low-M_W PMMA by PyAP-Ph+^{i}Bu$_2$AlBHT

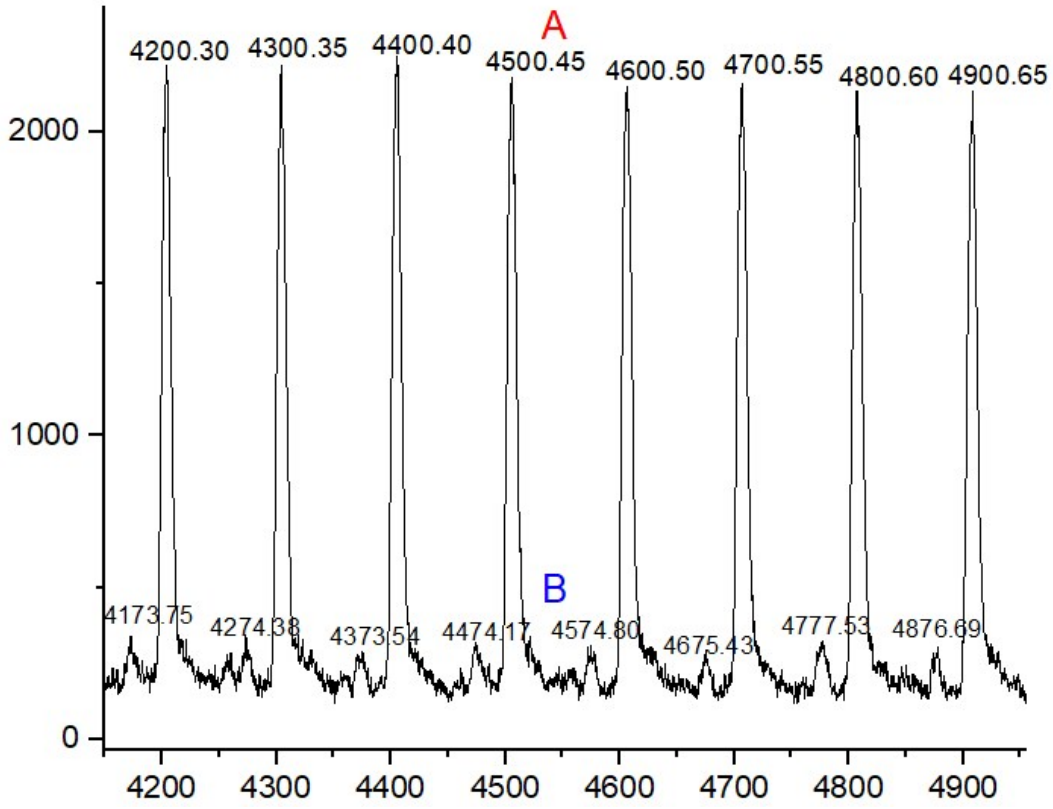

Figure S85. MALDI-TOF MS spectrum of the low-M_W PMMA sample produced by PyAP-Ph+^{i}Bu$_2$AlBHT in toluene at ambient temperature

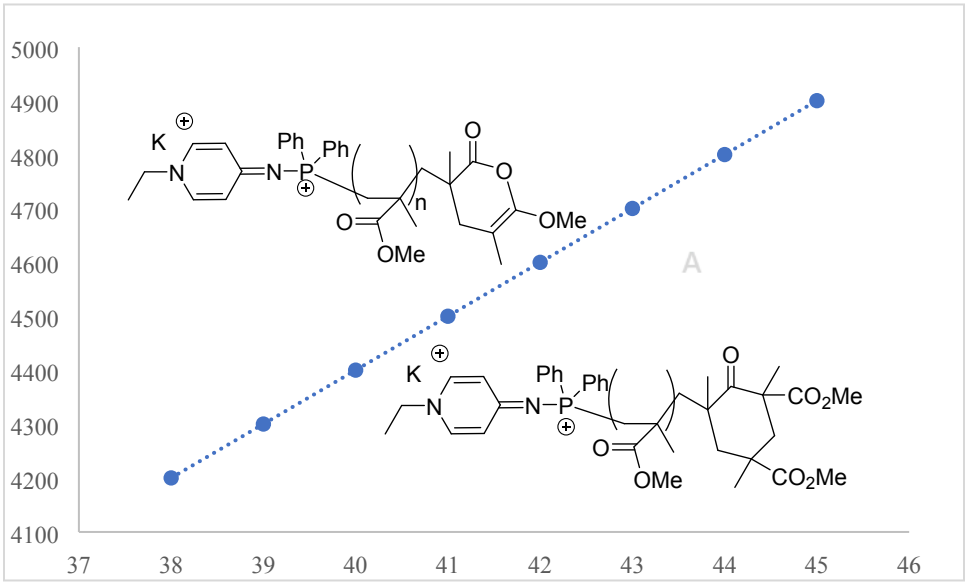

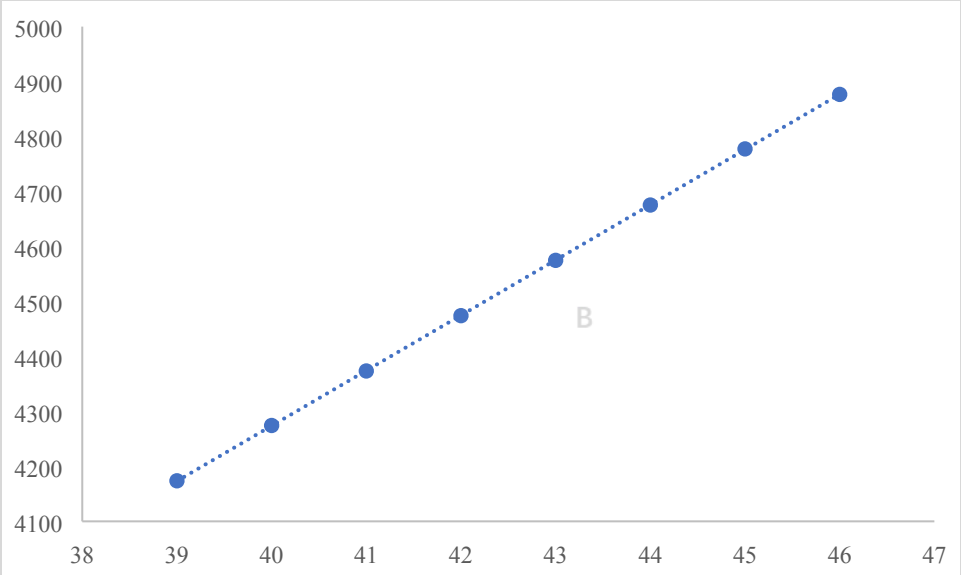

Figure S86. Plot of m/z values taken from Figure S85 vs the number of MMA repeat units (n) and the deduced corresponding polymer chain structure produced by PyAP-Ph+^{i}Bu$_2$AlBHT, upper: major peaks (**A**), bottom: minor peaks (**B**). Species B was not identified.

5 X-ray data of PyAP-^{t}Bu and INT1

CCDC numbers of PyAP-^{t}Bu is 1996418. These data can be obtained free of charge from The Cambridge Crystallographic Data Centre via www.ccdc.cam.ac.uk/data_request/cif.

Table S2 Crystal data and structure refinement for 1996418.

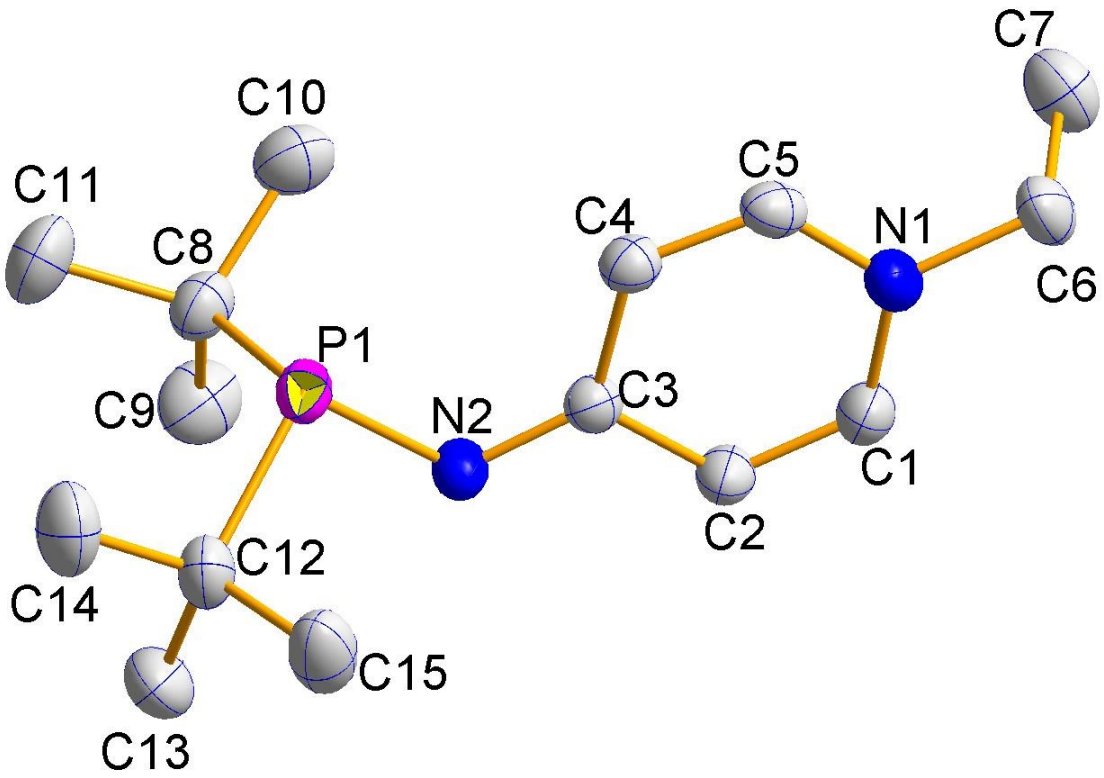

Figure S87. X-ray crystal structure of zwitterion **PyAP-^{t}Bu**. Hydrogen atoms and Fluorine atom are omitted for clarity and ellipsoids drawn at 30% probability (CCDC # 1996418).

Table S7 X-ray diffraction data of PyAP-^{t}Bu

Identification	
Code	1996418
Formula sum	C15H27N2P
Formula weight	266.36 g/mol
Crystal system	monoclinic
Space-group	P 1 21/c 1 (14)
Cell parameters	a=12.9533(7) Å b=12.0272(4) Å c=11.7499(6) Å β=116.824(5)°
Cell ratio	a/b=1.0770 b/c=1.0236 c/a=0.9071
Cell volume	1633.57(15) Å^3
Z	4
Calc. density	1.08297 g/cm^3
Meas. density	
Melting point	
RAll	0.0529
RObs	

Pearson code	mP180
Formula type	NO2P15Q27
Wyckoff sequence	e45

Selected geometric informations

Atoms 1,2	d 1,2 [Å]	Atoms 1,2	d 1,2 [Å]
N1-C5	1.357(2)	C8-C10	1.539(3)
N1-C1	1.359(2)	C9-H9A	0.9600
N1-C6	1.468(2)	C9-H9B	0.9600
N2-C3	1.306(2)	C9-H9C	0.9600
N2-P1	1.7196(15)	C10-H10A	0.9600
P1-C12	1.878(2)	C10-H10B	0.9600
P1-C8	1.886(2)	C10-H10C	0.9600
C1-C2	1.343(3)	C11-H11A	0.9600
C1-H1	0.9300	C11-H11B	0.9600
C2-C3	1.440(2)	C11-H11C	0.9600
C2-H2	0.9300	C12-C13	1.524(3)
C3-C4	1.446(2)	C12-C15	1.541(3)
C4-C5	1.344(3)	C12-C14	1.541(3)
C4-H4	0.9300	C13-H13A	0.9600
C5-H5	0.9300	C13-H13B	0.9600
C6-C7	1.497(3)	C13-H13C	0.9600
C6-H6A	0.9700	C14-H14A	0.9600
C6-H6B	0.9700	C14-H14B	0.9600
C7-H7A	0.9600	C14-H14C	0.9600
C7-H7B	0.9600	C15-H15A	0.9600
C7-H7C	0.9600	C15-H15B	0.9600
C8-C11	1.529(3)	C15-H15C	0.9600
C8-C9	1.532(3)		

Atoms 1,2,3	Angle 1,2,3 [°]	Atoms 1,2,3	Angle 1,2,3 [°]
C5-N1-C1	117.68(15)	C8-C9-H9B	109.500
C5-N1-C6	121.08(16)	H9A-C9-H9B	109.500
C1-N1-C6	121.12(17)	C8-C9-H9C	109.500
C3-N2-P1	119.59(12)	H9A-C9-H9C	109.500
N2-P1-C12	99.09(9)	H9B-C9-H9C	109.500
N2-P1-C8	100.03(9)	C8-C10-H10A	109.500
C12-P1-C8	110.07(9)	C8-C10-H10B	109.500
C2-C1-N1	122.31(18)	H10A-C10-H10B	109.500
C2-C1-H1	118.800	C8-C10-H10C	109.500
N1-C1-H1	118.800	H10A-C10-H10C	109.500
C1-C2-C3	122.74(17)	H10B-C10-H10C	109.500
C1-C2-H2	118.600	C8-C11-H11A	109.500
C3-C2-H2	118.600	C8-C11-H11B	109.500
N2-C3-C2	119.54(15)	H11A-C11-H11B	109.500
N2-C3-C4	128.16(16)	C8-C11-H11C	109.500
C2-C3-C4	112.29(15)	H11A-C11-H11C	109.500

C5-C4-C3	121.83(17)	H11B-C11-H11C	109.500
C5-C4-H4	119.100	C13-C12-C15	109.1(2)
C3-C4-H4	119.100	C13-C12-C14	110.55(19)
C4-C5-N1	123.13(16)	C15-C12-C14	107.1(2)
C4-C5-H5	118.400	C13-C12-P1	116.95(17)
N1-C5-H5	118.400	C15-C12-P1	104.43(14)
N1-C6-C7	112.21(18)	C14-C12-P1	108.21(16)
N1-C6-H6A	109.200	C12-C13-H13A	109.500
C7-C6-H6A	109.200	C12-C13-H13B	109.500
N1-C6-H6B	109.200	H13A-C13-H13B	109.500
C7-C6-H6B	109.200	C12-C13-H13C	109.500
H6A-C6-H6B	107.900	H13A-C13-H13C	109.500
C6-C7-H7A	109.500	H13B-C13-H13C	109.500
C6-C7-H7B	109.500	C12-C14-H14A	109.500
H7A-C7-H7B	109.500	C12-C14-H14B	109.500
C6-C7-H7C	109.500	H14A-C14-H14B	109.500
H7A-C7-H7C	109.500	C12-C14-H14C	109.500
H7B-C7-H7C	109.500	H14A-C14-H14C	109.500
C11-C8-C9	110.4(2)	H14B-C14-H14C	109.500
C11-C8-C10	108.30(19)	C12-C15-H15A	109.500
C9-C8-C10	107.9(2)	C12-C15-H15B	109.500
C11-C8-P1	110.14(16)	H15A-C15-H15B	109.500
C9-C8-P1	116.44(15)	C12-C15-H15C	109.500
C10-C8-P1	103.12(14)	H15A-C15-H15C	109.500
C8-C9-H9A	109.500	H15B-C15-H15C	109.500

Atoms 1,2,3,4	**Tors. an. 1,2,3,4 [°]**	**Atoms 1,2,3,4**	**Tors. an. 1,2,3,4 [°]**
C3-N2-P1-C12	-141.28(15)	C5-N1-C6-C7	-80.1(3)
C3-N2-P1-C8	106.32(16)	C1-N1-C6-C7	95.8(2)
C5-N1-C1-C2	0.0(3)	N2-P1-C8-C11	167.32(16)
C6-N1-C1-C2	-176.01(19)	C12-P1-C8-C11	63.71(18)
N1-C1-C2-C3	1.1(3)	N2-P1-C8-C9	40.70(19)
P1-N2-C3-C2	176.01(13)	C12-P1-C8-C9	-62.9(2)
P1-N2-C3-C4	-3.7(3)	N2-P1-C8-C10	-77.28(14)
C1-C2-C3-N2	179.01(19)	C12-P1-C8-C10	179.10(14)
C1-C2-C3-C4	-1.3(3)	N2-P1-C12-C13	-60.10(17)
N2-C3-C4-C5	-179.79(19)	C8-P1-C12-C13	44.15(19)
C2-C3-C4-C5	0.5(3)	N2-P1-C12-C15	60.50(18)
C3-C4-C5-N1	0.5(3)	C8-P1-C12-C15	164.75(17)
C1-N1-C5-C4	-0.8(3)	N2-P1-C12-C14	174.31(15)
C6-N1-C5-C4	175.23(18)	C8-P1-C12-C14	-81.44(17)

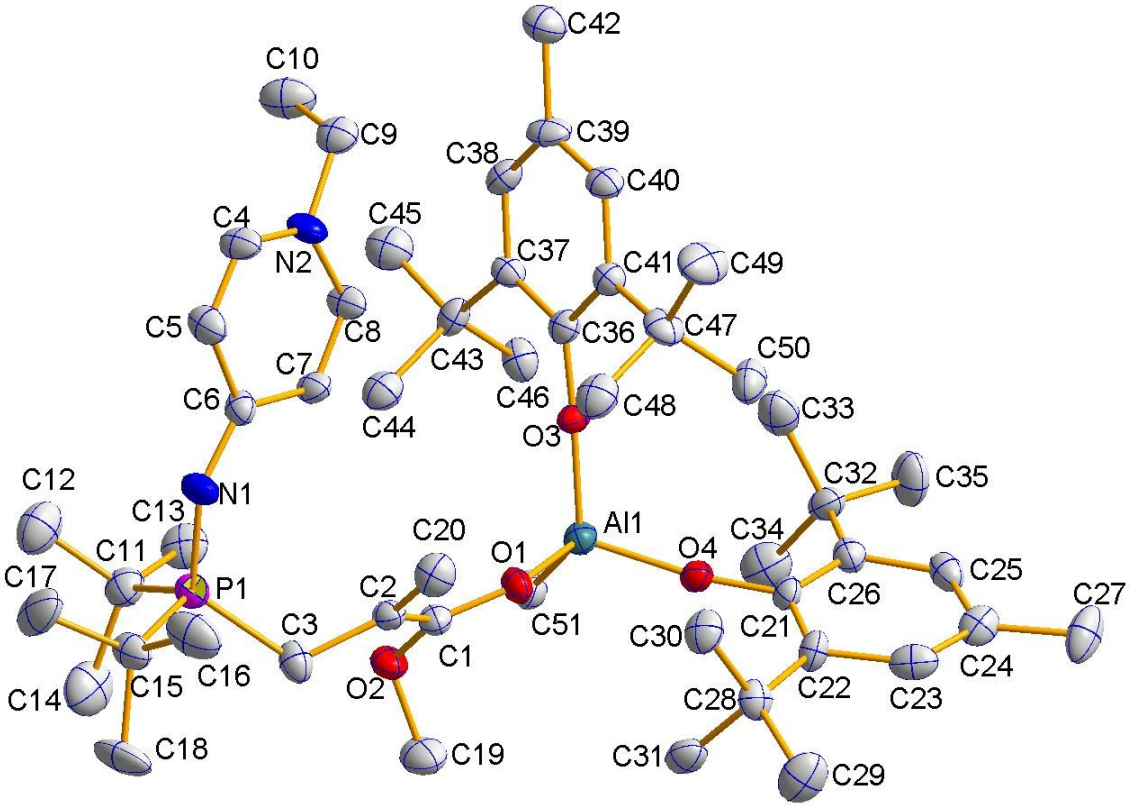

Figure S88. X-ray crystal structure of zwitterion **INT1**. Hydrogen atoms and Fluorine atom are omitted for clarity and ellipsoids drawn at 15% probability (CCDC # 2011850).

Table S8 X-ray diffraction data of INT1.

Identification	
Code	C51H84AlN2O4P
Formula weight	847.15 g/mol
Crystal system	orthorhombic
Space-group	P n a 21 (33)
Cell parameters	a=23.690(2) Å b=12.7455(11) Å c=23.188(2) Å
Cell ratio	a/b=1.8587 b/c=0.5497 c/a=0.9788
Cell volume	7001.41(104) Å^3
Z	4
Calc. density	0.803634 g/cm^3
Meas. density	0 g/cm^3
Melting point	
RAll	0.1243
RObs	
Pearson code	oP572
Formula type	NOP2Q4R51...
Wyckoff sequence	a143

Selected geometric informations

Atoms 1,2	d 1,2 [?]	Atoms 1,2	d 1,2 [?]
Al1-O3	1.729(3)	C24-C27	1.527(6)
Al1-O1	1.748(3)	C25-C26	1.431(6)
Al1-O4	1.749(3)	C25-H25	0.9300

Al1-C51	1.961(4)	C26-C32	1.506(6)
P1-N1	1.550(4)	C27-H27A	0.9600
P1-C3	1.814(4)	C27-H27B	0.9600
P1-C15	1.840(5)	C27-H27C	0.9600
P1-C11	1.860(6)	C28-C31	1.489(5)
N1-C6	1.316(5)	C28-C30	1.508(5)
N2-C4	1.324(5)	C28-C29	1.567(5)
N2-C8	1.329(5)	C29-H29A	0.9600
N2-C9	1.446(5)	C29-H29B	0.9600
O1-C1	1.282(5)	C29-H29C	0.9600
O2-C1	1.369(5)	C30-H30A	0.9600
O2-C19	1.434(5)	C30-H30B	0.9600
O3-C36	1.327(5)	C30-H30C	0.9600
O4-C21	1.318(5)	C31-H31A	0.9600
C1-C2	1.323(6)	C31-H31B	0.9600
C2-C3	1.506(5)	C31-H31C	0.9600
C2-C20	1.525(6)	C32-C33	1.509(6)
C3-H3A	0.9700	C32-C35	1.521(6)
C3-H3B	0.9700	C32-C34	1.528(6)
C4-C5	1.275(5)	C33-H33A	0.9600
C4-H4	0.9300	C33-H33B	0.9600
C5-C6	1.417(6)	C33-H33C	0.9600
C5-H5	0.9300	C34-H34A	0.9600
C6-C7	1.408(5)	C34-H34B	0.9600
C7-C8	1.314(5)	C34-H34C	0.9600
C7-H7	0.9300	C35-H35A	0.9600
C8-H8	0.9300	C35-H35B	0.9600
C9-C10	1.445(5)	C35-H35C	0.9600
C9-H9A	0.9700	C36-C41	1.387(6)
C9-H9B	0.9700	C36-C37	1.435(5)
C10-H10A	0.9600	C37-C38	1.363(5)
C10-H10B	0.9600	C37-C43	1.503(5)
C10-H10C	0.9600	C38-C39	1.313(6)
C11-C13	1.472(6)	C38-H38	0.9300
C11-C12	1.487(6)	C39-C40	1.389(6)
C11-C14	1.589(6)	C39-C42	1.540(6)
C12-H12A	0.9600	C40-C41	1.378(5)
C12-H12B	0.9600	C40-H40	0.9300
C12-H12C	0.9600	C41-C47	1.481(6)
C13-H13A	0.9600	C42-H42A	0.9600
C13-H13B	0.9600	C42-H42B	0.9600
C13-H13C	0.9600	C42-H42C	0.9600
C14-H14A	0.9600	C43-C45	1.528(5)
C14-H14B	0.9600	C43-C44	1.536(5)
C14-H14C	0.9600	C43-C46	1.542(5)
C15-C17	1.469(6)	C44-H44A	0.9600
C15-C16	1.502(7)	C44-H44B	0.9600
C15-C18	1.533(6)	C44-H44C	0.9600
C16-H16A	0.9600	C45-H45A	0.9600
C16-H16B	0.9600	C45-H45B	0.9600
C16-H16C	0.9600	C45-H45C	0.9600
C17-H17A	0.9600	C46-H46A	0.9600
C17-H17B	0.9600	C46-H46B	0.9600
C17-H17C	0.9600	C46-H46C	0.9600
C18-H18A	0.9600	C47-C50	1.536(6)
C18-H18B	0.9600	C47-C49	1.539(6)
C18-H18C	0.9600	C47-C48	1.553(6)
C19-H19A	0.9600	C48-H48A	0.9600
C19-H19B	0.9600	C48-H48B	0.9600
C19-H19C	0.9600	C48-H48C	0.9600
C20-H20A	0.9600	C49-H49A	0.9600
C20-H20B	0.9600	C49-H49B	0.9600
C20-H20C	0.9600	C49-H49C	0.9600
C21-C22	1.352(5)	C50-H50A	0.9600
C21-C26	1.375(6)	C50-H50B	0.9600
C22-C23	1.444(6)	C50-H50C	0.9600

C22-C28	1.474(6)	C51-H51A	0.9600
C23-C24	1.300(6)	C51-H51B	0.9600
C23-H23	0.9300	C51-H51C	0.9600
C24-C25	1.377(6)		

Atoms 1,2,3	Angle 1,2,3 [°]	Atoms 1,2,3	Angle 1,2,3 [°]
O3-Al1-O1	103.47(15)	C21-C26-C32	127.4(6)
O3-Al1-O4	110.21(15)	C25-C26-C32	116.8(6)
O1-Al1-O4	108.34(15)	C24-C27-H27A	109.500
O3-Al1-C51	118.52(16)	C24-C27-H27B	109.500
O1-Al1-C51	108.57(18)	H27A-C27-H27B	109.500
O4-Al1-C51	107.34(16)	C24-C27-H27C	109.500
N1-P1-C3	121.1(2)	H27A-C27-H27C	109.500
N1-P1-C15	102.4(2)	H27B-C27-H27C	109.500
C3-P1-C15	104.4(2)	C22-C28-C31	105.9(4)
N1-P1-C11	107.8(2)	C22-C28-C30	111.7(5)
C3-P1-C11	106.9(2)	C31-C28-C30	109.8(4)
C15-P1-C11	114.5(3)	C22-C28-C29	117.8(5)
C6-N1-P1	141.6(4)	C31-C28-C29	101.7(4)
C4-N2-C8	117.6(4)	C30-C28-C29	109.2(4)
C4-N2-C9	123.3(5)	C28-C29-H29A	109.500
C8-N2-C9	119.1(5)	C28-C29-H29B	109.500
C1-O1-Al1	138.6(3)	H29A-C29-H29B	109.500
C1-O2-C19	112.2(4)	C28-C29-H29C	109.500
C36-O3-Al1	177.3(3)	H29A-C29-H29C	109.500
C21-O4-Al1	172.3(3)	H29B-C29-H29C	109.500
O1-C1-C2	125.9(5)	C28-C30-H30A	109.500
O1-C1-O2	118.4(5)	C28-C30-H30B	109.500
C2-C1-O2	115.6(5)	H30A-C30-H30B	109.500
C1-C2-C3	124.6(5)	C28-C30-H30C	109.500
C1-C2-C20	120.5(5)	H30A-C30-H30C	109.500
C3-C2-C20	114.1(4)	H30B-C30-H30C	109.500
C2-C3-P1	120.2(3)	C28-C31-H31A	109.500
C2-C3-H3A	107.300	C28-C31-H31B	109.500
A1-C3-H3A	107.300	H31A-C31-H31B	109.500
C2-C3-H3B	107.300	C28-C31-H31C	109.500
A1-C3-H3B	107.300	H31A-C31-H31C	109.500
H3A-C3-H3B	106.900	H31B-C31-H31C	109.500
C5-C4-N2	123.3(5)	C26-C32-C33	107.8(5)
C5-C4-H4	118.300	C26-C32-C35	115.6(5)
N2-C4-H4	118.300	C33-C32-C35	107.3(5)
C4-C5-C6	123.2(5)	C26-C32-C34	109.9(5)
C4-C5-H5	118.400	C33-C32-C34	112.5(5)
C6-C5-H5	118.400	C35-C32-C34	103.9(5)
N1-C6-C7	129.4(5)	C32-C33-H33A	109.500
N1-C6-C5	119.8(5)	C32-C33-H33B	109.500
C7-C6-C5	110.8(5)	H33A-C33-H33B	109.500
C8-C7-C6	123.5(5)	C32-C33-H33C	109.500
C8-C7-H7	118.200	H33A-C33-H33C	109.500
C6-C7-H7	118.200	H33B-C33-H33C	109.500
C7-C8-N2	121.2(5)	C32-C34-H34A	109.500
C7-C8-H8	119.400	C32-C34-H34B	109.500
N2-C8-H8	119.400	H34A-C34-H34B	109.500
C10-C9-N2	113.8(5)	C32-C34-H34C	109.500
C10-C9-H9A	108.800	H34A-C34-H34C	109.500
N2-C9-H9A	108.800	H34B-C34-H34C	109.500
C10-C9-H9B	108.800	C32-C35-H35A	109.500
N2-C9-H9B	108.800	C32-C35-H35B	109.500
H9A-C9-H9B	107.700	H35A-C35-H35B	109.500
C9-C10-H10A	109.500	C32-C35-H35C	109.500
C9-C10-H10B	109.500	H35A-C35-H35C	109.500
H10A-C10-H10B	109.500	H35B-C35-H35C	109.500
C9-C10-H10C	109.500	O3-C36-C41	122.8(5)
H10A-C10-H10C	109.500	O3-C36-C37	120.2(5)
H10B-C10-H10C	109.500	C41-C36-C37	116.9(5)
C13-C11-C12	108.6(5)	C38-C37-C36	118.8(5)

C13-C11-C14	110.9(5)	C38-C37-C43	120.1(6)
C12-C11-C14	106.0(5)	C36-C37-C43	121.1(5)
C13-C11-P1	108.9(4)	C39-C38-C37	123.9(5)
C12-C11-P1	110.7(4)	C39-C38-H38	118.100
C14-C11-P1	111.7(4)	C37-C38-H38	118.100
C11-C12-H12A	109.500	C38-C39-C40	119.2(5)
C11-C12-H12B	109.500	C38-C39-C42	122.2(7)
H12A-C12-H12B	109.500	C40-C39-C42	118.6(6)
C11-C12-H12C	109.500	C41-C40-C39	120.0(5)
H12A-C12-H12C	109.500	C41-C40-H40	120.000
H12B-C12-H12C	109.500	C39-C40-H40	120.000
C11-C13-H13A	109.500	C40-C41-C36	121.1(5)
C11-C13-H-13B	109.500	C40-C41-C47	115.7(5)
H13A-C13-H13B	109.500	C36-C41-C47	123.2(5)
C11-C13-H13C	109.500	C39-C42-H42A	109.500
H13A-C13-H13C	109.500	C39-C42-H42B	109.500
H13B-C13-H13C	109.500	H42A-C42-H42B	109.500
C11-C14-H14A	109.500	C39-C42-H42C	109.500
C11-C14-H14B	109.500	H42A-C42-H42C	109.500
H14A-C14-H14B	109.500	H42B-C42-H42C	109.500
C11-C14-H14C	109.500	C37-C43-C45	112.9(5)
H14A-C14-H14C	109.500	C37-C43-C44	113.6(4)
H14B-C14-H14C	109.500	C45-C43-C44	101.5(4)
C17-C15-C16	105.7(5)	C37-C43-C46	110.7(4)
C17-C15-C18	109.5(5)	C45-C43-C46	107.1(4)
C16-C15-C18	108.4(5)	C44-C43-C46	110.4(4)
C17-C15-P1	115.0(4)	C43-C44-H44A	109.500
C16-C15-P1	104.6(4)	C43-C44-H44B	109.500
C18-C15-P1	113.0(4)	H44A-C44-H44B	109.500
C15-C16-H16A	109.500	C43-C44-H44C	109.500
C15-C16-H16B	109.500	H44A-C44-H44C	109.500
H16A-C16-H16B	109.500	H44B-C44-H44C	109.500
C15-C16-H16C	109.500	C43-C45-H45A	109.500
H16A-C16-H16C	109.500	C43-C45-H45B	109.500
H16B-C16-H16C	109.500	H45A-C45-H45B	109.500
C15-C17-H17A	109.500	C43-C45-H45C	109.500
C15-C17-H17B	109.500	H45A-C45-H45C	109.500
H17A-C17-H17B	109.500	H45B-C45-H45C	109.500
C15C17H17C	109.500	C43-C46-H46A	109.500
H17A-C17-H17C	109.500	C43-C46-H46B	109.500
H17B-C17-H17C	109.500	H46A-C46-H46B	109.500
C15-C18-H18A	109.500	C43-C46-H46C	109.500
C15-C18-H18B	109.500	H46A-C46-H46C	109.500
H18A-C18-H18B	109.500	H46B-C46-H46C	109.500
C15-C18-H18C	109.500	C41-C47-C50	114.1(5)
H18A-C18-H18C	109.500	C41-C47-C49	115.9(5)
H18B-C18-H18C	109.500	C50-C47-C49	104.7(5)
O2-C19-H19A	109.500	C41-C47-C48	108.1(5)
O2-C19-H19B	109.500	C5-0C47-C48	108.9(5)
H19A-C19-H19B	109.500	C49-C47-C48	104.5(5)
O2-C19-H19C	109.500	C47-C48-H48A	109.500
H19A-C19-H19C	109.500	C47-C48-H48B	109.500
H19B-C19-H19C	109.500	H48A-C48-H48B	109.500
C2-C20-H20A	109.500	C47-C48-H48C	109.500
C2-C20-H20B	109.500	H48A-C48-H48C	109.500
H20A-C20-H20B	109.500	H48B-C48-H48C	109.500
C2-C20-H20C	109.500	C47-C49-H49A	109.500
H20A-C20-H20C	109.500	C47-C49-H49B	109.500
H20B-C20-H20C	109.500	H49A-C49-H49B	109.500
O4-C21-C22	117.8(5)	C47-C49-H49C	109.500
O4-C21-C26	119.2(6)	H49A-C49-H49C	109.500
C22-C21-C26	122.9(5)	H49B-C49-H49C	109.500
C21-C22-C23	115.5(5)	C47-C50-H50A	109.500
C21-C22-C28	129.1(5)	C47-C50-H50B	109.500
C23-C22-C28	115.4(6)	H50A-C50-H50B	109.500
C24-C23-C22	126.6(6)	C47-C50-H50C	109.500

C24-C23-H23	116.700	H50A-C50-H50C	109.500
C22-C23-H23	116.700	H50B-C50-H50C	109.500
C23-C24-C25	114.7(6)	Al1-C51-H51A	109.500
C23-C24-C27	126.3(7)	Al1-C51-H51B	109.500
C25-C24-C27	119.0(6)	H51A-C51-H51B	109.500
C24-C25-C26	124.4(5)	Al1-C51-H51C	109.500
C24-C25-H25	117.800	H51A-C51-H51C	109.500
C26-C25-H25	117.800	H51B-C51-H51C	109.500
C21-C26-C25	115.7(5)		

Atoms 1,2,3,4	Tors. an. 1,2,3,4 [°]	Atoms 1,2,3,4	Tors. an. 1,2,3,4 [°]
C3-P1-N1-C6	54.3(6)	O4-C21-C22-C23	-176.1(4)
C15-P1-N1-C6	169.8(6)	C26-C21-C22-C23	6.8(7)
C11-P1-N1-C6	-69.1(6)	O4-C21-C22-C28	-0.1(8)
O3-Al1-O1-C1	101.3(5)	C26-C21-C22-C28	-177.2(5)
O4-Al1-O1-C1	-141.7(4)	C21-C22-C23-C24	-3.1(8)
C51-Al1-O1-C1	-25.4(5)	C28-C22-C23-C24	-179.7(5)
O1-Al1-O3-C36	-67.(7)	C22-C23-C24-C25	-0.4(8)
O4-Al1-O3-C36	178.(100)	C22-C23-C24-C27	177.3(4)
C51-Al1-O3-C36	54.(7)	C23-C24-C25-C26	0.5(7)
O3-Al1-O4-C21	4.(3)	C27-C24-C25-C26	-177.4(4)
O1-Al1-O4-C21	-108.(3)	O4-C21-C26-C25	176.2(4)
C51-Al1-O4-C21	135.(3)	C22-C21-C26-C25	-6.8(7)
Al1-O1-C1-C2	-149.3(4)	O4-C21-C26-C32	-8.1(8)
Al1-O1-C1-O2	28.0(7)	C22-C21-C26-C32	168.9(5)
C19-O2-C1-O1	78.4(5)	C24-C25-C26-C21	2.9(7)
C19-O2-C1-C2	-104.1(5)	C24-C25-C26-C32	-173.2(5)
O1-C1-C2-C3	-175.9(4)	C21-C22-C28-C31	56.0(7)
O2-C1-C2-C3	6.8(7)	C23-C22-C28-C31	-128.0(5)
O1-C1-C2-C20	-6.7(8)	C21-C22-C28-C30	-63.5(7)
O2-C1-C2-C20	176.0(4)	C23-C22-C28-C30	112.5(5)
C1-C2-C3-P1	-114.8(5)	C21-C22-C28-C29	168.8(5)
C20-C2-C3-P1	75.4(5)	C23-C22-C28-C29	-15.1(7)
N1-P1-C3-C2	-23.4(5)	C21-C26-C32-C33	66.5(7)
C15-P1-C3-C2	-137.8(4)	C25-C26-C32-C33	-117.9(5)
C11-P1-C3-C2	100.4(4)	C21-C26-C32-C35	-173.5(5)
C8-N2-C4-C5	-6.4(8)	C25-C26-C32-C35	2.1(7)
C9-N2-C4-C5	172.8(5)	C21-C26-C32-C34	-56.4(7)
N2-C4-C5-C6	2.4(9)	C25-C26-C32-C34	119.2(5)
Al1-N1-C6-C7	-13.5(9)	Al1-O3-C36-C41	138.(7)
Al1-N1-C6-C5	164.0(4)	Al1-O3-C36-C37	-44.(7)
C4-C5-C6-N1	-177.2(5)	O3-C36-C37-C38	-176.4(4)
C4-C5-C6-C7	0.8(7)	C41-C36-C37-C38	1.8(6)
N1-C6-C7-C8	178.0(5)	O3-C36-C37-C43	4.4(6)
C5-C6-C7-C8	0.2(7)	C41-C36-C37-C43	-177.3(4)
C6-C7-C8-N2	-4.4(8)	C36-C37-C38-C39	-0.1(7)
C4-N2-C8-C7	7.3(7)	C43-C37-C38-C39	179.1(5)
C9-N2-C8-C7	-171.9(5)	C37-C38-C39-C40	0.6(8)
C4-N2-C9-C10	-92.0(6)	C37-C38-C39-C42	178.2(4)
C8-N2-C9-C10	87.1(5)	C38-C39-C40-C41	-2.9(8)
N1-P1-C11-C13	72.7(4)	C42-C39-C40-C41	179.4(4)
C3-P1-C11-C13	-59.0(4)	C39-C40-C41-C36	4.8(7)
C15-P1-C11-C13	-174.1(4)	C39-C40-C41-C47	-174.8(5)
N1-P1-C11-C12	-46.6(5)	O3-C36-C41-C40	174.0(4)
C3-P1-C11-C12	-178.3(4)	C37-C36-C41-C40	-4.2(6)
C15-P1-C11-C12	66.5(5)	O3-C36-C41-C47	-6.3(7)
N1-P1-C11-C14	-164.5(4)	C37-C36-C41-C47	175.4(4)
C3-P1-C11-C14	63.8(5)	C38-C37-C43-C45	-6.0(6)
C15-P1-C11-C14	-51.3(5)	C36-C37-C43-C45	173.1(4)
N1-P1-C15-C17	58.5(5)	C38-C37-C43-C44	-120.9(5)
C3-P1-C15-C17	-174.4(4)	C36-C37-C43-C44	58.2(6)
C11-P1-C15-C17	-57.8(5)	C38-C37-C43-C46	114.1(5)
N1-P1-C15-C16	-57.0(4)	C36-C37-C43-C46	-66.8(5)
C3-P1-C15-C16	70.1(4)	C40-C41-C47-C50	-118.0(5)
C11-P1-C15-C16	-173.3(4)	C36-C41-C47-C50	62.3(6)

N1-P1-C15-C18	-174.7(4)	C40-C41-C47-C49	3.7(7)
C3-P1-C15-C18	-47.7(5)	C36-C41-C47-C49	-175.9(5)
C11-P1-C15-C18	69.0(5)	C40-C41-C47-C48	120.6(4)
Al1-O4-C21-C22	114.(2)	C36-C41-C47-C48	-59.0(6)
Al1-O4-C21-C26	-69.(3)		

6 Proposed Polymerization Mechanism

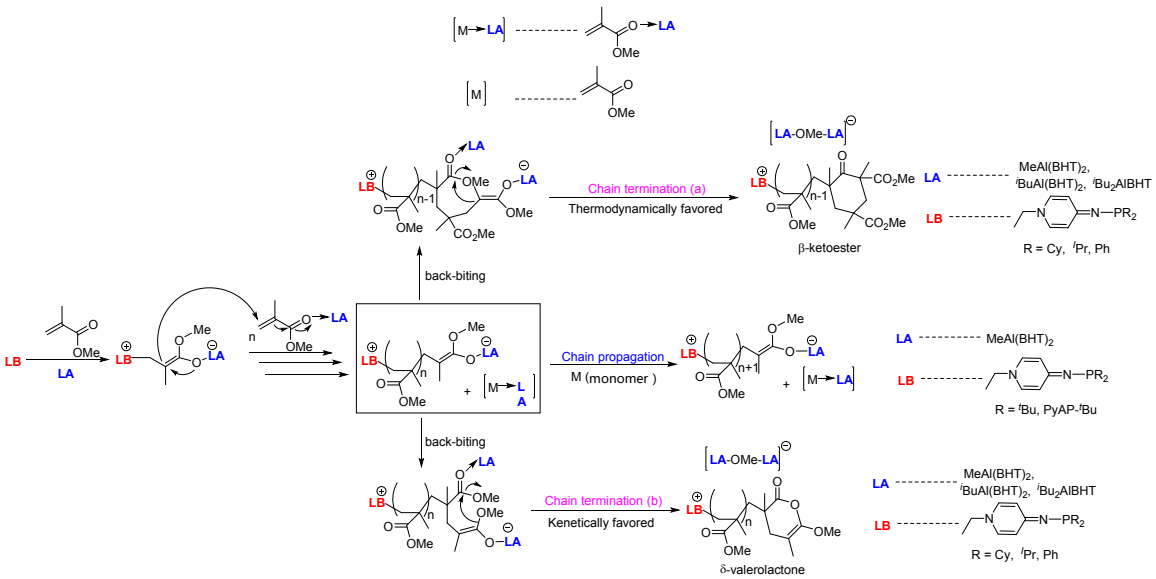

Scheme S1. Proposed Mechanism for Polymerization of MMA by PyAP-Based LPs